

**MASARYKOVA UNIVERZITA**  
**PŘÍRODOVĚDECKÁ FAKULTA**  
ÚSTAV TEORETICKÉ FYZIKY A ASTROFYZIKY

# **Diplomová práce**

**BRNO 2024**

**KATEŘINA PIVOŇKOVÁ**



MASARYKOVA  
UNIVERZITA  
PŘÍRODOVĚDECKÁ FAKULTA  
ÚSTAV TEORETICKÉ FYZIKY A ASTROFYZIKY

---

# Study of high-velocity absorption events in spectra of $\alpha$ Cygni variables

Diplomová práce

**Kateřina Pivoňková**

Vedoucí práce: Olga Viktorovna Maryeva, Ph.D.

Brno 2024





# Bibliografický záznam

<b>Autor:</b>	Bc. Kateřina Pivoňková Přírodovědecká fakulta, Masarykova univerzita Ústav teoretické fyziky a astrofyziky
<b>Název práce:</b>	Studium vysokorychlostních absorpčních událostí ve spektech proměnných hvězd typu $\alpha$ Cygni
<b>Studijní program:</b>	Fyzika
<b>Studijní obor:</b>	Astrofyzika
<b>Vedoucí práce:</b>	Olga Viktorovna Maryeva, Ph.D.
<b>Akademický rok:</b>	2023/2024
<b>Počet stran:</b>	xvi + 105
<b>Klíčová slova:</b>	proměnné typu $\alpha$ Cygni; modří veleobři; vysokorychlostní absorpční událost; Balmerova série; konvektivní vrstvy; metody: spektroskopie



# Bibliographic Entry

**Author:** Bc. Kateřina Pivoňková  
Faculty of Science, Masaryk University  
Department of Theoretical Physics and Astrophysics

**Title of Thesis:** Study of high-velocity absorption events in spectra of  $\alpha$  Cygni variables

**Degree Programme:** Physics

**Field of Study:** Astrophysics

**Supervisor:** Olga Viktorovna Maryeva, Ph.D.

**Academic Year:** 2023/2024

**Number of Pages:** xvi + 105

**Keywords:**  $\alpha$  Cygni variables; blue supergiants; High-Velocity Absorption event; Balmer series; convective zones; techniques: spectroscopy



# Abstrakt

Přestože je jev známý jako vysokorychlostní absorpční události, zkráceně HVA z anglického High-Velocity Absorption, pozorovaný ve spektrech pozdních B a raných A typveleobr, znám již od konce minulého století, stále zůstává záhadou. Tyto události jsou charakteristické náhlým prohloubením absorpčních profilů Balmerovy série, zvláště prominentní u čáry  $H\alpha$ , a též výrazným dopplerovským posunem směrem do modré oblasti spektra.

Pro pochopení podstaty událostí HVA jsme zkoumali dříve publikované výsledky a archivní spektrální data z rychlých zdrojů, včetně databáze projektu IACOB a databáze 2m Perkovala dalekohledu Astronomického ústavu Akademie věd České republiky. Snažili jsme se odlišit události HVA od běžných variací ve spektrech hvězd na základě jejich časových, spektrálních a kauzálních charakteristik. Se zaměřením na morfologický vývoj a kinematické vlastnosti spojené s událostmi HVA jsme rozšířili naši analýzu na čáry vyšší Balmerovy série a vybrané fotosférické čáry. Na základě shromážděných dat jsme navrhli potenciální souvislost mezi fenoménem HVA a vnitřními konvektivními zónami v atmosférách hvězd spektrálního typu B.



# Abstract

The phenomenon of high-velocity absorption (HVA) events observed in the spectra of late B and early A-type supergiants remains enigmatic, even decades after its discovery. These events are characterized by a sudden increase in the depth of absorption lines, accompanied by a significant blue shift and are particularly prominent in the hydrogen Balmer series such as the  $H\alpha$  line.

To understand the nature of HVA phenomenon we investigated previously published results and archival spectral data from various sources, including the IACOB project database and the database of Perek 2m telescope of the Astronomical Institute of the Czech Academy of Sciences. We aimed to distinguish HVA events from ordinary variations in stellar spectra based on their temporal, spectral, and causal characteristics. By focusing on the morphological evolution and kinematic properties associated with HVA events, we extended our analysis beyond the  $H\alpha$  line to include higher Balmer lines and selected photospheric lines. Based on collected data we proposed a potential link between the HVA phenomenon and inner convective zones in the atmospheres B-type stars.





ZADÁNÍ  
DIPLOMOVÉ PRÁCE

Akademický rok: 2023/2024

Ústav:	Ústav teoretické fyziky a astrofyziky
Studentka:	Bc. Kateřina Pivoňková
Program:	Fyzika
Specializace:	Astrofyzika

Ředitel ústavu PŘF MU Vám ve smyslu Studijního a zkušebního řádu MU určuje diplomovou práci s názvem:

Název práce:	Studium vysokorychlostních absorpčních událostí ve spektrech proměnných hvězd typu $\alpha$ Cygni
Název práce anglicky:	Study of high-velocity absorption events in spectra of $\alpha$ Cygni variables
Jazyk závěrečné práce:	angličtina

**Oficiální zadání:**

Late B- and early A-type supergiants are post-main-sequence massive stars. Some of them are evolving red-wards just after the termination of the main sequence, while others have evolved back from the red supergiant (RSG) stage. Among late B- and early A-type supergiants there is a group of variable stars named after its prototype – alpha Cygni. These variables – alpha Cygni variables – show both changes in brightness and variability of spectral lines (mainly the intensity and shape of H $\alpha$  emission line). They also sometimes display a rare and peculiar phenomenon – high-velocity absorption events (HVAs), occasional appearance of deep and highly blue-shifted absorptions. This effect is still little known, as it was detected only for a few late B- and early A-type supergiants. There is no established theory of the appearance of HVA, which can explain the scarcity of objects with HVA and long intervals between these events. Therefore, the search for new HVA events is very important. The work will consist of the search for new cases of HVA events among the archival spectra from the archive of Perek 2-m telescope and in IACOB spectroscopic database, as well as statistical analysis of both newly detected and known from literature HVA events in order to reveal the mechanisms of their appearance and physics behind this rare and peculiar phenomenon.

Vedoucí práce:	Olga Viktorovna Maryeva, Ph.D.
Datum zadání práce:	21. 11. 2022
V Brně dne:	2. 4. 2024

Zadání bylo schváleno prostřednictvím IS MU.

Bc. Kateřina Pivoňková, 28. 3. 2024

Olga Viktorovna Maryeva, Ph.D., 28. 3. 2024

Mgr. Dušan Hemzal, Ph.D., 31. 3. 2024



# Acknowledgment

First I would like to express my gratitude to my supervisor Olga Viktorovna Maryeva, Ph.D., for her invaluable guidance, endless patience and support throughout this research journey. I would like to thank to Sergio Simon-Diaz, Ph.D., for providing the data from the IACOB project and for his mentorship during my internship at the Instituto de Astrofísica de Canarias (IAC).

Furthermore, I extend my sincere thanks to Mgr. Michal Kajan for providing the essential MESA models, which greatly contributed to this research. I am also grateful to doc. Jiří Kubát, Ph.D. and prof. Jiří Krtička, Ph.D., for their insightful discussions and substantial feedback on the results.

Additionally, I would like to express my heartfelt appreciation to my family and close friend. Their unwavering support has been instrumental in enabling me to complete this thesis successfully.

# Declaration

I declare that I have done my diploma thesis independently under the guidance of the supervisor with the use of cited studies.

Brno, May 2024

.....  
Kateřina Pivoňková



# Contents

<b>Introduction</b> .....	<b>1</b>
<b>1. <math>\alpha</math> Cygni variables and High-Velocity Absorption events</b> .....	<b>3</b>
1.1 $\alpha$ Cygni variables .....	3
1.2 High-Velocity Absorption events and Discrete Absorption Components .....	5
<b>2. Supergiants exhibiting HVAs</b> .....	<b>7</b>
2.1 HD 21389 .....	11
2.2 HD 199478 .....	11
2.3 HD 21291 .....	12
2.4 HD 34085 (Rigel) .....	13
2.5 HD 223960 .....	14
2.6 HD 197345 (Deneb) .....	14
2.7 HD 207260 .....	15
2.8 HD 91619 .....	16
2.9 HD 96919 .....	17
2.10 HD 14489 .....	17
2.11 HD 92207 .....	17
<b>3. Analysis of Archival Data</b> .....	<b>21</b>
3.1 Spectral data .....	21
3.1.1 Tools for analysis .....	21
3.2 HD 92207 .....	23
3.3 HD 21389 .....	24
3.4 HD 199478 .....	27
3.5 HD 96919 and HD 91619 .....	32
3.6 HD 207260 and HD 223960 .....	33
3.7 HD 21291 .....	36
3.8 HD 34085 (Rigel) .....	38
3.9 HD 197345 (Deneb) .....	48
3.10 Broad emission wings around $H\alpha$ .....	61
<b>4. Explanation for HVA events</b> .....	<b>65</b>
4.1 Evolutionary status .....	65

4.2 Hypothesis behind HVA events . . . . .	68
4.3 Hypothesis based on the results of this work . . . . .	70
<b>Conclusion and Future Insights . . . . .</b>	<b>79</b>
<b>Bibliography . . . . .</b>	<b>81</b>
<b>Appendix . . . . .</b>	<b>93</b>

# Introduction

For over a century, late B- and early A-type supergiants have intrigued astronomers with their spectral variability, yet the driving mechanism behind these observed variations remains unknown despite decades of extensive research.

Among the poorly understood phenomena in this context are High-Velocity Absorption (HVA) events. Manifesting as a sudden and dramatic change in absorption line profiles accompanied by significant blue shifts which are prominent in Balmer hydrogen series, particularly in  $H\alpha$  line. Up to now the events were observed in very few supergiants and despite extensive research, fundamental questions about the triggering mechanism and the limited occurrence of HVA events in certain stars remain unanswered. Although these rare HVA events, discovered decades ago, are known only to a narrow circle of specialists, their study holds potential for understanding the internal structure and evolution of blue supergiants.

Based on the analysis of historically published results, as well as the study of spectral data collected at the Canary Islands Institute of Astrophysics (IACOB project) and at the Astronomical Institute of the Czech Academy of Sciences, we aim to describe in detail the observational properties of HVA events.

Focusing mainly on  $H\alpha$  line where the events manifest the most, we traced the morphological evolution of the event and also the evolution of its parameters such as blue-edge velocity, line intensities and the duration of the event to establish whether they display any repetitive behavior. Additionally higher Balmer lines and selected photospheric line are also analysed to see the imprint of the event in different layers of the atmosphere.

With use of observational properties of several HVA events recorded for a few supergiants, we proposed potential scenario how this extraordinary phenomenon is triggered.





# Chapter 1

## $\alpha$ Cygni variables and High-Velocity Absorption events

### 1.1 $\alpha$ Cygni variables

Deneb ( $\alpha$  Cyg), owing to its distinctive type of variability, has emerged as a prototype of a class of pulsating post-main sequence stars characterized by both, spectroscopic and photometric variability. This relatively poorly studied class of  $\alpha$  Cyg variables is primarily identified by low-amplitude light variations (generally less than tenth of magnitude) occurring over a wide range of periods, spanning from days to several months (Catelan and Smith, 2015).

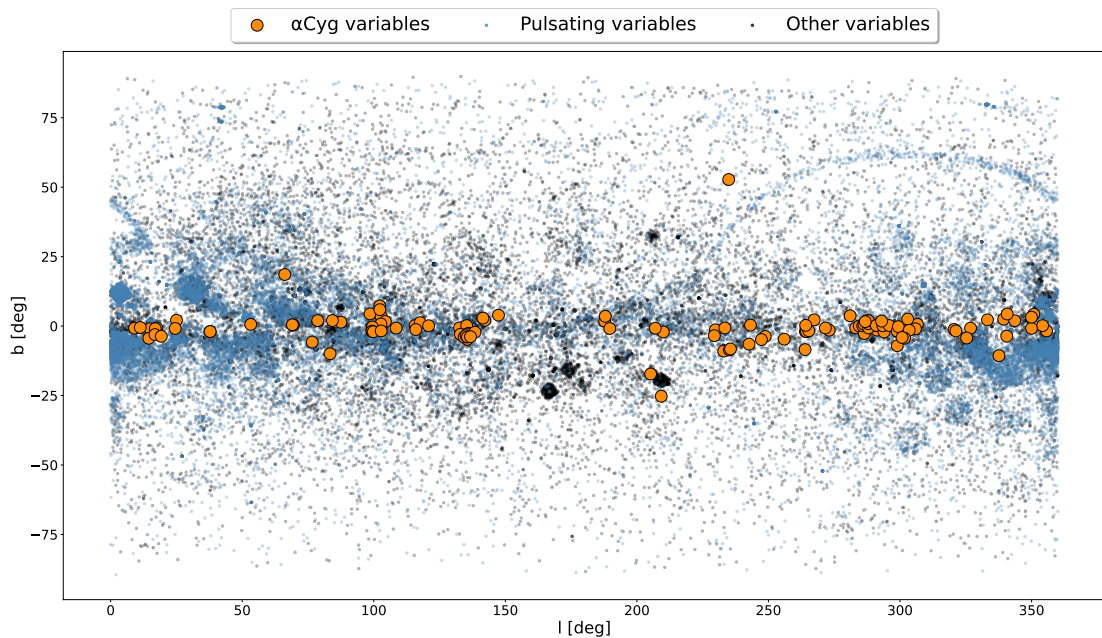


Figure 1.1: The distribution of  $\alpha$  Cyg variables in the Milky Way galaxy. Data used in this figure were collected from Samus' et al. (2017).

These objects exhibit variability not only in their light but also in the profiles

and radial velocities of spectral lines. The  $H\alpha$  line, in particular, undergoes dramatic changes in profile strength and even type. Variability in photospheric lines is generally lower compared to that observed in the  $H\alpha$  line. The variations in radial velocities are attributed to stellar pulsations, most likely non-radial (Achmad et al., 1997), and observations indicate a correlation between changes in brightness and variations in the radial velocities of lines (Fath, 1935).

Considering the position of  $\alpha$  Cygni variables in the HR diagram (Fig. 1.2), the evolutionary status and therefore their current age remain uncertain. These stars are all evolved objects situated in the transitional region between the Main Sequence (MS) and the Red Supergiant Stage (RSGs). However, the pathway by which massive stars enter this region is not definitively established, as they may enter directly from the MS or evolve leftward after previously undergoing the RSG phase.

Fig. 1.2 reveals a significant scatter in both luminosity and  $\log(T_{\text{eff}})$  among  $\alpha$  Cyg variables. This raises questions about whether such a wide range is governed by the same pulsational mechanism or if these stars are grouped into the class based solely on similar manifestations of different underlying causes. The wide range of  $\log(T_{\text{eff}})$  poses a potential challenge if the pulsations originate from an instability specific to  $\alpha$  Cyg stars, as pulsational mechanisms are typically found to operate within narrow temperature ranges (Gautschy, 1992), such as RR Lyrae,  $\delta$  Scuti, etc.

In light of this, the mechanism proposed by Saio et al. (2006) to explain the long-period oscillations observed in HD 163899 (classified as SPBsg - Slowly Pulsating B supergiant) may offer promise. The observed behavior could be interpreted as over-stable g-mode pulsations trapped in the envelope just above the convective zone overlaying the H-burning shell. This concept was further developed a few years later by Gautschy (2009), who studied the properties of over-stable low-degree modes and their significance in clarification of the  $\alpha$  Cyg phenomenon. One of the suggested statements from discussion should be pinpointed, and it is the one supporting the paper by Glatzel and Mehren (1996) saying that the  $\alpha$  Cyg variables are not homogenous in sense pulsation excitation mechanism even though the observed manifestation is similar or the same.

In conclusion, despite significant progress made in both observational and theoretical directions, the long timescale observations and low-amplitude variability associated with  $\alpha$  Cyg variables still leave many open questions. This is particularly challenging given that the typical variability characteristic of  $\alpha$  Cyg type decreases in both timescale and amplitude with increasing effective temperature. Consequently, observing such processes is considerably more straightforward in cooler supergiants such as Deneb, as discussed in e.g., Lefever et al. (2007).

These stars continue to pose intriguing questions that challenge our current understanding. However, ongoing research efforts hold promise not only for further unraveling the complexities of these pulsating variable stars but also for discovering new candidates e.g. Dorn-Wallenstein et al. (2020) that may not yet be classified. Additionally, determining the variability properties of Deneb as a prototype with precision is crucial so that it can serve as a reliable template for classification purposes.

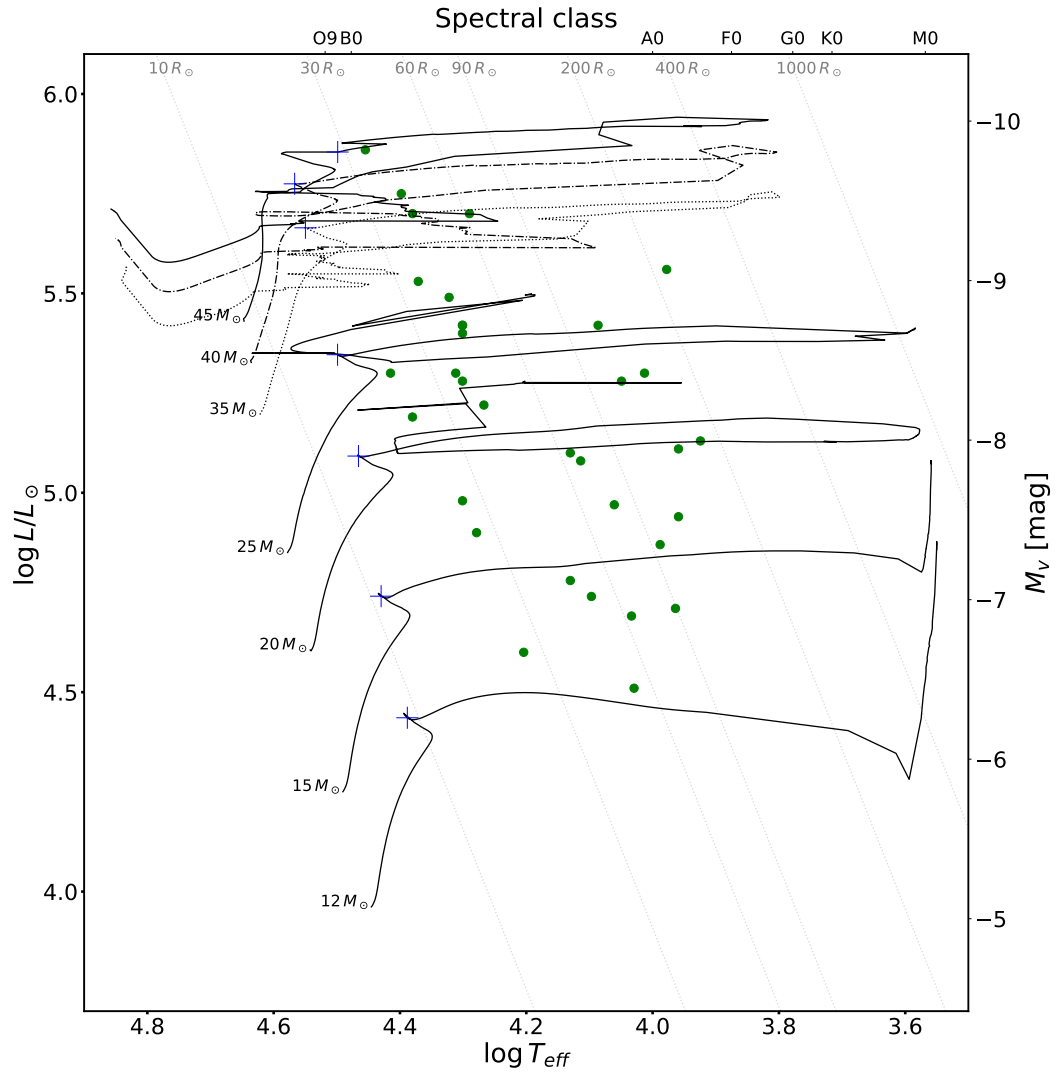


Figure 1.2: Sample of  $\alpha$  Cyg variables in the HR diagram. Evolutionary tracks with blue crosses marking the end of the Main Sequence for massive stars were collected from (Yusof et al., 2022). The data for individual stars are taken from (Kudritzki et al., 1999; Lefever et al., 2007) and Tab. 2.2, Tab. 2.3 for the stars analyzed in the frame of this work as they are classified as  $\alpha$  Cyg variables.

## 1.2 High-Velocity Absorption events and Discrete Absorption Components

The variability in  $H\alpha$  line of blue supergiants was early noted in papers e.g. by Sanford (1947) and Snow and Morton (1976) and later by e.g. Kaufer et al. (1996b) and Markova et al. (2008). A group from Heidelberg took a significant step forward by initiating a long-term, high-resolution monitoring of B- and A-type supergiants. As a result, subsequent publications by Kaufer et al. (1996a), Kaufer et al. (1996b), and Kaufer et al. (1997b) became the first to discuss the appearance of peculiar

events observed in the H $\alpha$  line for Rigel.

These events are characterized by a significant increase in absorption line depth accompanied by a pronounced blue shift encompassing a considerable fraction of the terminal velocity. They most prominently observed in the hydrogen Balmer series, especially in the H $\alpha$  line. In some cases, the deepening may be accompanied by the appearance of a secondary absorption component, which evolves over time as the event progresses. Based on these characteristics, this feature is commonly referred to as an HVA event, an abbreviation for High-Velocity Absorption.

Since their initial discovery, HVA events have been observed multiple times (e.g. Israelian et al. (1997), Morrison et al. (2008), Markova et al. (2008), Chesneau et al. (2014), Ismailov and Ismayilova (2019), and Corliss et al. (2015)), yet they remain restricted to a very select group of objects, all identified as late B- and early A-type supergiants exhibiting  $\alpha$  Cyg type variability. The limited occurrence of HVA events, with only sporadic observations over a decade, poses a significant challenge. Although the number of documented HVA events has gradually increased since their first observation, numerous unanswered questions persist regarding these extraordinary phenomena.

Beside HVA events, there are similar features commonly referred to as Discrete Absorption Components (DACs) which are prominent structures observed in the stellar winds of massive hot stars with line-driven winds. These structures appear as localized narrow absorption features moving blueward from the line center and are typically observed in resonance lines in ultraviolet (UV) range. Their nature is generally assumed to be rooted in Corotating Interacting Regions (CIRs), as suggested by Mullan (1984).

Systematic investigations of DACs, carried out by e.g. Snow (1977) and Prinja and Howarth (1985), have revealed their variability on timescales shorter than one hour. On the other hand, for A-type supergiants was observed by Verdugo et al. (1999a) they may stay unchanged for years.

It is important to note that such features differ from what is observed in H $\alpha$  as HVA events, primarily in their kinematic properties. However, both phenomena have a similar explanation working with large-scale wind structures grounded in the photosphere (Markova et al., 2008).

# Chapter 2

## Supergiants exhibiting HVAs

Current research on HVA events aims to characterize the triggering mechanism behind this phenomenon. The first step in achieving this goal is to thoroughly understand their observational properties, including the general characteristics of stars that sporadically exhibit these extraordinary events.

In this chapter we discuss the physical parameters of known stars exhibiting HVA events, accompanied by an analysis of their previously observed spectral variability. Table 2.1 presents list of eleven supergiants with detected HVA events, while their parameters are collected in Tables 2.2-2.4.

The values of absolute visual magnitude  $M_V$  were calculated using distance estimation listed in Tab. 2.2 - 2.3:

$$M_V = m_V - 5 \log(r) + 5 - A_V, \quad (2.1)$$

where  $A_V$  is interstellar extinction estimated as:

$$A_V = 3.1[(B - V) - (B - V)_0]. \quad (2.2)$$

The values for intrinsic colour indices  $(B - V)_0$  were taken according to individual spectral type from *Stellar Classification Table* (n.d.).

Table 2.1: List of supergiants with detected HVA components.

Supergiants showing HVA	Sp. type	Notes
HD 91619	B6 Iab	HVA event observed once. Strong and weak
HD 34085/Rigel*	B8 Iae	HVA events observed multiple times. Only strong events with large blue shifts were observed.
HD 199478*	B8 Ia	HVA event observed once.
HD 21291*	B9 Ia	Strong and weak events observed.
HD 96919	B9.5 Ia	Mostly exhibits weak events.
HD 21389*	A0 Ia	Shows HVA-like events.
HD 92207	A0 Ia	Suspected to show HVA events.
HD 223960	A0.1 Ia	Only small fractions of event. Shows weak and strong
HD 207260	A2 Iae	HVA events with low frequency of appearance.
HD 197345/Deneb*	A2 Ia	No data about the event.
HD 14489	A1 Ia	

\* – supergiants for which the HVA events were detected in this study or in the study by Pivoňková (2022)

Parameters	Values			
Names <sup>1</sup>	<b>HD 21389</b> HR 1040 V* CE Cam	<b>HD 34085</b> HR 1713 V* bet Ori	<b>HD 199478</b> HR 8020 V* V2140 Cyg	<b>HD 197345</b> HR 7924 V* alf Cyg
				<b>HD 21291</b> HR 1035 V* CS Cam
<b>Observed Parameters</b>				
RA J2000	$3^h 29^m 54.7^s$ <sup>2</sup>	$5^h 14^m 32.3^s$ <sup>12</sup>	$20^h 55^m 49.8^s$ <sup>2</sup>	$20^h 41^m 25.9^s$ <sup>12</sup>
DEC J2000	$58^\circ 52' 43.5''$ <sup>2</sup>	$-8^\circ 12' 5.9''$ <sup>12</sup>	$47^\circ 25' 3.6''$ <sup>2</sup>	$45^\circ 16' 49.2''$ <sup>12</sup>
$M_V$ [mag]	-7.56	-7.3	-8.27	-8.7
$V$ [mag]	4.54 <sup>3</sup>	0.13 <sup>3</sup>	5.64 <sup>3</sup>	1.25 <sup>3</sup>
$B$ [mag]	5.10 <sup>3</sup>	0.10 <sup>3</sup>	6.12 <sup>3</sup>	1.34 <sup>3</sup>
Spectral Type	A0 Ia <sup>4</sup>	B8 Iae <sup>13</sup>	B8 Ia <sup>17</sup>	A2 Ia <sup>21</sup>
Parallax [mas]	$0.930 \pm 0.119$ <sup>2</sup>	$3.78 \pm 0.34$ <sup>12</sup>	$0.392 \pm 0.040$ <sup>2</sup>	$2.31 \pm 0.32$ <sup>12</sup>
Membership	Cam OB1 <sup>28</sup>	Ori OB1 <sup>31</sup>	NGC 6991 <sup>30</sup>	Cyg OB7 <sup>28</sup>
				Cam OB1 <sup>28</sup>
<b>Estimated Parameters</b>				
$T_{eff}$ [kK]	9.73 <sup>5</sup>	11.2 <sup>14</sup>	13.0 <sup>18</sup>	9.1 <sup>14</sup>
$M$ [ $M_\odot$ ]	19.3 <sup>5</sup>	23 <sup>14</sup>	$9^{+5}_{-3}$ <sup>18</sup>	18 <sup>14</sup>
$R$ [ $R_\odot$ ]	97 <sup>5</sup>	116 <sup>14</sup>	68 <sup>18</sup>	119 <sup>14</sup>
$\log L/L_\odot$	4.87 <sup>6</sup>	5.28 <sup>14</sup>	5.08 <sup>18</sup>	4.94 <sup>14</sup>
$\log g$ [cgs]	1.7 <sup>7</sup>	1.67 <sup>14</sup>	1.3 <sup>18</sup>	1.54 <sup>14</sup>
$v_{esc}$ [ $\text{km} \cdot \text{s}^{-1}$ ]	233 <sup>8</sup>	244 <sup>14</sup>	225 <sup>14</sup>	-
$v_\infty$ [ $\text{km} \cdot \text{s}^{-1}$ ]	218 <sup>8</sup>	$155 \pm 46$ <sup>26</sup>	230 <sup>18</sup>	-
$v \cdot \sin i$ [ $\text{km} \cdot \text{s}^{-1}$ ]	53 <sup>5</sup>	55 <sup>14</sup>	41 <sup>18</sup>	50 <sup>14</sup>
$\dot{M}$ [ $M_\odot \cdot \text{yr}^{-1}$ ]	$4.2 \cdot 10^{-7}$ <sup>9</sup>	$1.1 \cdot 10^{-7}$ <sup>25</sup>	$6.73 \cdot 10^{-6}$ <sup>18</sup>	$3.1 \cdot 10^{-7}$ <sup>22</sup>
$V_{macro}$ [ $\text{km} \cdot \text{s}^{-1}$ ]	-	$52 \pm 3$ <sup>26</sup>	40 <sup>19</sup>	-
$R_p$ [ $\text{km} \cdot \text{s}^{-1}$ ]	$-4.9 \pm 0.8$ <sup>27</sup>	$17.8 \pm 0.4$ <sup>15</sup>	$-15.0 \pm 7.4$ <sup>20</sup>	$-4.9 \pm 0.3$ <sup>15</sup>
Distance [pc]	$1084^{+124}_{-112}$ <sup>11</sup>	$260 \pm 20$ <sup>16</sup>	$2466^{+354}_{-247}$ <sup>11</sup>	$802 \pm 66$ <sup>22</sup>
				$949^{+143}_{-88}$ <sup>11</sup>

Table 2.2: Stellar parameters for stars known to show HVA events.

<sup>1</sup> adopted from Simbad, <sup>2</sup> Gaia Collaboration (2020), <sup>3</sup> Ducati (2002), <sup>4</sup> Lyder (2001), <sup>5</sup> Verdugo et al. (1999b), <sup>6</sup> de Jager et al. (1988), <sup>7</sup> Takeda and Takada-Hidai (2000), <sup>8</sup> Talavera and Gomez de Castro (1987), <sup>9</sup> Barlow and Cohen (1977), <sup>10</sup> Bailer-Jones et al. (2018), <sup>11</sup> Bailer-Jones et al. (2021), <sup>12</sup> van Leeuwen (2007), <sup>13</sup> Merrill and Burwell (1943), <sup>14</sup> Kauter et al. (1996a), <sup>15</sup> Gontcharov (2006), <sup>16</sup> de Almeida et al. (2022), <sup>17</sup> Wegmayer et al. (2022), <sup>18</sup> Markova and Puls (2008), <sup>19</sup> Markova et al. (2008), <sup>20</sup> Kharchenko et al. (2007), <sup>21</sup> Morgan and Roman (1950), <sup>22</sup> Schiller and Przybilla (2008), <sup>23</sup> Garrison and Gray (1994), <sup>24</sup> Firnstein and Przybilla (2012), <sup>25</sup> Shultz et al. (2014), <sup>26</sup> Haucke et al. (2018), <sup>27</sup> Gaia Collaboration (2022), <sup>28</sup> Straizys and Laugalys (2008), <sup>29</sup> Lamers (1981), <sup>30</sup> Humphreys (1978), <sup>31</sup> Bouy and Alves (2015)



Parameters	Values			
	HD 223960	HD 207260	HD 91619	HD 96919
Names <sup>1</sup>	HD 223960 BD+60 2636 V* V819 Cas	HD 207260 HR 8334 V* nu. Cep	HD 91619 HR 4147 V* V369 Car	HD 14489 HR 685 V* V474 Per
<b>Observed Parameters</b>				
RA J2000	23 <sup>h</sup> 53 <sup>m</sup> 50.0 <sup>s</sup> <sup>2</sup>	21 <sup>h</sup> 45 <sup>m</sup> 26.9 <sup>s</sup> <sup>10</sup>	10 <sup>h</sup> 33 <sup>m</sup> 25.4 <sup>s</sup> <sup>2</sup>	11 <sup>h</sup> 8 <sup>m</sup> 34.0 <sup>s</sup> <sup>2</sup>
DEC J2000	60°51'12.2" <sup>2</sup>	61°7'14.9" <sup>10</sup>	-58°11'24.5" <sup>2</sup>	-61°56'49.8" <sup>2</sup>
$M_V$ [mag]	-7.7 <sup>3</sup>	-7.6	-7.3	-8.0
$V$ [mag]	6.90 <sup>3</sup>	4.29 <sup>3</sup>	6.26 <sup>3</sup>	5.19 <sup>3</sup>
$B$ [mag]	7.61 <sup>3</sup>	4.81 <sup>3</sup>	6.61 <sup>3</sup>	5.42 <sup>3</sup>
Spectral Type	A0.1 Ia <sup>4</sup>	A2 Iae <sup>11</sup>	B6 Iab <sup>18</sup>	B9.5 Ia <sup>23</sup>
Parallax [mas]	0.341 ± 0.015 <sup>2</sup>	0.48 ± 0.14 <sup>10</sup>	0.4191 ± 0.0218 <sup>2</sup>	0.39 ± 0.07 <sup>2</sup>
Membership	Cas OB5 <sup>31</sup>	Cep OB2 <sup>12</sup>	NGC 3293 <sup>19</sup>	Per OB1 <sup>29</sup>
<b>Estimated Parameters</b>				
$T_{eff}$ [kK]	10.7 ± 0.2 <sup>5</sup>	9.2 ± 0.2 <sup>13</sup>	12.2 <sup>20</sup>	10.3 <sup>20</sup>
$M$ [ $M_{\odot}$ ]	19 <sup>6</sup>	14.7 <sup>14</sup>	27 <sup>21</sup>	23 <sup>20</sup>
$R$ [ $R_{\odot}$ ]	68 <sup>6</sup>	92 <sup>14</sup>	114 <sup>20</sup>	141 <sup>20</sup>
$\log L/L_{\odot}$	4.51 <sup>7</sup>	4.71 <sup>14</sup>	5.42 <sup>20</sup>	5.3 <sup>20</sup>
$\log g$ [cgs]	1.6 ± 0.1 <sup>5</sup>	1.4 ± 0.2 <sup>13</sup>	1.75 <sup>20</sup>	1.5 <sup>20</sup>
$v_{esc}$ [ $\text{km} \cdot \text{s}^{-1}$ ]	-	-	261 <sup>20</sup>	220 <sup>20</sup>
$v_{\infty}$ [ $\text{km} \cdot \text{s}^{-1}$ ]	273 <sup>8</sup>	166 <sup>15</sup>	-	-
$v \cdot \sin i$ [ $\text{km} \cdot \text{s}^{-1}$ ]	54 <sup>6</sup>	44 <sup>14</sup>	60 <sup>20</sup>	25 <sup>25</sup>
$\dot{M}$ [ $M_{\odot} \cdot \text{yr}^{-1}$ ]	-	1.4 · 10 <sup>-6</sup> <sup>16</sup>	-	-
$R_v$ [ $\text{km} \cdot \text{s}^{-1}$ ]	-48.1 ± 2.0 <sup>30</sup>	-18.26 ± 0.76 <sup>17</sup>	7.0 ± 4.3 <sup>22</sup>	-22.4 ± 2.0 <sup>30</sup>
Distance [pc]	2716 <sup>+130</sup> <sub>-111</sub> <sup>9</sup>	1080 <sup>+118</sup> <sub>-109</sub> <sup>9</sup>	2313 <sup>+112</sup> <sub>-98</sub> <sup>9</sup>	2670 <sup>+591</sup> <sub>-388</sub> <sup>9</sup>

Table 2.3: Stellar parameters for stars known to show HVA events.

<sup>1</sup> adopted from Simbad, <sup>2</sup> Gaia Collaboration (2020), <sup>3</sup> Ducati (2002), <sup>4</sup> Bartaya et al. (1994), <sup>5</sup> Firnstein and Przybilla (2012), <sup>6</sup> Verdugo et al. (1999a), <sup>7</sup> Gaia Collaboration et al. (2018), <sup>8</sup> Talavera and Gomez de Castro (1987), <sup>9</sup> Bailer-Jones et al. (2021), <sup>10</sup> van Leeuwen (2007), <sup>11</sup> Gray and Garrison (1987), <sup>12</sup> Hill et al. (1986), <sup>13</sup> Samedov et al. (2021), <sup>14</sup> Verdugo et al. (1999b), <sup>15</sup> Shultz et al. (2014), <sup>16</sup> Vink et al. (1999), Vink et al. (2000), and Vink et al. (2001), <sup>17</sup> Gaia Collaboration (2022), <sup>18</sup> Houk and Cowley (1975), <sup>19</sup> Harris (1976), <sup>20</sup> Kaufer et al. (1996a), <sup>21</sup> Schaller et al. (1992), <sup>22</sup> Gontcharov (2006), <sup>23</sup> Houk and Cowley (1975), <sup>24</sup> Abt and Morrell (1995), <sup>25</sup> Venn (1995), <sup>26</sup> de Jager et al. (1988), <sup>27</sup> Kervella et al. (2019), <sup>28</sup> Kervella et al. (2004), <sup>29</sup> de Burgos et al. (2020), <sup>30</sup> Wilson (1953), <sup>31</sup> Bartaya et al. (1994)



## 2.1 HD 21389

Spectroscopic variability of HD 21389 has been known since the beginning of last century (Campbell et al., 1911) when it was suspected as a spectroscopic binary. However, until now we do not have any satisfactory proof of HD 21389 being a binary or multiple system.

Radial velocity measurements of selected lines (Si II and Fe II) by Abt (1957) revealed a period of about 7.7 days. The analysis also indicated that motions of the atmosphere across the regions of Si II and Fe II are similar, with radial velocity curves exhibiting the same shape but being shifted relative to each other. Additionally, Percy and Welch (1983) estimated a period ranging from 6 to 15 days based on photometric observations.

Aydin (1972) proposed complex pulsations as the likely source of the observed variability in Balmer lines as same as in metallic lines. Later, the variability in metallic lines was found by several authors, e.g. Denizman and Hack (1988), Maharramov and Baloglanov (2015), and Zeinalov and Rzaev (1990a). The latter work specifically aimed to investigate the evolution of the  $H\alpha$  line profile. Despite the persistent complexity of the line profile structure, they proposed a scenario involving transitions from absorption to P Cygni profile, then to inverse P Cygni profile, and back to absorption (or in the reverse order). However, long-term spectroscopic analyses of this star by Corliss et al. (2015) and Pivoňková (2022) have presented a broader range of profiles, including double-peak, multi-component absorption or peculiar profiles of highly asymmetric nature. However, none of these studies found any discernible pattern in the observations.

The most comprehensive study of HD 21389 was conducted by Corliss et al. (2015). This investigation is based on 14 years (1993 - 2007) of spectroscopic observations, with some seasons simultaneously covered by photometric observations. The results revealed a strong correlation of variability (both spectroscopic and photometric) with the phase of a star, whether it is active or relatively quiet. Furthermore, HD 21389 experienced two HVA events, the first occurring in 1993 and the second just a year later in 1994. Subsequent events for HD 21389 were also captured by Richardson et al. (2011) (without any supporting data) and by Pivonková et al. (2022) in 2018.

## 2.2 HD 199478

HD 199478 stands out as the most peculiar supergiant among the HVA targets studied in this work, as it is the only one that exhibits High-Velocity Emission (HVE) events (Ismailov and Ismayilova, 2019).

HD 199478 become first spectroscopically studied by Merrill and Burwell (1933), who noted some kind of variability in  $H\beta$  line. They also found He I lines ( $\lambda 5876$ ,  $\lambda 6678$ ) to double and suggested the star to be possibly a binary. Later Rosendhal (1973a) studied spectra of this star and found that  $H\alpha$  line profile consisted of an emission on both sides of an absorption core. Beside that, observed He I lines as Merrill and Burwell (1933) and also found double structure.

The star was most extensively spectroscopically studied by N. Markova (Markova and Valchev, 2000; Markova and Puls, 2008; Markova et al., 2008) and by N. Z. Ismailov (Ismailov and Ismayilova, 2021; Ismayilova and Ismailov, 2020) who several times observed and described observational properties of HVA. The first-ever observed HVA event for HD 199478 occurred in 2000, as discussed in Markova et al. (2008). In this case, they did not find any influence of the HVA event on photospheric lines, contrary to the findings published by Kaufer et al. (1997b) for different stars during HVA event. They also speculated on the interpretation of the emission found in the  $H\alpha$  line, attributing it to originate in the complex structured stellar envelope.

Ismailov and Ismayilova (2019) conducted an analysis of  $H\alpha$  and  $H\beta$  lines of HD 199478. The data revealed that HD 199478 experienced an HVA event in 2011 lasting 13 – 27 days. This event is likely the strongest HVA event ever detected in terms of blue shift. The depth of absorption component of  $H\alpha$  line reached almost 0.8 of continuum level and radial velocity was blue-shifted to  $-510 \text{ km s}^{-1}$ . That was first ever taken observation of HVA with velocities higher (more than two times) than terminal velocity  $v_\infty$  which is reported by Markova and Puls (2008) to be  $230 \text{ km s}^{-1}$ . Interestingly, the event was also observed in the  $H\beta$  line. By estimating the parameters of these two lines over the whole observational time (2011, 2013 – 2015), they established a variability period of around 22 days, during which the profile remained stable. Additionally, they detected quasi-periodic variability on a timescale of 90 – 100 days. The work of Ismailov and Ismayilova (2021) suggests that the behavior of  $H\alpha$  line during the spectacular events is correlated with variability in the photospheric lines.

HD 199478 was recently identified as Blue Hypergiant (BHG) (Clark et al., 2012) and also found to be a binary. The secondary component has a mass of  $M_2 = 864.54 M_J$  and orbiting at an estimated distance of 4.624 au (Kervella et al., 2019).

## 2.3 HD 21291

The stellar parameters of HD 21291 are listed in Tab. 2.2.

As reported in Maíz Apellániz et al. (2021), HD 21291 is identified as a primary component of a binary system. The secondary component is classified as a less luminous giant with a spectral type B2. Given its separation of  $2.3''$ , the secondary component often lies outside the aperture and is notably fainter. Even from the combined spectra, the secondary component remains unresolved, with only minor changes discernible in certain He I lines.

Rosendhal (1973b) reports this star as a rare type of supergiant exhibiting an  $H\alpha$  line profile in the shape of an inverse P Cygni, although such profiles are now commonly observed in stars of a similar type.

The spectral variability of HD 21291 was extensively studied by the end of the last century, beginning with the work of Zvereva et al. (1984) and Rzaev et al. (1989), who suggested some form of stratification in its atmosphere. It was then followed by Zeinalov and Rzaev (1990a) and Zeinalov and Rzaev (1990b) where, despite focusing on long time variability, they observed the variability in line profiles on a time scale

of an hour for Balmer and photospheric lines. They also speculated on the cyclical evolution of the  $H\alpha$  line profile. Overall, the structure of the  $H\alpha$  line remained complicated and variable, which the authors attributed to non-radial pulsations.

Although Richardson et al. (2011) reports HVA events in HD 21291, no supporting data are provided.

## 2.4 HD 34085 (Rigel)

The fundamental stellar parameters for Rigel are presented in Tab. 2.2. With a visual magnitude  $V = 0.13$  mag, Rigel stands as one of the brightest stars in the night sky. Additionally, it is a member of a multiple system composed of four components, as illustrated schematically in Fig. 2.1.

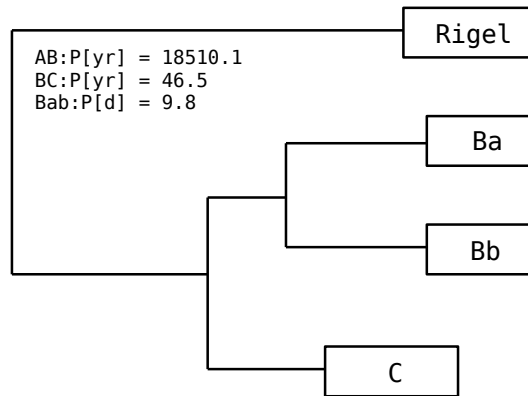


Figure 2.1: Scheme of the hierarchy of Rigel’s multiple system. Data for the scheme were taken from Tokovinin (1997).

One of the earliest studies to conclude on the peculiar spectral behavior of Rigel was conducted by Plaskett (1909). He attempted to establish a period of binary motion based on velocity curves. Unfortunately, due to the quality and low frequency of observations at the time, the result of 21.9 day could not be considered final and was proposed more as a rough estimation. The effort of Sanford (1947) to revisit the period in some sense failed, but a quasi-period of similar span was identified. As a tendency to uncover any periodic signatures in Rigel’s spectra grew, Kikuchi (1968) examined a line profile variations of  $H\alpha$  line. However, no recurrent patterns were recognized.

Rigel (its photosphere and wind region) has been most extensively studied by Kaufer et al. (1996a) and Kaufer et al. (1996b) who analyzed the time-series observation in the optical region. As they summarized  $H\alpha$  line presents a broad variety of profiles among which are also Be-stars-like ones which suggests the presence of an extended equatorial disk-like structure. The reported timescale of spectroscopic variability ranges from several days to months. Additionally, the HVA event was caught for Rigel in 1993 and for the first time analyzed in detail. For an explanation of discovered HVA events Kaufer et al. (1996a) and Kaufer et al. (1996b) suggested

few physical mechanisms of HVA formation. One of them is mass-loss ejecta, other – critical ionization structure in the envelope. These mechanisms are presented in detail in the Section 4.2. Subsequently, Israelian et al. (1997) found the same event in spectra obtained during spectroscopic monitoring 1993-1997 and suggested magnetic loops mechanism as reason of HVA formation (more details in Section 4.2) .

A decade-long spectroscopic monitoring of Rigel by Morrison et al. (2008) revealed that the  $H\alpha$  line is preferably found in the shapes of P Cygni profile, inverse P Cygni one, or pure absorption. Morrison et al. (2008) captured few HVA events, the strongest of them (of 2006 year) was comparable in intensity to the one detected by Kaufer et al. (1996a). The same strong event is also reported by Chesneau et al. (2014), who caught it just a few days before Morrison et al. (2008).

Except for HVA events, the so called DACs (more details about DACs in Section 1.2), stellar wind features were detected in UV Mg II lines of Rigel (e.g. Bates et al. (1986) and Bates et al. (1988)).

## 2.5 HD 223960

Verdugo et al. (1999a) and Verdugo et al. (1999b) highlight that within their sample, HD 223960 stands out as the sole supergiant displaying asymmetric profiles in  $H\beta$ ,  $H\gamma$ , and  $H\delta$  lines. Consequently, this asymmetry poses a challenge in estimating the surface gravity of this star. These distinctive features were suggested by authors to originate from an unusually structured stellar wind.

In a study by Fischer and Morrison (2001), significant emphasis is placed on the morphology of  $H\alpha$  profile for HD 223960, which predominantly exhibits double-peaked emission. This behavior, characterized by the entirety of the  $H\alpha$  line appearing above the continuum, is unusually observed among other Galactic A-type supergiants. The exception to this pattern is perhaps only observed in HD 199478, as reported by Markova and Valchev (2000). The work by Fischer and Morrison (2001) presents a discussion of the atypical nature of the  $H\alpha$  line, suggesting its origin within a system of interacting binaries. However, despite extensive investigation, no indication of radial velocity variability in HD 223960 was uncovered, suggesting its non-binary nature. They also propose that the presence of a double-peaked profile may indicate similarities between this A-type supergiant and Be stars, possibly implying the existence of an equatorial circumstellar disk. However, the conclusion ultimately based on spectroscopic evidence points to a low-density and fast stellar wind. But no clear statement about the appearance of the  $H\alpha$  line profile is presented.

## 2.6 HD 197345 (Deneb)

Deneb, an early A-type supergiant, stands as a prototype of  $\alpha$  Cyg-type variables. The investigation of its behavior started more than a century ago and continues to these days, yet the underlying processes remain incompletely understood. Spectral variability studies of Deneb have been conducted numerous times since the early

1900s. One of the earliest results on variability in radial velocities was presented in a paper by Lee (1911). This was followed by further studies, such as that by Fath (1935), who conducted the first variability study using photometry. Additionally, Abt (1957) analyzed several supergiants, including Deneb, and discovered atmospheric oscillations in early- and intermediate-type supergiants.

A harmonic analysis of Deneb performed by Lucy (1976) revealed multi-periodic oscillations within its atmosphere. Moreover, due to its variability in radial velocities, suspicions arose regarding Deneb's potential binary system membership, although its spectral binarity remains unconfirmed. Years later, Inoue (1979) discovered signs of stratification in Deneb's atmosphere. Measurements of radial velocities of lines of various ions revealed different values dependent on the layer where the line arises. For the bottom part, in the photosphere, the velocity was about  $6 \text{ km s}^{-1}$ . For the layer above, where higher Balmer lines are formed, found an amplitude of  $15 \text{ km} \cdot \text{s}^{-1}$  and finally for the upper part, the  $\text{H}\alpha$  region found an amplitude of  $50 \text{ km s}^{-1}$ .

In the works by Kaufer et al. (1996a) and Kaufer et al. (1996b), radial velocity and line profile variations of  $\text{H}\alpha$  in Deneb and five other supergiants were examined. The analysis unveiled multi-periodicity in radial velocities and equivalent widths of  $\text{H}\alpha$ . In contrast to the above-mentioned variability of Deneb, they observed much more active behavior in  $\text{H}\alpha$ . It was recognized as an HVA event that Deneb underwent in 1991. A few years later, in August 1997, Morrison and Mulliss (1998) found another HVA event. During this event, lasting approximately 40 days, a secondary blue-shifted absorption component appeared. This sudden appearance of the secondary absorption component of  $\text{H}\alpha$  seems to be consistent across all supergiants with recorded strong events (Kaufer et al., 1996b; Morrison et al., 2008; Ismailov and Ismayilova, 2019; Shultz et al., 2014).

In the work by Richardson et al. (2011) the detailed analysis of 5-year observations of Deneb is performed. They found quite rare radial pulsations in the atmosphere of Deneb. Within the time-series spectra they detected HVA events in 1997 and in 2001, both lasting approximately 40 days, consistent with the findings of Morrison and Mulliss (1998). Notably, the behavior of the  $\text{H}\alpha$  line was highly variable over the whole observational period.

More recently, Rzaev (2023) published the results of a four-year (1998-2001, 2007) spectroscopic analysis of Deneb, primarily investigating He I and  $\text{H}\beta$  lines. The study revealed variability in radial velocities of lines likely due to pulsational motions. They established a period of radial pulsations at about 14 days and a period of non-radial pulsations at 22 days. These periods seem to be realistic, supported by evidence from Gautschy (2009), who pointed to the existence of a subphotospheric convective zone possibly driving the observed variability in Deneb. The derived periods of a dozen to several tens of days should be very stable for  $\alpha$  Cyg-type variables.

## 2.7 HD 207260

The first spectral study of HD 207260 was conducted by Abt (1957), who estimated a period of variability to be 7.6 days by measuring radial velocities of Fe II lines ( $\lambda 4508$ ,  $\lambda 4515$ ,  $\lambda 4520$ , and  $\lambda 4522$ ).

Later, Scholz and Gerth (1981) determined the effective magnetic field of  $\nu$  Cep based on 55 Zeeman spectrograms, showing several years of variations. At the beginning of the observational period, the effective magnetic field was moderate, while in 1978, it reached +2000 G. Additionally, they reported on an approximately 40 days period of radial velocity variations observed in Balmer lines, as well as lines of other elements and ions.

Ten years later, Gerth et al. (1991) performed measurements to confirm the presence of a magnetic field using the same photoelectric method and found the magnetic field to be temporal with a clear period of 4.7 years. The magnetic field was found to vary and sometimes disappear from the data. However, this variability may be attributed to the lower accuracy of the photographic method for measuring magnetic fields.

In a study by Takeda and Takada-Hidai (1995), the atmospheric parameters for HD 207260 were derived, along with N-abundances, where it was noted that the star exhibits a large N/H ratio compared to solar values. This suggests that HD 207260 has likely undergone some form of nitrogen enrichment.

The CNO abundances derived for HD 207260 by Yüce (2003) do not indicate atmospheric enrichment by the products of the CNO cycle. This suggests that the star is likely in a pre-RSG stage.

In a study by Verdugo et al. (2003), a search for magnetic fields among A-type supergiants, including  $\nu$  Cep, was conducted. However, no Zeeman splitting was observed for any of them.

Regarding the magnetic wind confinement for  $\nu$  Cep, investigated by Shultz et al. (2014), no Zeeman signature was detected. Additionally they found two HVA events for HD 207260 (in 2010 and again in 2012), even though Richardson et al. (2011) reported that  $\nu$  Cep does not exhibit any HVA events.

Study by Kervella et al. (2019) revealed that  $\nu$  Cep is a binary, with secondary component having a mass of  $M_2 = 86.67 M_J$  and orbiting at a distance of 3.810 au.

## 2.8 HD 91619

The spectroscopic monitoring of HD 91619, along with HD 96919, was conducted by Wolf and Sterken (1976), in conjunction with *ubvy* photometric observations. Throughout the entire observational period, HD 91619 exhibited peculiar H $\alpha$  line profiles characterized by irregular variations without any discernible pattern. Photometric observations also revealed a quasi-periodicity of approximately 20 days.

Subsequently, Kaufer et al. (1994) focused mainly on the H $\alpha$  line variability of HD 91619, demonstrating a broad range of variability. This study was further extended by Kaufer et al. (1996a) to provide a detailed view of the H $\alpha$  variations. The results indicated evidence of an HVA event that HD 91619 underwent in 1994 (further details about the event can be found in the relevant table in the Chapter 3.5).

Furthermore, Chini et al. (2012) reported HD 91619 to be a single-line spectroscopic binary based on high-resolution spectra.



## 2.9 HD 96919

The first comprehensive study of HD 96919 was conducted by Wolf and Sterken (1976), aiming to characterize the variability in the  $H\alpha$  line, as they noted to exhibit a peculiar profile. The observations were partially accompanied by simultaneous photometric observations. Despite no significant strong variations captured, the period photometric variability was established to be approximately 20 days. More pronounced changes were observed in the  $H\alpha$  line. Besides exhibiting extended emission wings, the  $H\alpha$  line showed variations that correlated with changes in its radial velocities. Additionally, it displayed Be stars-like characteristics, with V/R radial velocity variations completing an entire cycle in less than a year. In contrast, no significant changes were found in the  $H\beta$  line.

The most extensive spectral monitoring of HD 96919 has been presented in a series of papers by Kaufer et al. (1994), Kaufer et al. (1996a), Kaufer et al. (1996b), and Kaufer et al. (1997b). Through an analysis of the  $H\alpha$  line, they identified three distinct HVA events, occurring in 1993, 1994, and 1995, respectively. Similar behavior was observed in higher Balmer lines during each event. Additionally, they emphasized the noticeable effect of these extreme wind events, such as HVAs, on strong lines (with line widths exceeding  $500 \text{ m}\text{\AA}$ ), excluding Balmer lines.

Based on proper motion anomaly analysis, HD 96919 is now identified as the primary component of a binary system, with the second component having a mass of  $M_2 = 409.73 M_J$  and orbiting at a distance of 4.203 au (Kervella et al., 2019).

## 2.10 HD 14489

This particular supergiant is very rarely studied one among the sample of stars showing peculiar HVA events. Consequently, the number of publications discussing it is limited. The only mention of an HVA component for this star is found in a footnote in a paper by Richardson et al. (2011), discovered in the spectral data from the Ritter Observatory. The comment notes variability similar to that observed in Deneb, leading to the assumption that this star also exhibits HVA events.

According to a study by Kervella et al. (2019), HD 14489 is identified as a binary. The secondary component, with a mass of  $M_2 = 296.23 M_J$ , orbits at an estimated distance of 3.881 au.

## 2.11 HD 92207

HD 92207 was found as a primary component of a spectroscopic binary (Levato, 1972) and later it has been confirmed by Kervella et al. (2019). The secondary component with a mass of  $M_2 = 141.62 M_J$  orbits at the distance of 4.066 au.

In a study by Buscombe (1973) and Buscombe (1974) HD 92207 has been found to display a large range of variability in spectral lines, consequently in atmospheric parameters and therefore was denoted as the most variable known A-type supergiant.

Kaufer et al. (1994) found the H $\alpha$  line of HD 92207 to be highly variable on a time scale of days to several weeks. Kaufer et al. (1996a) report on an extraordinary event observed in 1994, where the absorption component of H $\alpha$  line reached the velocity of  $-230 \text{ km s}^{-1}$  and persisted in the spectra for  $\approx 150$  days. This event also left an imprint on the wind-sensitive line FeII( $\lambda 5169$ ), with related variations suggesting the event was more likely a DAC than an HVA event (Kaufer et al., 1996a).

Table 2.4: Stellar parameters for HD 92207.

Parameters	Values	References
	HD 92207	
Names	V* V370 Car	adopted from Simbad
	HR 4169	
<b>Observed Parameters</b>		
RA J2000	$10^{\text{h}}37^{\text{m}}27.1^{\text{s}}$	Gaia Collaboration (2020)
DEC J2000	$-58^{\circ}44'0.0''$	Gaia Collaboration (2020)
$V$ [mag]	5.45	Ducati (2002)
$B$ [mag]	5.95	Ducati (2002)
$M_V$ [mag]	-7.9	
Spectral Type	A0 Ia	Houk and Cowley (1975)
Parallax [mas]	$0.468 \pm 0.062$	Gaia Collaboration (2020)
Membership	NGC 3324	Kharchenko and Roeser (2009)
<b>Estimated Parameters</b>		
$T_{eff}$ [kK]	$9500 \pm 200$	Przybilla et al. (2006)
$M$ [ $M_{\odot}$ ]	$25 \pm 3$	Przybilla et al. (2006)
$R$ [ $R_{\odot}$ ]	$223 \pm 24$	Przybilla et al. (2006)
$\log L/L_{\odot}$	$5.56 \pm 0.08$	Przybilla et al. (2006)
$\log g$ [cgs]	$1.2 \pm 0.1$	Przybilla et al. (2006)
$v_{\infty}$ [ $\text{km} \cdot \text{s}^{-1}$ ]	235	Kudritzki et al. (1999)
$v \cdot \sin i$ [ $\text{km} \cdot \text{s}^{-1}$ ]	$30 \pm 5$	Przybilla et al. (2006)
$\dot{M}$ [ $M_{\odot} \cdot \text{yr}^{-1}$ ]	$1.31 \cdot 10^{-6}$	Kudritzki et al. (1999)
$R_v$ [ $\text{km} \cdot \text{s}^{-1}$ ]	$-8.5 \pm 4.2$	Gontcharov (2006)
Distance [pc]	$2091^{+291}_{-235}$	Bailer-Jones et al. (2021)

However, we assume it was an HVA event. The strong P Cygni appearance of the H $\alpha$  line during the event is only a consequence of the fact that the star has strong wind, due to which the manifestation of H $\alpha$  appears differently than what is usually observed during HVA events. Another supporting argument against this event being a DAC is the span of the suddenly appeared component, which in this case is  $3\text{\AA}$ , while DACs are assumed to be narrow (Howarth, 1992).

Kaufer et al. (1997b) observed weak blue wings of strong lines (with line widths exceeding  $500 \text{ m\AA}$  - Balmer lines excluded), indicating stronger wind compared to other analyzed stars (Rigel, Deneb, HD 91619, HD 96919, HD 100262). HD 92207 was the only star monitored by *ubvy*-Strömgren photometry. The light variations seem to be correlated with radial-velocity curves, which led to the assumption that the both



kinds of variations have the same nature, likely variations in radius. Furthermore, a clear periodicity of approximately 27 days was found based on line profile variations.

A recent study by Hubrig et al. (2012) reported the presence of a magnetic field within HD 92207, with a longitudinal magnetic field strength of several hundred Gauss. However, Bagnulo et al. (2013) reanalyzed the same data a year later and convincingly demonstrated that no measurable magnetic field is present in HD 92207.



# Chapter 3

## Analysis of Archival Data

### 3.1 Spectral data

With the aim of searching for HVA events, we analyzed archival high- and medium-resolution optical spectra of all known objects showing HVA events that were accessible via the IACOB database (Simón-Díaz et al., 2011) or the database of the Perek 2m telescope of the Astronomical Institute of the Czech Academy of Science.

While the Perek 2m database contains only spectra taken by the Perek 2m telescope, the IACOB database offers a wider range of instruments used for acquiring the spectra. Details regarding the instruments, number of spectra, and other properties can be found in Tab. 3.1 - 3.2.

All the archival data were then searched through and subsequently analyzed for HVA events. Due to the non-systematic nature (in the sense of this study) of the archival observations, the time series contains numerous gaps without any observations. It's important to note that many spectra were acquired for various purposes, such as high-cadence observations to study pulsations, and therefore not all the lines of interest for this study are included.

All data obtained from the IACOB or Perek 2m database were reduced using standard IRAF tasks or IDL-based procedures that follow IRAF tasks. Additional processes, such as barycentric velocity correction or normalization, were performed using custom Python code. It's important to note that telluric correction was not performed. Previous research (Pivoňková, 2022) revealed that telluric correction may artificially affect the spectrum, particularly in the region of interest, which is the H $\alpha$  region.

#### 3.1.1 Tools for analysis

For investigation of line profile variability the Temporal Variance Spectrum (TVS) analysis and residual dynamic spectra were used.

To systematically explore a global variability in spectral lines through time-series observations, a variant of the TVS was employed. This method, originally introduced by Fullerton et al. (1996), was utilized to track the variations in absorption line profiles of O-type stars. The method involves computing the average spectrum

Table 3.1: Instruments used for acquiring the analyzed spectra.

Instrument	Observatory	Resolution	Sp. range	Ref.
D700	Ondřejov	13000	6260-6765	[1]
OES	Ondřejov	50000	3950-8730	[9]
Feros	ESO La Silla	48000	3530 - 9200	[2]
Fies low	La Palma	46000	3600 - 7200	[3]
Fies high	La Palma	67000	3700 - 9000	[3]
Hermes	La Palma	85000	3760 - 9000	[4]
SONG	Teide	35000	4380 - 6900	[5]
HEROS	ESO La Silla	20000	5700 - 8600	[6]
Fairborn echelle	Fairborn	30000	4900 - 7100	[7]
FLASH	ESO La Silla	20000	4000 - 6800	[8]

[1] Slechta and Skoda (2002); [2] Kaufer et al. (1997a); [3] Telting et al. (2014); [4] Raskin et al. (2011); [5] Grundahl et al. (2011); [6] Kaufer (1998) [7] Eaton and Williamson (2004); [8] Mandel (1988); [9] Koubský et al. (2004)

Table 3.2: Number of spectra per star used for the analysis.

	D700	OES	Feros	Fies low	Fies high	Hermes	SONG	Fairborn echelle	HEROS	FLASH
HD 21291	29				24	16	211			
HD 21389	86*	10*		1	2	7				
HD 34085 (Rigel)	36		16		21	101	4335	6653	667	206
HD 91619			6							
HD 96919			6							
HD 197345 (Deneb)	160			2		1				
HD 199478	28			9		18				
HD 207260						2				
HD 223960						3				

\* were published in Pivonková et al. (2022)

through the time series and determining the corresponding deviation, denoted as  $\sigma$ :

$$\sigma = \sqrt{\frac{\sum_{i=1}^N |x_i - \bar{x}|^2}{N}} \quad (3.1)$$

As mentioned in the Section. 1.2, the characteristic features for HVA events appear in the spectra sporadically amidst random profile variations. Sometimes, the event manifests as a deep absorption, significantly shifted H $\alpha$  line, while at other times, only a weak shift is observed. Establishing criteria to determine whether a specific profile corresponds to an event or a normal profile is challenging, particularly because stars exhibiting these events often have peculiar H $\alpha$  profiles even during quiescent phases with no observable HVA.

To address this challenge, the “residual dynamic spectra” method was employed. This method operates on the assumption that the HVA profile significantly deviates from the average profile. Consequently, each spectrum is subtracted from the average spectrum to obtain residual fluxes. After that these residual fluxes are compared to each other, with pixel values being colored according to the minimal and maximal values.

Given the fact that the time series data are acquired using various instruments, pixel values may be subject to shifts. Additionally, the barycentric velocity correction can induce shifts even among spectra obtained by the same instrument. Therefore, adjustments are made to ensure accurate representation of line profile variability. Specifically, all spectra in the series are interpolated to the same wavelength grid in both the TVS and residual dynamic spectra. This interpolation step is crucial for computing  $\sigma$  and also residual fluxes, as it is calculated for each corresponding flux point separately. However, it’s important to emphasize that this interpolation is performed for illustrative purposes only, and further analysis and measurements of line properties are conducted on the original spectra.

Additionally, equivalent widths (EW) and radial velocities (RV) of selected spectral lines were measured to study of dynamics of atmospheric layers below the wind during HVA events. Equivalent widths were measured using custom Python code based on the `equivalent_width` function from the `Specutils` Python library. Radial velocities, apart from those derived from Balmer lines, were determined using Gaussian fitting methods. However, due to the complexity of highly asymmetric line profiles, particularly those seen in the H $\alpha$  line during HVA events, only visual estimation of the position of the core and the blue edge of the line was feasible. This method was chosen as the most appropriate way to describe the observational properties of HVA events.

## 3.2 HD 92207

HD 92207 was studied by Kaufer et al. (1996a), who focused mainly on variations in the H $\alpha$  region. A peculiar event was identified in the 1994 campaign, where an additional blue-shifted absorption component of a P Cygni profile was observed. This component propagated at a velocity around  $-230 \text{ km s}^{-1}$ , starting at approximately

$-205 \text{ km s}^{-1}$  on JD2449390 and evolving to about  $-255 \text{ km s}^{-1}$  over roughly 140 days.

Unfortunately, the authors did not discuss the appearance of such a feature in higher Balmer lines. However, a similar, weaker component was found in the wind-sensitive line of Fe II ( $\lambda 5169$ ). As a result, this feature was attributed to a DACs-like effect.

### 3.3 HD 21389

The results of previous spectroscopic analysis of HD 21389 are summarized in Pivonková et al. (2022) (attached in the Appendix). Ongoing spectral monitoring with the Perek 2-m telescope indicates that no new HVA events have occurred over the past two years. Additionally, 10 spectra of HD 21389 from 8 different observational nights were available in the IACOB database, none of which display signs of an HVA event.

The radial velocity measurements of selected spectral lines during a 5-year campaign by the Perek 2-m telescope are plotted in Fig. 3.1. Fig. 3.2 presents the temporal variability spectrum (TVS) for selected spectral lines, including  $H\alpha$ ,  $H\beta$ ,  $H\gamma$ ,  $H\delta$ , He I  $\lambda 6678$ , He I  $\lambda 5875$ , and Si II  $\lambda 6347$ .

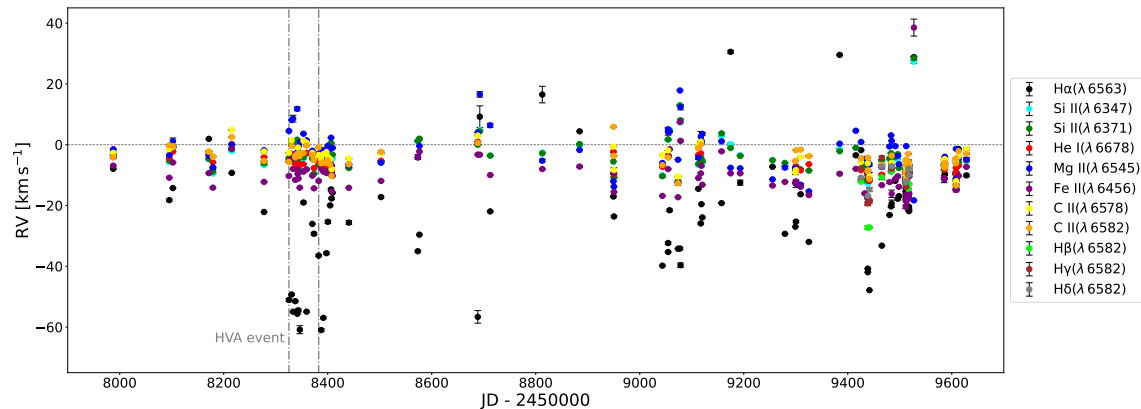


Figure 3.1: The radial velocities of selected lines from 2017 up to 2022. The data includes a portion of the HVA event that HD 21389 underwent in 2018.

Recent HVA event (2018) recognized in  $H\alpha$  line of HD 21389 is recorded in Pivonková et al. (2022). The event was probably caught around its maximum or after since the depth of profile decreases (seen from Tab. 3.3) – it seems to be common behavior observed in  $H\alpha$  line that depth of profile increasing towards the maximum of the event where we see also maximum of blue-shifted velocity and then in again decrease towards its end (Kaufer et al., 1996a; Corliss et al., 2015; Morrison et al., 2008). Another supporting fact about the event from 2018 being caught around its maximum is duration of the event with 46 days being approximately a half of what was observed by Corliss et al. (2015).

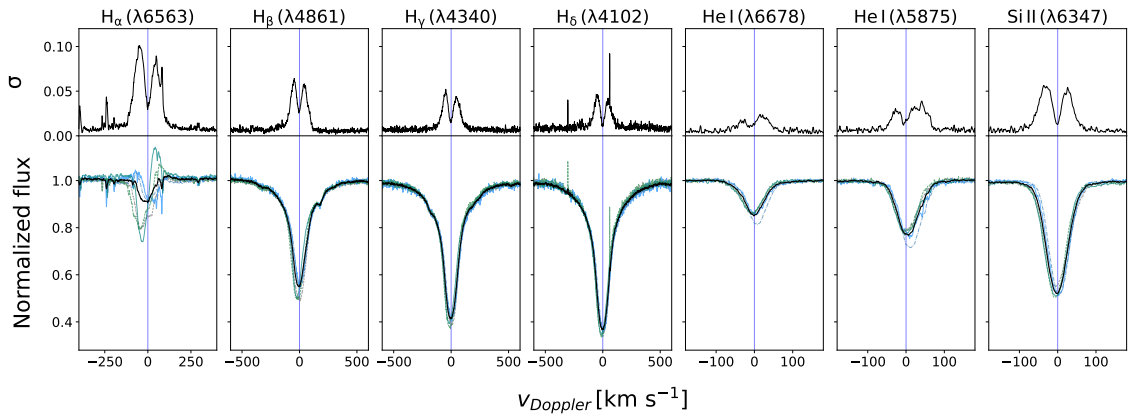


Figure 3.2: The Temporal Variance Spectrum (TVS) of HD 21389 focusing on seven selected spectral lines. Bottom panels: the black line represents the averaged spectrum, while selected composite spectra are illustrated in different colors. Top panels: the deviation from the average spectra, providing insights into the general variability observed in each line.

Due to the lack of observations at the very beginning of the event in 2018, there is no information about the  $H\alpha$  profile before the event. However, at the end of the event, the  $H\alpha$  line exhibited a P Cygni shape. This was already seen (HVA event is closed by P Cygni profile) in a work by Chesneau et al. (2014) in Fig. 2 for Rigel's HVA event in 2010. Additionally, as seen from Fig. 3.1 no correlation in RV of other spectral lines was observed during HVA event which span  $> 46$  days. And since the spectra were taken by D700 spectrograph in only  $H\alpha$  region, the evolution of the event cannot be traced from higher Balmer lines.

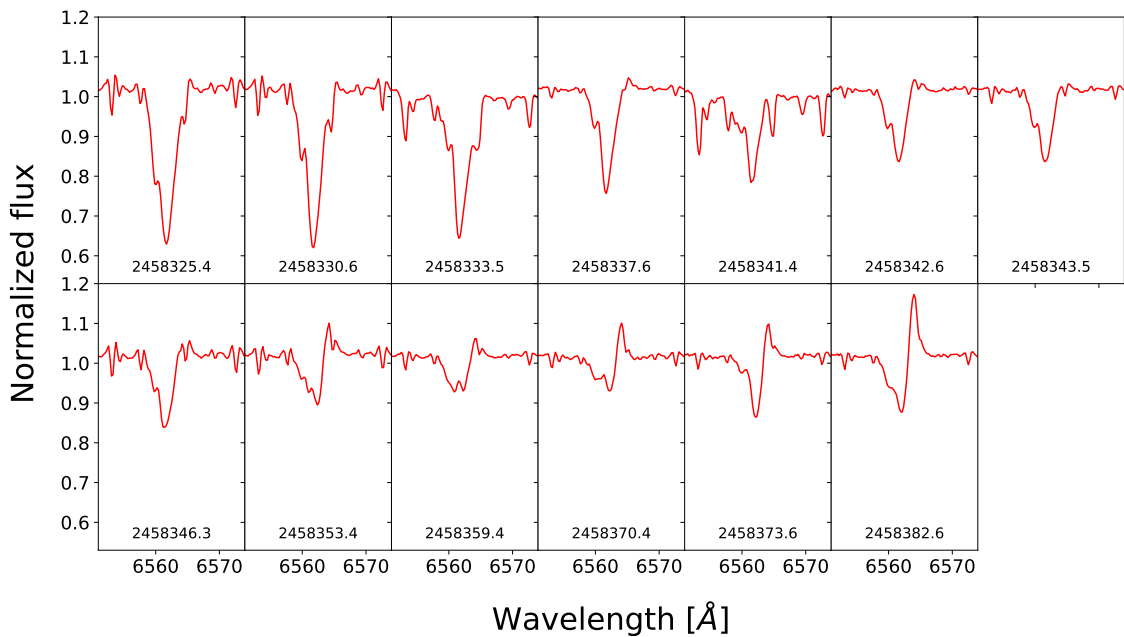


Figure 3.3:  $H\alpha$  line profiles taken during HVA event for HD 21389 in 2018.

Table 3.3: Estimated velocities and intensities of H $\alpha$  during HVA event recorded for HD 21389 in 2018.

JD	max. depth [cont. lvl]	Velocity [km s <sup>-1</sup> ]	
		blue-edge	blue-shifted core
2458325.4	0.63	-206.8	-49.6
2458330.6	0.62	-214.2	-47.6
2458333.5	0.64	-269.3	-54.0
2458337.6	0.76	-213.4	-49.1
2458341.4	0.78	-226.5	-57.2
2458342.6	0.84	-208.0	-54.4
2458343.5	0.84	-211.4	-57.8
2458346.3	0.84	-213.5	-66.4
<b>P Cygni feature appears</b>			
2458353.4	0.89	-206.8	-17.6
2458359.4	0.93	-207.8	-86.1
2458370.4	0.93	-210.9	-109.3
2458373.6	0.86	-206.8	-28.4
2458382.6	0.88	-213.9	-126.5

Table 3.4: Characteristics of HVA event recorded for HD 21389.

	Corliss et al. (2015)	Corliss et al. (2015)
JD	2449301 – 2449390	2449595 – 2449709
Dates	Nov 9. 1993 - Feb 6. 1994	Aug 30. - Dec 22. 1994
$v_{blue\ core}$ [km s <sup>-1</sup> ]	$\approx -120$	$\approx -80$
$v_{blue\ edge}$ [km s <sup>-1</sup> ]	$\approx -190$	$\approx -180$
Depth*	$\approx 0.30$	$\approx 0.50$
Duration of event [d]	$\approx 90$	$\approx 114$
Pivonková et al. (2022)		
JD	2458325 – 2458383	
Dates	Jul 25. - Sept 21. 2018	
$v_{blue\ core}$ [km s <sup>-1</sup> ]	-109	
$v_{blue\ edge}$ [km s <sup>-1</sup> ]	-269	
Depth*	0.62	
Duration of event [d]	< 46	

\* Depth (in continuum lvl) of blue-shifted absorption component.

The very first identified HVA events for HD 21389 are analyzed in Corliss et al. (2015) with fundamental parameters listed in Tab. 3.4. First HVA event was observed in 1993 followed by the second one just a year after in both cases with high correlated behavior of blue-edge velocity and equivalent widths of H $\alpha$  line.

Comparing HVA events observed by Pivonková et al. (2022) and the ones taken by Corliss et al. (2015), two types can be distinguished. The strong ones are typical



by significant blue-shifted velocity  $> 100 \text{ km s}^{-1}$  and the weak ones in which the velocity does not cross the velocity  $\approx 100 \text{ km s}^{-1}$ . Example of  $\text{H}\alpha$  line profile from weak HVA event is seen in Fig. 3.3. The time evolution of both type of the events is also different. While during strong events additional absorption component appear, starts as minor component and as the passes the minor component become stronger then main absorption component, again decreases and finally disappears. The weak events manifests only as deep, broad and blue-shifted absorption.

### 3.4 HD 199478

HD 199478 with its effective temperature about 13 000 K (Tab. 2.2) is the hottest object known to exhibit HVA events and was recently classified as a blue hypergiant (BHG) by Clark et al. (2012).

As shown in Fig. 3.4,  $\text{H}\alpha$  line of HD 199478 tend to be found in emission. This characteristic is also confirmed by Markova and Valchev (2000), Markova et al. (2008), and Ismailov and Ismaylova (2019).

The variability of the  $\text{H}\alpha$  line profile occurs on a time scale of several days to weeks. Fig. 3.5 shows the number of occurrences of each profile type which examples may be found in Fig. 3.6. In addition to the  $\text{H}\alpha$  line, higher Balmer lines also

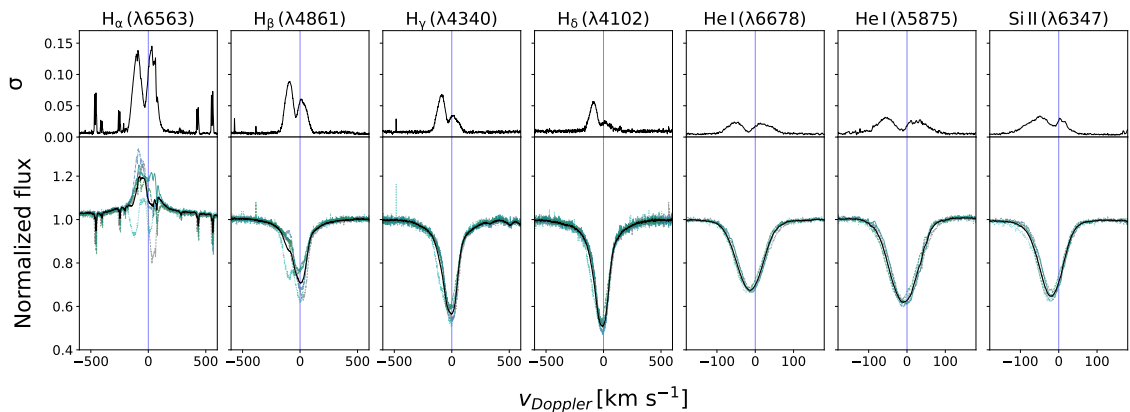


Figure 3.4: The Temporal Variance Spectrum (TVS) of HD 199478 focusing on seven selected spectral lines. Bottom panels: the black line represents the averaged spectrum, while selected composite spectra are illustrated in different colors. Top panels: the deviation from the average spectra, providing insights into the general variability observed in each line.

exhibit variability in their line profiles, which is most prominently observed during HVA events.

According to data collected in this study, the most recently HVA event for HD 199478 was captured in October 2017. Unfortunately, only one spectrum was taken during this event.  $\text{H}\alpha$  line from this event may be seen in Fig. 3.7 in blue color. Larger sample of profiles was taken during HVA event which HD 199478 underwent in 2015.  $\text{H}\alpha$  line from this event may be seen in Fig. 3.7 in red color. The measured properties of both HVA events from  $\text{H}\alpha$  line are listed in Tab. 3.5.

The HVA event from 2015, with the duration of more than 4 days, is recognized from dynamic spectra in Fig. 3.9 as magenta regions and could be traced for  $H\alpha$  (a),  $H\beta$  (b),  $H\gamma$  (c), and  $H\delta$  (d) lines. Comparing all these lines, it is evident that the HVA event feature appears first in higher Balmer lines and is last seen in the  $H\alpha$  line, indicating that the event arises at deeper layers in the atmosphere.

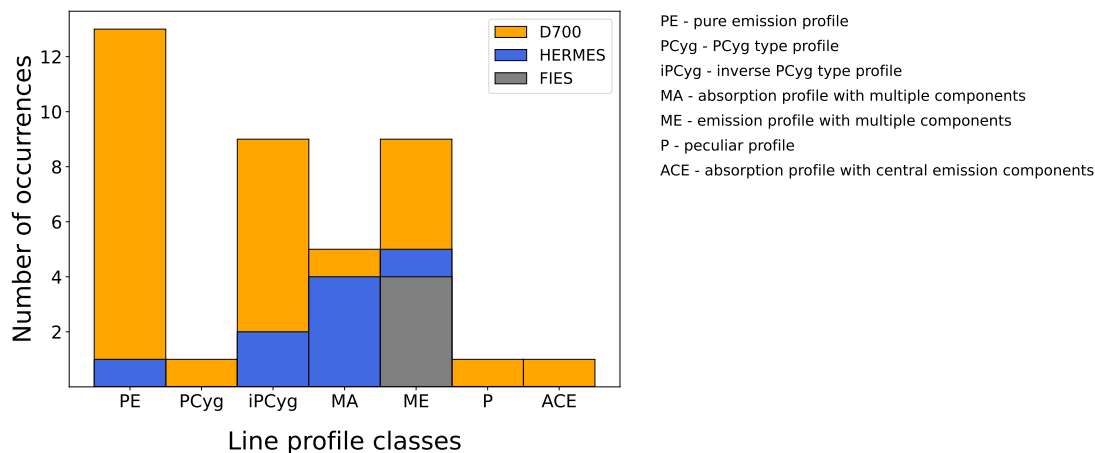


Figure 3.5:  $H\alpha$  line profile morphology histogram for HD 199478 with only one profile taken from each night observations.

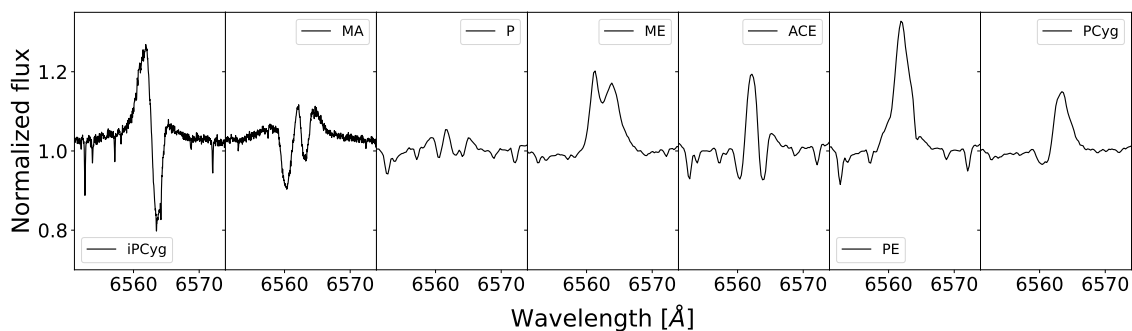


Figure 3.6: Example profiles for different classes shown in Fig. 3.5.

In the spectra of HD 199478, the  $H\alpha$  line profiles exhibit the highest blue-shifted velocities during the events compared to other stars with HVA. Concurrently, an emission component is consistently present in the  $H\alpha$  line throughout most of the observational period. Consequently, the observed profile during HVA events represents a combination of blue-shifted absorption and emission, with the emission component filling the absorption feature. The presence of this emission component obscures the core of the HVA absorption component, making it impossible to determine its radial velocity. As a result, a reliable velocity estimate can only be obtained for the blue edge of the line.

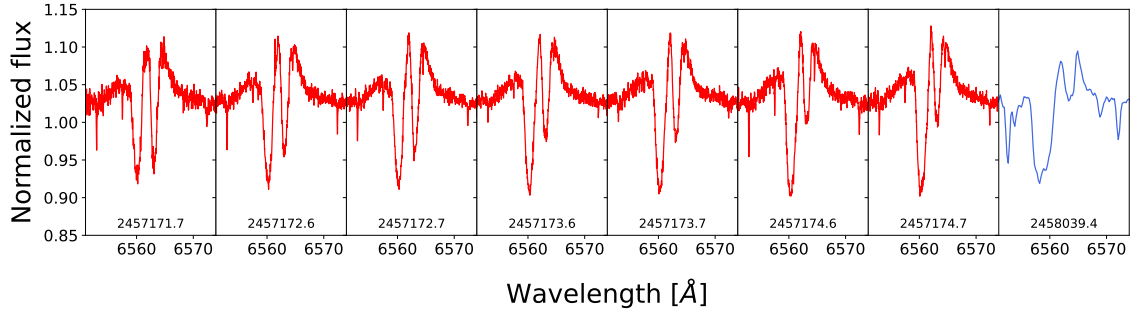


Figure 3.7:  $H\alpha$  line profiles of HD 199478 taken during HVA event in May/June 2015 (red) and October 2017 (lightblue).

Table 3.5: Estimated velocities and intensities of  $H\alpha$  during HVA event recorded for HD 199478 in 2015 and 2017 (last row).

JD	max. depth [cont. lvl]	Velocity [ $\text{km s}^{-1}$ ]	
		blue-edge	blue-shifted core
2457171.7	0.93	-258.6	-119.6
2457172.6	0.92	-222.0	-113.9
2457172.7	0.92	-251.5	-118.4
2457173.6	0.91	-225.6	-112.7
2457173.7	0.91	-215.9	-113.7
2457174.6	0.90	-183.1	-108.2
2457174.7	0.90	-213.7	-119.9
2458039.4	0.92	-303.3	-207.6

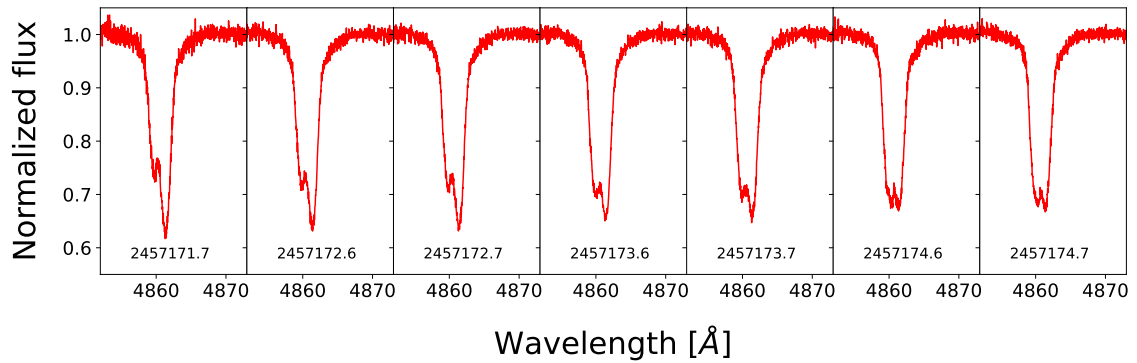


Figure 3.8:  $H\beta$  line profiles of HD 199478 taken during HVA event in May/June 2015.

In addition to the HVA event from 2015 observed in the Balmer lines, traces of the HVA event can be detected in photospheric lines, particularly in He I ( $\lambda 5876$ ) and Si II ( $\lambda 6347$ ), Si II ( $\lambda 6371$ ). Example of He I and Si II lines are depicted in dynamic spectra shown in Fig. 3.10. In both cases, the event manifests as asymmetries present

on the blue side of the line. This was for the first time observed by Ismailov and Ismayilova (2021) for HD 199478, when an increase in equivalent width during the HVA event was observed for photospheric lines. Until now, HD 199478 is the only star with an HVA event traceable from photospheric lines.

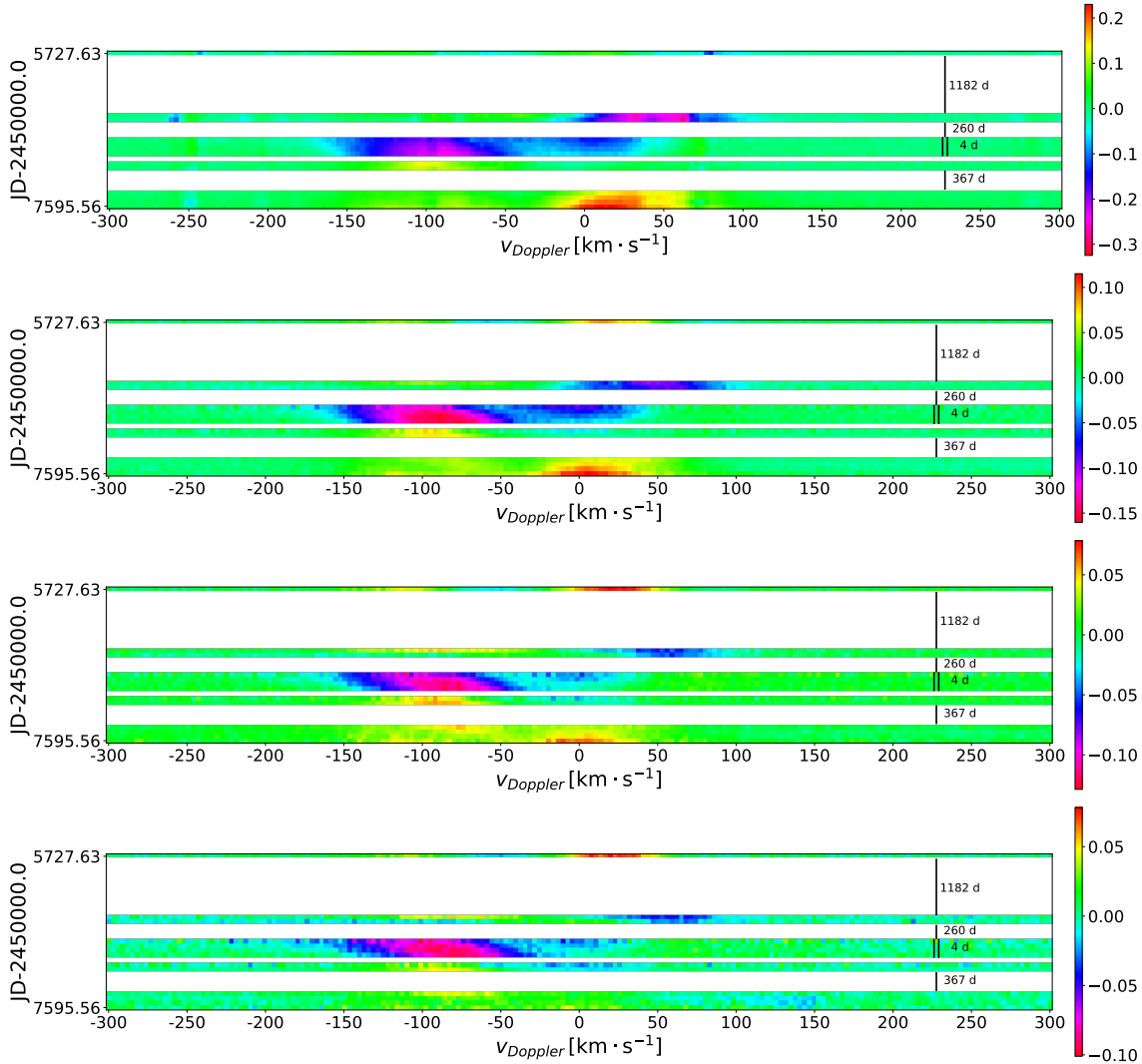


Figure 3.9: Dynamical spectrum of  $H\alpha$ ,  $H\beta$ ,  $H\gamma$ ,  $H\delta$  line, from top to bottom respectively, for HD 199478.

The first ever detected HVA event for HD199478 was observed by Markova et al. (2008) during a simultaneous spectroscopic and photometric campaign conducted between 1999 and 2000. HD199478 experienced an extraordinary event in 2000, spanning over 60 days. The line profile of  $H\alpha$  during this event resembled that shown in Fig. 3.5 in red color. Measures of this event (in 2000) are listed in the Tab. 3.6. Additionally, the authors noted that the star was approximately one magnitude fainter at the onset of the event compared to the moment of maximum absorption in the  $H\alpha$  line.

HD 199478 has experienced several peculiar HVA events since its initial detection.

At least one such event was detected by Richardson et al. (2011) during observations conducted at the Ritter Observatory between 2000 and 2006. However, the authors did not provide any supporting data regarding the event or the number of detection.

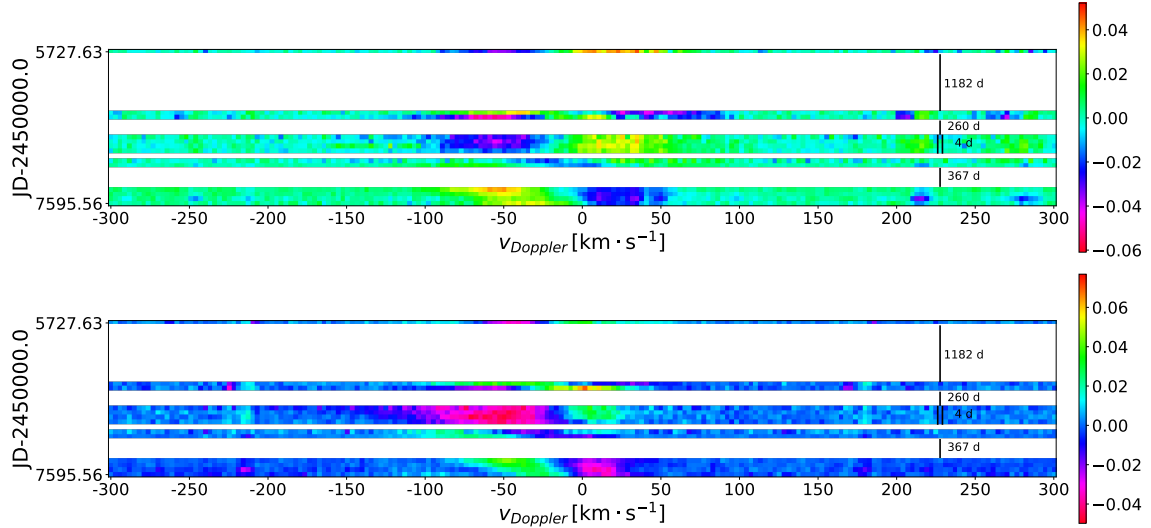


Figure 3.10: Dynamical spectrum of He I  $\lambda 5876$  and Si II  $\lambda 6347$  line, from top to bottom respectively, for HD 199478.

The most recent published HVA event for HD 199478 is reported by Ismailov and Ismayilova (2019). They observed an HVA event in 2011 and conclude about it as the strongest ever detected HVA event (not only for HD 199478, but among all SGs which have been recognised to show HVA events). This particular event differed from the typical  $H\alpha$  line profile observed during HVA events (for more details see Tab. 3.6). Instead of the profile recognized by Markova et al. (2008), it consisted of emission centered at zero velocity and blue-shifted absorption, similar to a P Cygni profile. Over a period of approximately 13 days, the blue-shifted absorption increased in depth, reaching its maximum around 8 days after initiation before decreasing again. This behavior remained consistent across all HVA events observed.

Before the onset of the event and just after, the  $H\alpha$  line was found in emission, with noticeable variations in its strength and shape. Additionally, Ismailov and Ismayilova (2019) reported on an HVA event traceable in the  $H\beta$  line. It's important to note that the behavior of the  $H\beta$  line during the 2011 event differed from that analyzed in this thesis during the 2015 event. While in Fig. 3.8, the double-peaked absorption appear in both peaks with comparable strength, in the 2011 event (Ismailov and Ismayilova, 2019) only blue-shifted minor absorption component was found (similar to what is seen in Fig. 3.21 for Rigel's  $H\beta$  line during HVA event).

In addition to the 2011 HVA event, Ismailov and Ismayilova (2019) also mentioned a feature similar to the HVA phenomenon, which manifested as double-peaked emission with a blue-shifted component. This kind of event was detected in 2013, with a blue-shifted velocity of around  $-72 \text{ km s}^{-1}$ , and a separation of approximately  $110 \text{ km s}^{-1}$  between the two peaks. However, the authors did not provide detailed information about this event.

Table 3.6: Characteristics of HVA event recorded for HD 199478.

	Markova et al. (2008)	Ismailov and Ismayilova (2019)
JD	2451827 – 2451877	2455764 – 2455776
Dates	Oct 9. - Nov 28. 2000	Jul 21. - Aug 2. 2011
$v_{blue\ core}$ [km s <sup>-1</sup> ]	-130	-300
$v_{blue\ edge}$ [km s <sup>-1</sup> ]	≈ -250	-510
Depth*	0.51	≈ 0.81
Duration of event [d]	50 < $t$ < 60	13 < $t$ < 27

\* Depth (in continuum lvl) of blue-shifted absorption component.

### 3.5 HD 96919 and HD 91619

The observations of HD 96919 from four different nights revealed three distinct H $\alpha$  line profiles: inverse P Cygni, asymmetric emission, and double-peaked profiles, as illustrated in Fig. 3.11. Similarly, observations of HD 91619 from three different nights showed H $\alpha$  line profiles including inverse P Cygni, P Cygni, and double-peaked profiles (see Fig. 3.12). Although no signature of HVA events was found for either star in our study, HVA events are discussed in the work by Kaufer et al. (1996a). The parameters of these events for HD 96919 are listed in Tab. 3.7, and for HD91619 in Tab. 3.8.

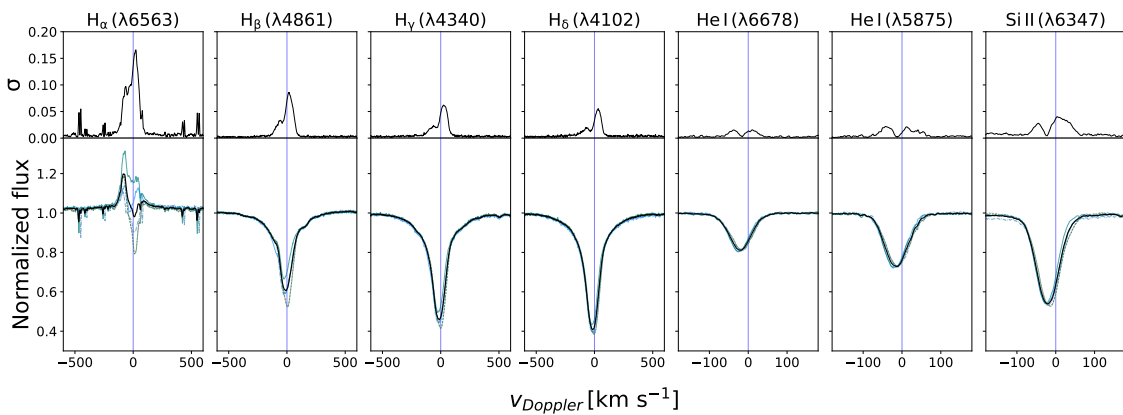


Figure 3.11: The Temporal Variance Spectrum (TVS) of HD 96919 focusing on seven selected spectral lines. Bottom panels: the black line represents the averaged spectrum, while selected composite spectra are illustrated in different colors. Top panels: the deviation from the average spectra, providing insights into the general variability observed in each line.

Table 3.7: Characteristics of HVA events recorded for HD 96919.

	Kaufer et al. (1996b)	Kaufer et al. (1996b)
JD	2449466	2449750 – 2449840
Dates	Apr 23. 1994	Feb 1. - May 2. 1995
$v_{blue\ core}$ [km s <sup>-1</sup> ]	-98	-108
$v_{blue\ edge}$ [km s <sup>-1</sup> ]	≈ -210	-160
Depth*	0.78	0.30
Duration of event [d]	–	< 90

\* Depth (in continuum lvl) of blue-shifted absorption component.

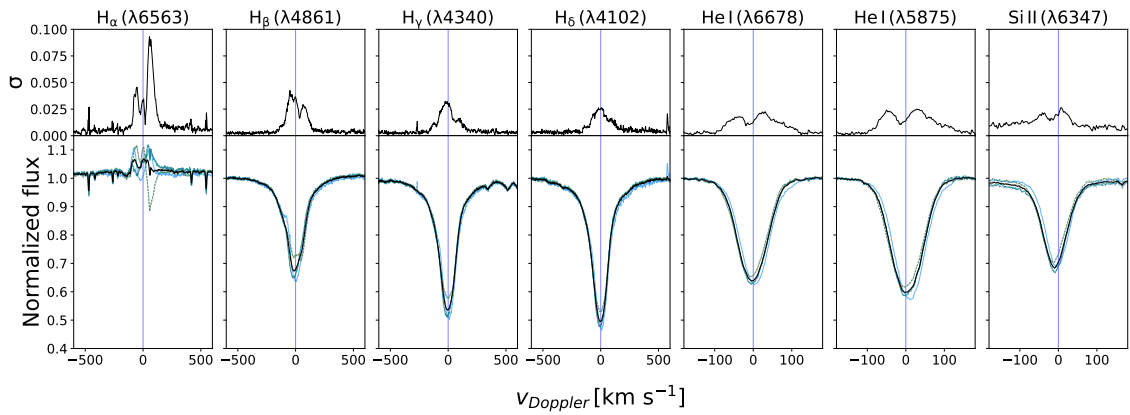


Figure 3.12: The Temporal Variance Spectrum (TVS) of HD 91619 focusing on seven selected spectral lines. Bottom panels: the black line represents the averaged spectrum, while selected composite spectra are illustrated in different colors. Top panels: the deviation from the average spectra, providing insights into the general variability observed in each line.

Table 3.8: Characteristics of HVA event recorded for HD 91619.

	Kaufer et al. (1996a)
JD	2449410 – 2449418
Dates	Feb 26. - Mar 6. 1994
$v_{blue\ core}$ [km s <sup>-1</sup> ]	≈ -130
$v_{blue\ edge}$ [km s <sup>-1</sup> ]	-200
Depth*	≈ 0.90
Duration of event [d]	> 8

\* Depth (in continuum lvl) of blue-shifted absorption component.

### 3.6 HD 207260 and HD 223960

For each of these two stars only three spectra were accessible from the IACOB database. As evident from Fig. 3.13 and Fig. 3.14, the signal-to-noise (S/N) ratio is

low, and both datasets consist of only two spectra. The last spectrum for each star, characterized by the lowest S/N ratio, was consequently excluded from the analysis due to the loss of most lines in the noisy continuum.

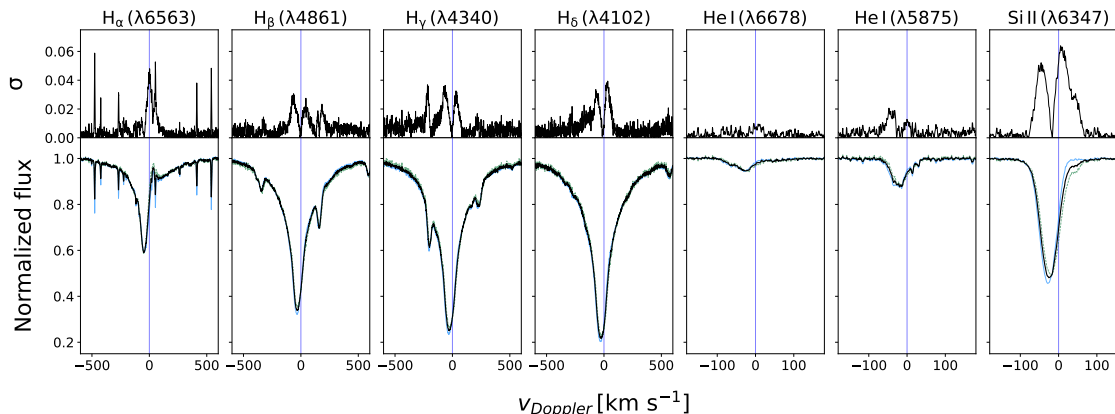


Figure 3.13: The Temporal Variance Spectrum (TVS) of HD 207260 focusing on seven selected spectral lines. Bottom panels: the black line represents the averaged spectrum, while selected composite spectra are illustrated in different colors. Top panels: the deviation from the average spectra, providing insights into the general variability observed in each line.

The spectrum of HD 207260 is in the range from 3900 Å up to 6800 Å similar to Deneb’s spectra, with only exceptions being interstellar (DIB and NaID) and water-vapour lines. In both spectra of HD 207260 analyzed in this study, no signs of HVA events were found, nor any peculiarities or features significantly deviating from what is seen in the spectra of Deneb. In both spectra of HD 207260 analyzed in this study, there are no evidences of HVA events. Although spectra were obtained with an interval in 9 years, we do not see variability in the H $\alpha$ .

Table 3.9: Characteristics of HVA event recorded for HD 207260.

	Shultz et al. (2014)	Shultz et al. (2014)
JD	2455402	2456197 – 2456201
Dates	Jul 24. 2010	Sep 27. - Oct 1. 2012
$v_{blue\ core}$ [km s $^{-1}$ ]	$\approx -130$	$\approx -100$
$v_{blue\ edge}$ [km s $^{-1}$ ]	$\approx -250$	$\approx -250$
Depth*	$\approx 0.77$	$\approx 0.68$
Duration of event [d]	–	> 4

\* Depth (in continuum lvl) of blue-shifted absorption component.

However, H $\alpha$  exhibits dramatic changes, as documented by Shultz et al. (2014), who were the first to observe HD 207260 during an HVA event. Their analysis revealed the presence of two events: one in 2010 (based on one snapshot) and the second one in 2012 (based on two snapshots). While HVA H $\alpha$  line profiles are typically observed in absorption with an additional blue-shifted component, during both



events, a P Cygni profile was present. Unfortunately, their paper does not provide data for other spectral lines, so it remains speculative whether the imprint of the event could be seen in wind-sensitive lines, since  $H\alpha$  shows stellar wind feature.

In contrast to HD 207260 the difference is seen in spectra of HD 223960 obtained on October 30 and December 17, 2013 (Fig. 3.14). Usually HD 223960 exhibits  $H\alpha$  line in emission, as described in the study by Fischer and Morrison (2001) and spectrum from December 17, 2013 is consistent with it. While in spectrum from October 30,  $H\alpha$  manifests complex absorption profile (Fig. 3.15). Unfortunately, available to us data are not enough to any speculation about HVA events. Even if the spectrum from October is taken during a potential HVA event, the lack of imprint in higher Balmer lines suggests that there is no peculiar event occurring. Moreover, HD 223960 has the highest radial velocity among the objects under study, around  $-49 \text{ km s}^{-1}$ , which is clearly visible in Fig. 3.14 as a substantial Doppler shift in all the lines.

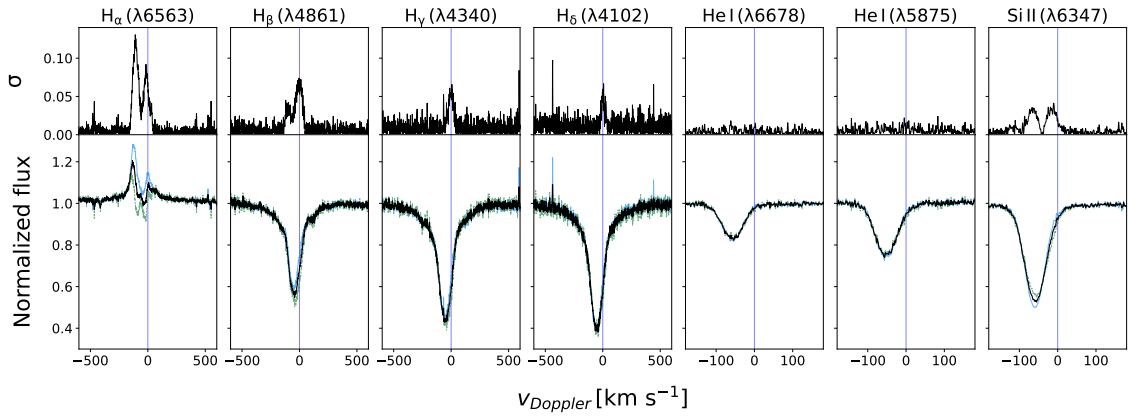


Figure 3.14: The Temporal Variance Spectrum (TVS) of HD 223960 focusing on seven selected spectral lines. Bottom panels: the black line represents the averaged spectrum, while selected composite spectra are illustrated in different colors. Top panels: the deviation from the average spectra, providing insights into the general variability observed in each line.

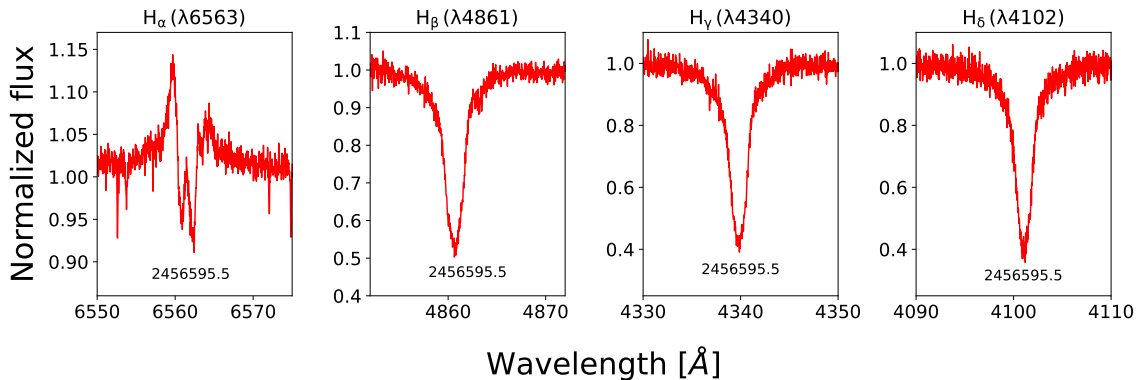


Figure 3.15: Line profiles of Balmer lines ( $H\alpha$ ,  $H\beta$ ,  $H\gamma$ ,  $H\delta$ ) during suspicious event for HD 223960.

Table 3.10: The date of the suspicious event recorded for HD 223960.

	This study
JD	2456595
Dates	Oct 30. 2013
$v_{blue\ core}$ [km s <sup>-1</sup> ]	-91
$v_{blue\ edge}$ [km s <sup>-1</sup> ]	≈ -500
Depth*	0.95

\* Depth (in continuum lvl) of blue-shifted absorption component.

### 3.7 HD 21291

The spectrum of HD 21291 corresponds to its spectral type B9 Ia. Variability in line profiles is detected only for few lines including H $\alpha$ , He I ( $\lambda$ 5875,  $\lambda$ 6678), and Si II ( $\lambda$ 6347,  $\lambda$ 6371) (Fig. 3.16).

The H $\alpha$  line profile generally remains stable on a time scale of several days, with exceptions during HVA events when the profile can change from day to day. The frequency of appearance for all observed H $\alpha$  line profiles can be seen in Fig. 3.17.

The first-ever observation of HVA event for HD 21291 was performed at the Ritter Observatory. However, only mention about HD 21291 showing peculiar events may be found in Richardson et al. (2011). The authors listed supergiants for which spectral time series were acquired at the Ritter Observatory, and noted the presence of one or more HVA events for some of these stars. Unfortunately, no data regarding the event for HD 21291 were provided in the publication.

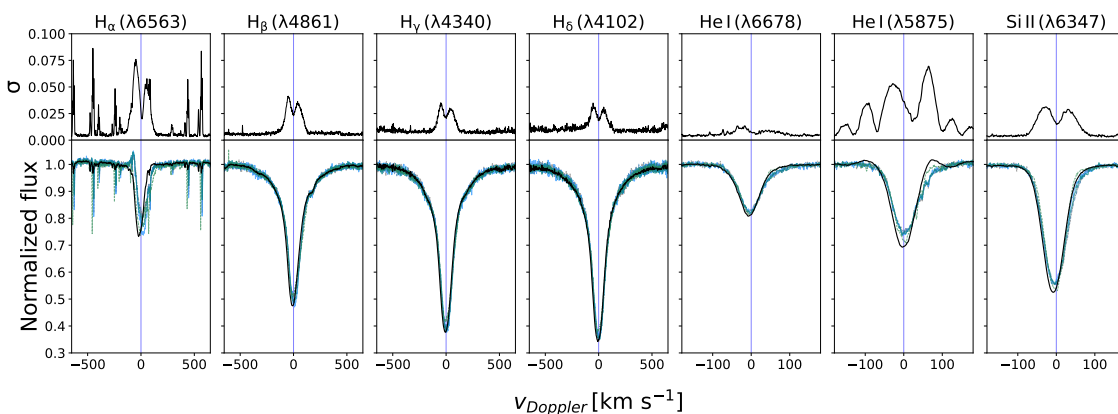


Figure 3.16: The Temporal Variance Spectrum (TVS) of HD 21291 focusing on seven selected spectral lines. Bottom panels: the black line represents the averaged spectrum, while selected composite spectra are illustrated in different colors. Top panels: the deviation from the average spectra, providing insights into the general variability observed in each line. Contains only data from Fies and Hermes (2011-2016).

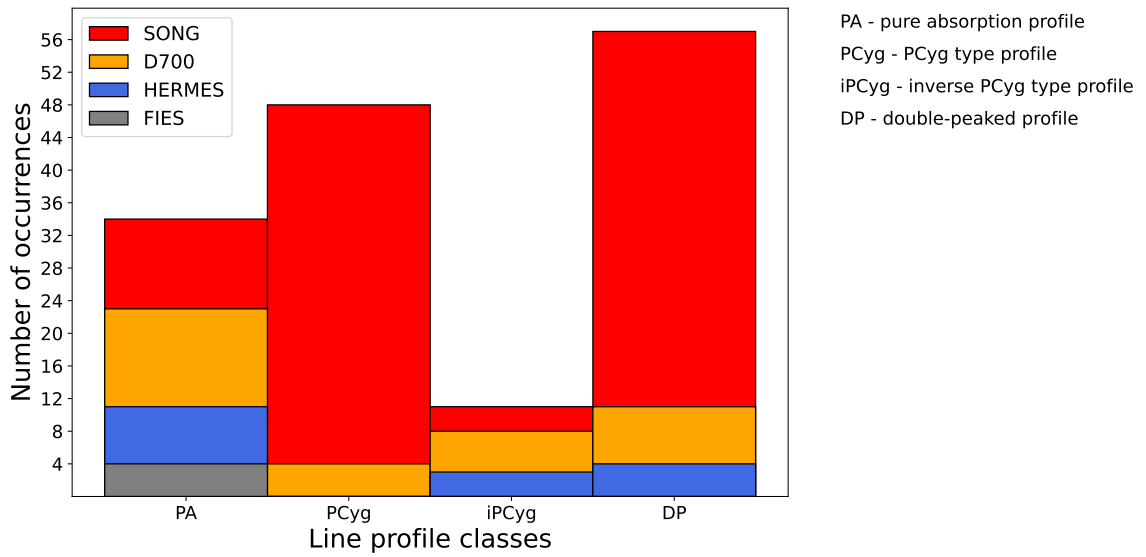


Figure 3.17:  $H\alpha$  line profile morphology histogram for HD 21291. Only one profile per night is accounted for.

The analysis of D700, FIES, and Hermes spectra did not reveal the presence of an HVA event for HD 21291. However, SONG data allowed to trace final part of an HVA event in September/October 2016. In the SONG time-series, the event ended on October 7th, 2016, and after 11-days interval, the time-series continued with HERMES data where the event disappeared. It is important to note that there was no significant blue-shift (around  $-10 \text{ km s}^{-1}$ ) in the  $H\alpha$  line core, so the blue region in the second section of Fig. 3.18 represents the blue wing line asymmetry, which remained even after the measurable signatures of the event disappeared. Hence, it is assumed that the duration of the event was more than 8 days.

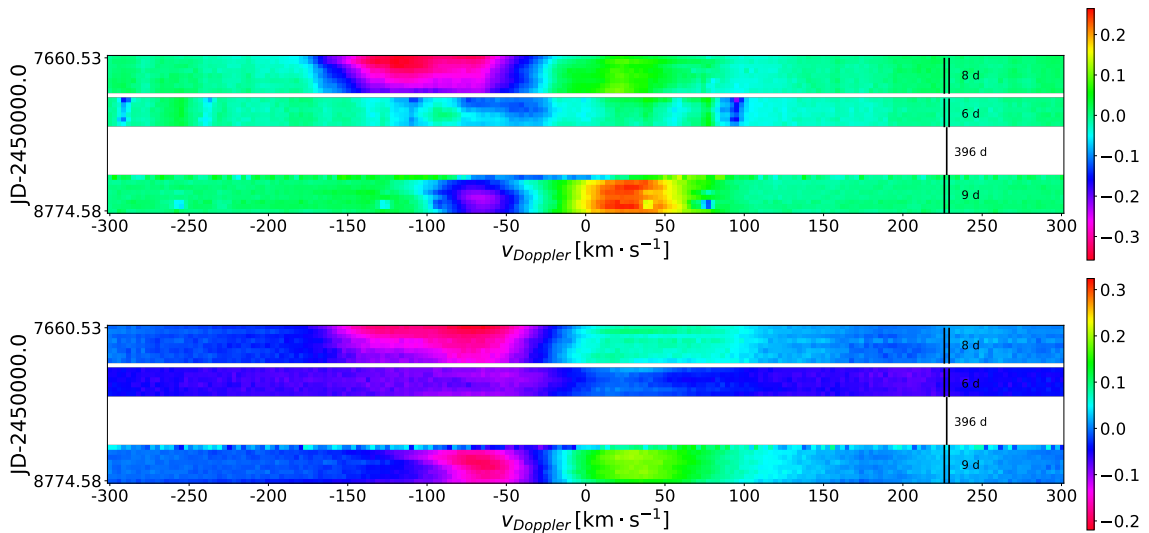


Figure 3.18: Dynamical spectrum of  $H\alpha$ , and  $H\beta$  line, from top to bottom respectively, for HD 21291 combined from SONG (first and third color section) and HERMES (second color section) spectra.

The detailed view on the line profiles from the 2016 event is presented in Fig. 3.19, and the measures of H $\alpha$  line are listed in Tab. 3.11. Unfortunately, the higher Balmer lines, except for H $\beta$ , are not covered by the SONG spectra, so the event cannot be traced in these lines.

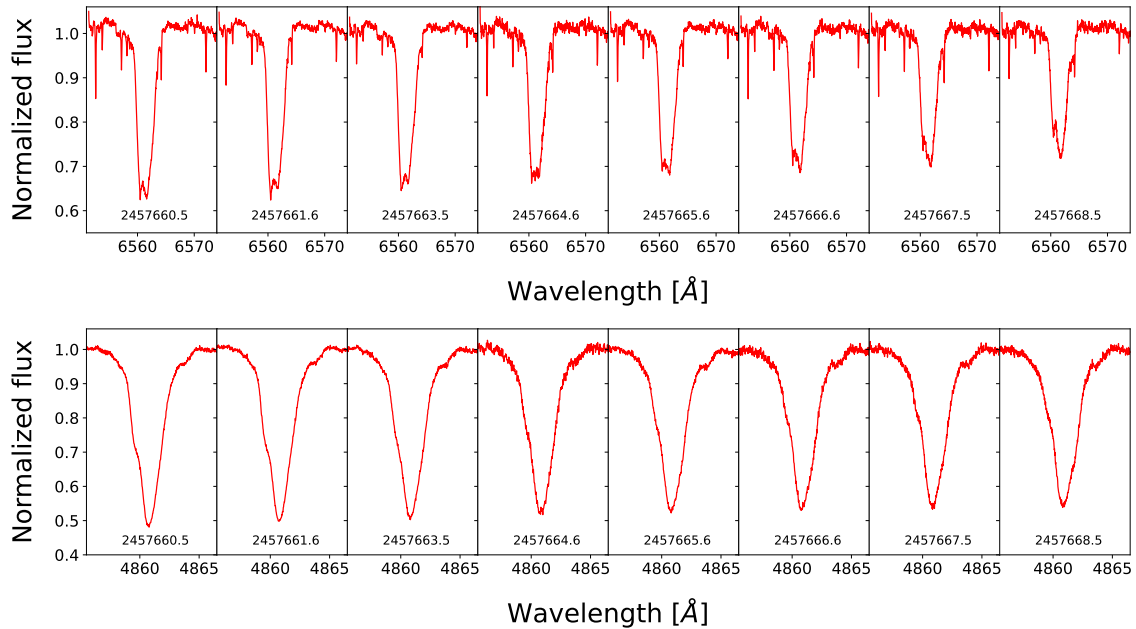


Figure 3.19: H $\alpha$  (upper panels) and H $\beta$  line profiles of HD 21291 taken during HVA event in September/October 2016.

Table 3.11: Estimated velocities and intensities of H $\alpha$  during HVA event recorded for HD 21291 in September/October 2016.

JD	max. depth [cont. lvl]	Velocity [km s <sup>-1</sup> ]	
		blue-edge	blue-shifted core
2457660.5	0.62	-305.4	-103.2
2457661.6	0.62	-304.8	-103.7
2457663.5	0.64	-303.6	-102.6
2457664.6	0.66	-368.6	-103.5
2457665.6	0.69	-359.8	-102.4
2457666.6	0.70	-361.8	-102.2
2457667.5	0.73	-354.3	-102.3
2457668.5	0.76	-358.7	-102.4

### 3.8 HD 34085 (Rigel)

At the outset of studying HVA events (Kaufer et al., 1996a; Kaufer et al., 1996b), only three supergiants, including Rigel, contributed to initiating the “hunt” for this

phenomenon.

The first identified HVA events for Rigel can be found in the study by Kaufer et al. (1996b). In particular, two events were identified, one strong in 1993 and the second weak just several months later in 1994, suggesting that such structures may persist across the star's rotational period ( $P_{\text{rot}} = 93$  days). However, no suspected behavior was observed in 1995, leading to the assumption that events occur sporadically. The measurements for both events are listed in Tab. 3.12. During 1994 event the blue-edge velocity of  $-278 \text{ km s}^{-1}$  even exceeded the wind terminal velocity (see Tab. 2.2). In both cases (events in 1993 and 1994) the event was also identified in higher Balmer lines, but as the authors emphasize, it was blended with photospheric lines. The 1993 event was simultaneously analyzed by Israelian et al. (1997), who found its maximum a day before Kaufer et al. (1996b). Israelian et al. (1997) especially highlighted the appearance of a red-shifted emission peak, which was found around  $200 \text{ km s}^{-1}$  and is assumed not to be related to extended emission wings (see Chapter 3.10). The

Table 3.12: Characteristics of HVA events recorded for  $\beta$  Ori.

	Kaufer et al. (1996b) Israelian et al. (1997)	Kaufer et al. (1996b)
JD	2449294 – 2449316	2449403.5
Date	Nov 2.-24. 1993	Feb 11. - 23. 1994
$v_{\text{blue core}}$ [ $\text{km s}^{-1}$ ]	-115	-139
$v_{\text{blue edge}}$ [ $\text{km s}^{-1}$ ]	-238	-278
Depth*	0.54	0.80
Duration of event [d]	> 22	40
	Morrison et al. (2008) Chesneau et al. (2014)	Shultz et al. (2014)
JD	2454038 – 2454046	2455167 – 2455177
Date	Oct 29. - Nov 6. 2006	Dec 1. - 11. 2009
$v_{\text{blue core}}$ [ $\text{km s}^{-1}$ ]	-200	$\approx -110$
$v_{\text{blue edge}}$ [ $\text{km s}^{-1}$ ]	-390	$\approx -160$
Depth*	$\approx 0.77$	$\approx 0.95$
Duration of event [d]	> 8	> 10
	Chesneau et al. (2014) Kaufer et al. (2012) Shultz et al. (2014)	
JD	2455240 – 24552865	
Date	Feb 12. - Mar 9. 2010	
$v_{\text{blue core}}$ [ $\text{km s}^{-1}$ ]	$\approx -160$	
$v_{\text{blue edge}}$ [ $\text{km s}^{-1}$ ]	-200	
Depth*	$\approx 0.85$	
Duration of event [d]	> 25	

\* Depth (in continuum lvl) of blue-shifted absorption component.

study by Morrison et al. (2008) also reports observing an HVA event. Besides several

weak events, one strong event in 2006 was identified with comparable properties to the one reported by Israelian et al. (1997). As previously mentioned in Kaufer et al. (1996a), the  $H\alpha$  line tended to be found in an inverse P Cygni shape just before and after the events. The same was observed by Morrison et al. (2008), who found that the  $H\alpha$  line exhibited an inverse P Cygni shape after the event, and by Shultz et al. (2014), who, on the other hand, reported that a weak HVA event observed in 2009 was also preceded by an inverse P Cygni profile.

Within this study the largest sample of spectra was obtained and analyzed for Rigel. However, as mentioned in the Section 3.1.1, the sample contains heterogeneous data obtained with different instruments. Due to this some interesting lines were not always covered by spectral range. Additionally, in some spectra, certain lines were included but found at the edge of the aperture, making their extraction impossible. Therefore, most recorded events are only shown in the  $H\alpha$  line.

Indeed, Rigel stands out as the supergiant with the most recorded HVA events, not only within the scope of this thesis but also in general among studies that discuss the appearance of extraordinary events (e.g. Kaufer et al. (1996a), Morrison et al. (2008), Israelian et al. (1997), and Chesneau et al. (2014)). The large amount of recorded events can be attributed to Rigel's status as one of the brightest supergiants, making it a prime and easily observable target. Consequently, regular observations contribute to the detection of numerous events associated with Rigel.

The only HVA event that could be traced in higher Balmer lines occurred in February/March 2014. The corresponding residual dynamic spectra can be found in Fig. 3.22 for the  $H\alpha$ ,  $H\beta$ ,  $H\gamma$ ,  $H\delta$  line.

A clear delay is evident in these plots as the event propagates through the atmosphere, with the event first appearing in the bottom (in the  $H\delta$  line) and then observed at the very end in the most upper part (in the  $H\alpha$  line). While the most dramatic changes in profile are observed for the  $H\alpha$  line, in the higher Balmer lines, it only alters as blue-wing asymmetries.

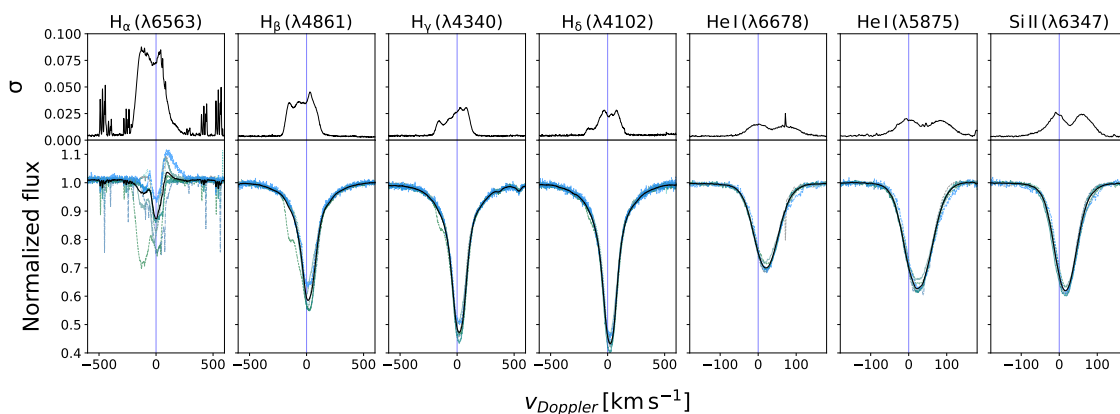


Figure 3.20: The Temporal Variance Spectrum (TVS) of HD 34085 focusing on seven selected spectral lines. *Bottom panels:* the black line represents the averaged spectrum, while selected composite spectra are illustrated in different colors. *Top panels:* the deviation from the average spectra, providing insights into the general variability observed in each line. Contains only data from Fies and Hermes (2011-2016).

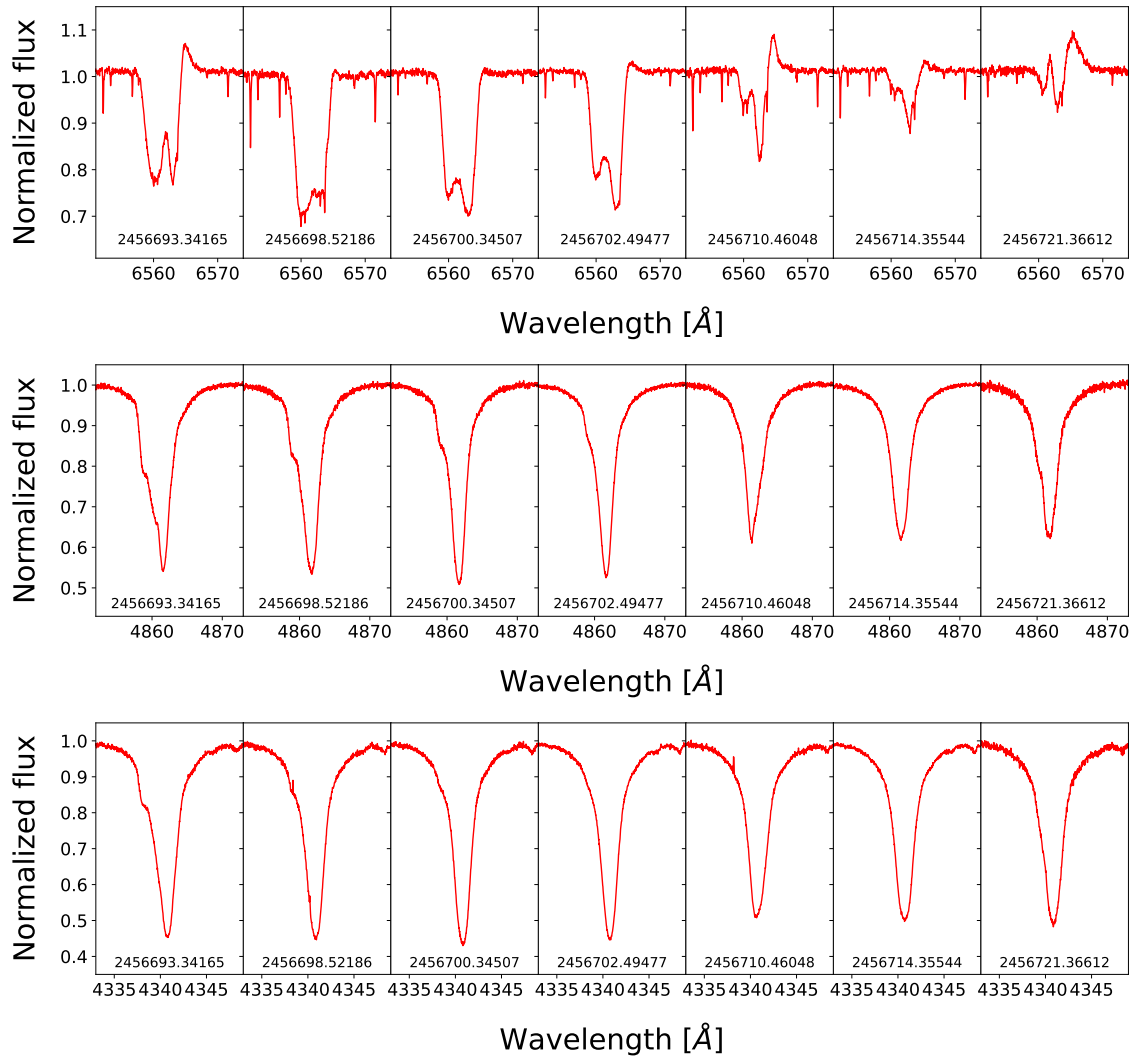


Figure 3.21: H $\alpha$  (*top*), H $\beta$  (*middle*), H $\gamma$  (*bottom*) line profiles of Rigel taken during HVA event in February/March 2014.

A detailed view of the time evolution of the line profiles of H $\alpha$ , H $\beta$  and H $\gamma$  can be seen in Fig. 3.21. Additionally from these plots, the delay in the appearance of the event's maximum is also clearly discernible. Particularly, the H $\alpha$  line profile captured at the maximum of the event (third panel in top row of Fig. 3.21) appears to exhibit the same shape as observed by Kaufer et al. (1996b), Israelian et al. (1997), Rother (2009), and Morrison et al. (2008).

Moreover, two selected photospheric lines were also examined (see lower panels of Fig. 3.23) with the aim of finding the imprint of the event, similar to the case of HD 199478. However, no sign has been identified, thus we assume that the Rigel's photospheric lines remain untouched by the event.

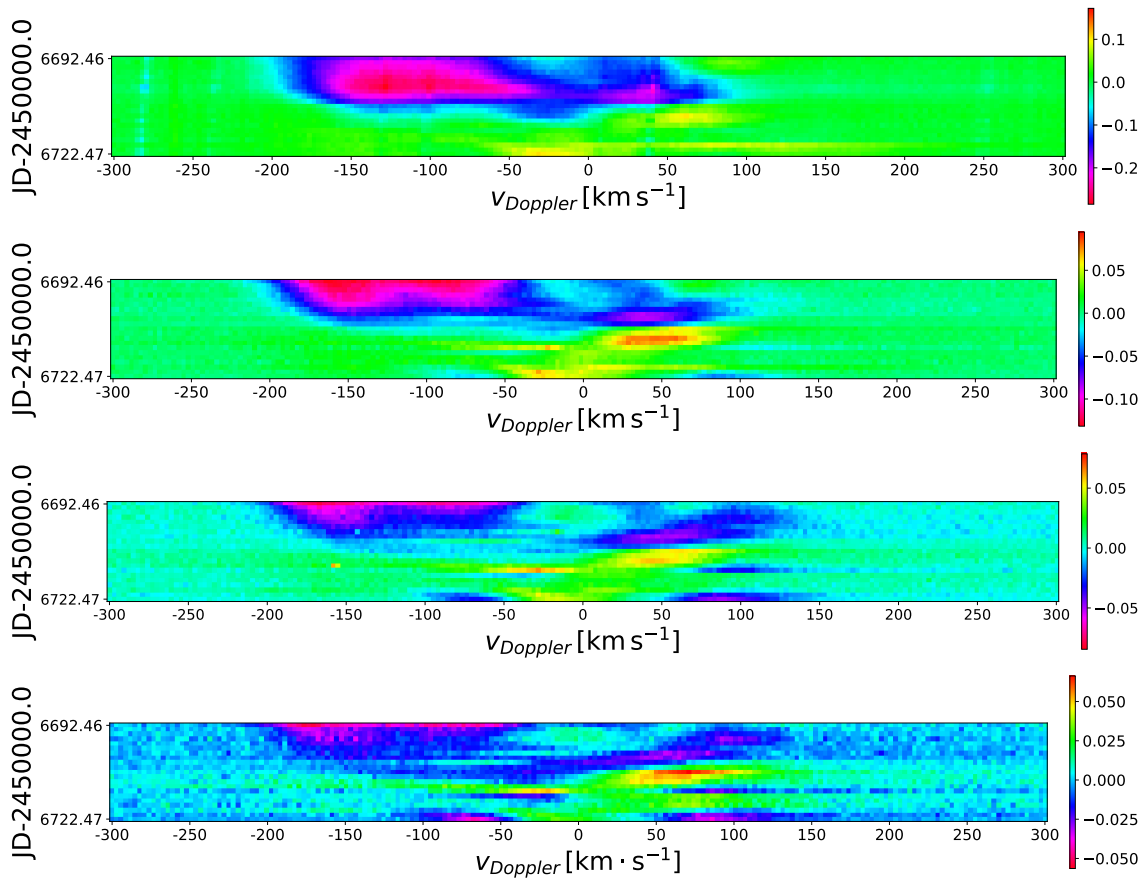


Figure 3.22: Dynamical spectrum of  $H\alpha$ ,  $H\beta$ ,  $H\gamma$ ,  $H\delta$  line, from top to bottom respectively, for Rigel taken during HVA event in January/March 2014.

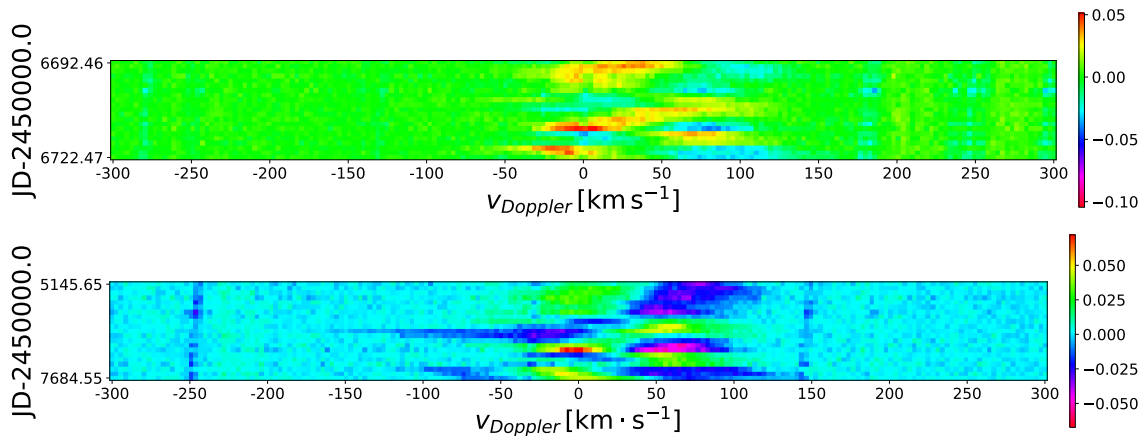


Figure 3.23: Dynamical spectrum of He I  $\lambda$  5876 (*top*) and Si II  $\lambda$  6347 (*bottom*) lines during HVA event in February/March 2014.

The analysis of the last obtained data set from the Fairborn Observatory completed the HVA event from 2014 in the  $H\alpha$  line. Fig. 3.24 presents entire event,



where the additional data revealed the presence of a weak event just a couple of days before the strong one appeared.

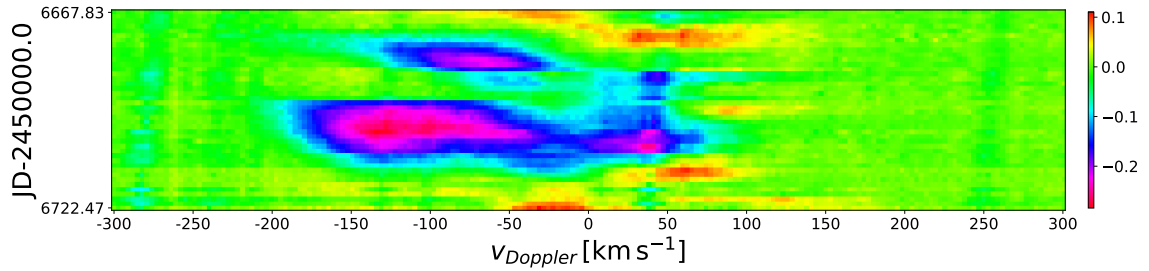


Figure 3.24: Dynamical spectrum of H $\alpha$  line during HVA event in January/March 2014.

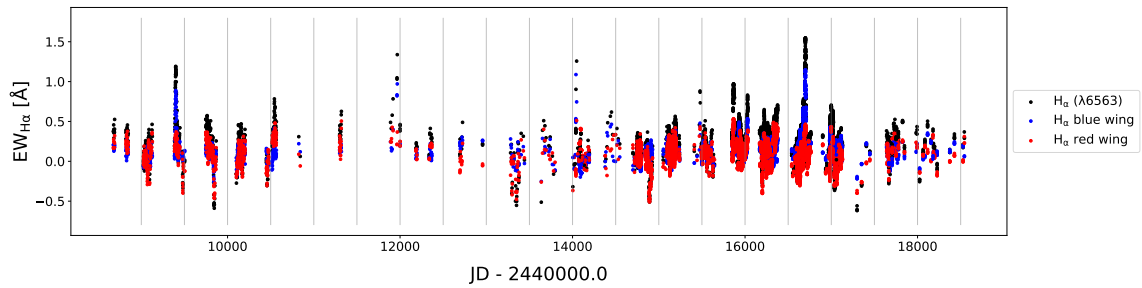


Figure 3.25: Equivalent widths of H $\alpha$  line measured across whole observational period from February 1992 to February 2019.

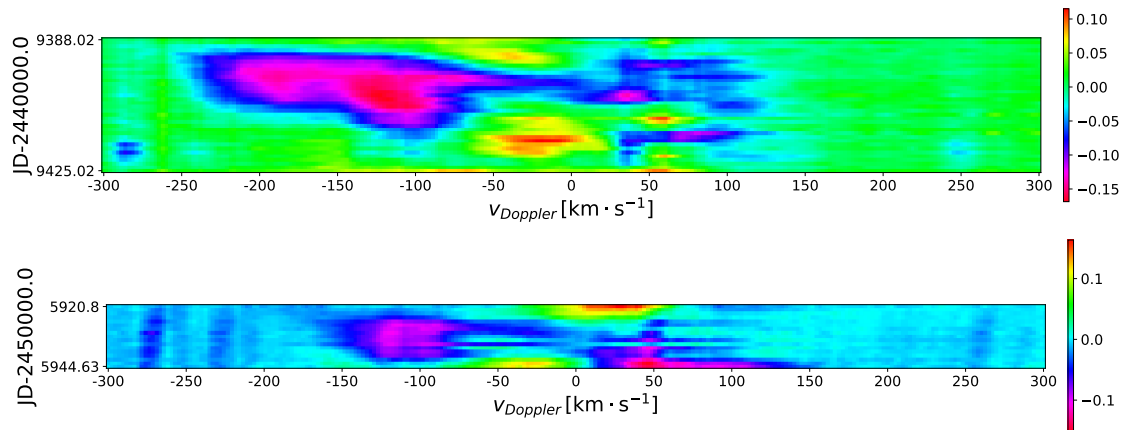


Figure 3.26: Dynamical spectra of H $\alpha$  line during HVA event in February/March 1994 (*top*) and December 2011/January 2012 (*bottom*).

The behavior of H $\alpha$  line was also traced via equivalent widths. The measurements across a whole observational period are shown in Fig. 3.25 with a detailed view on Fig. 3.27 - 3.29. As the strength of profile increase while the event evolves towards its

maximum and decrease when going back to normal, HVA events are also identified as peaks mainly in blue part of the line exceeding  $1.0 \text{ \AA}$  in EW. Additionally, oscillations in EW with the period of  $\approx 11$  years may be clearly identified from Fig. 3.25.

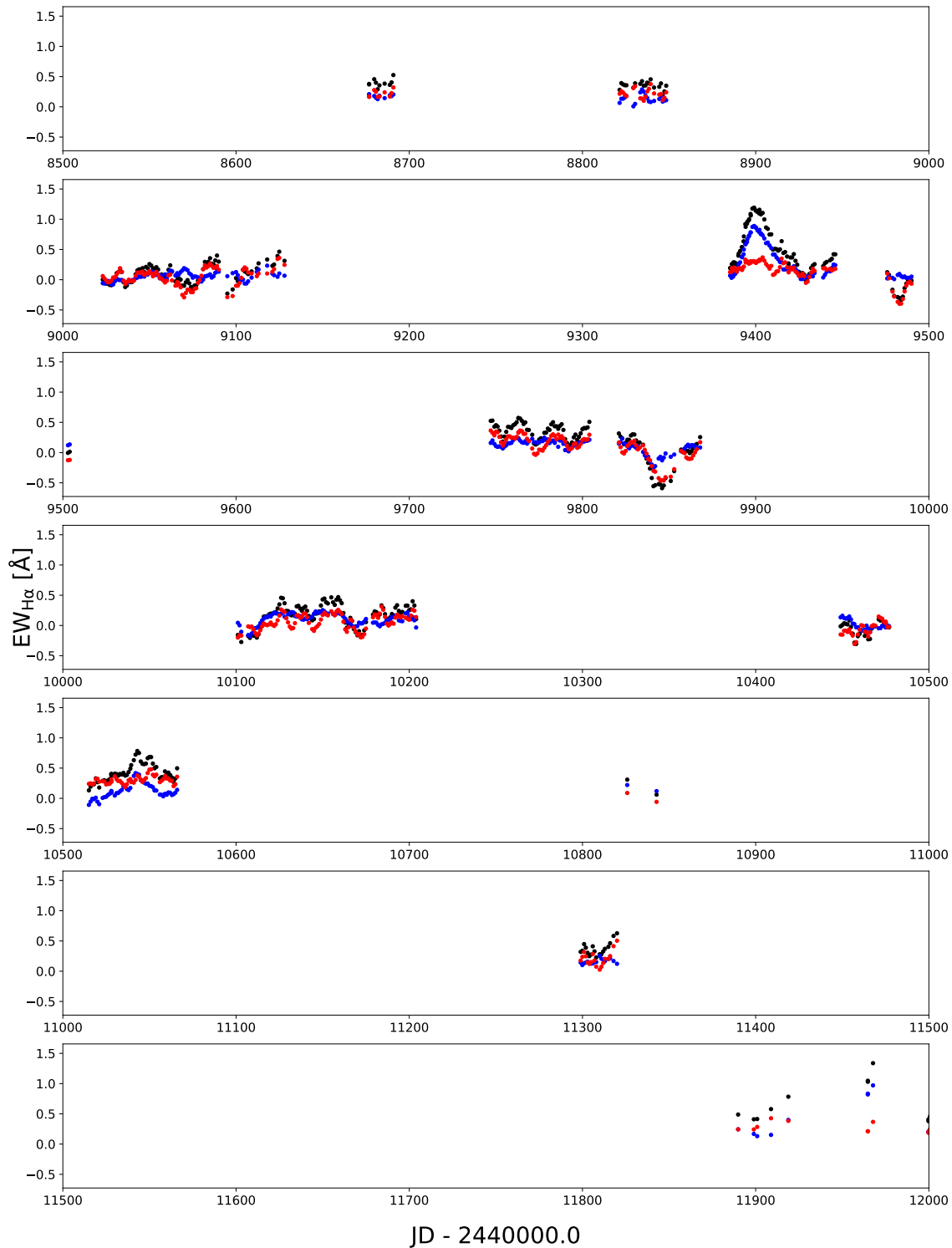


Figure 3.27: Zoomed part of Fig. 3.25.

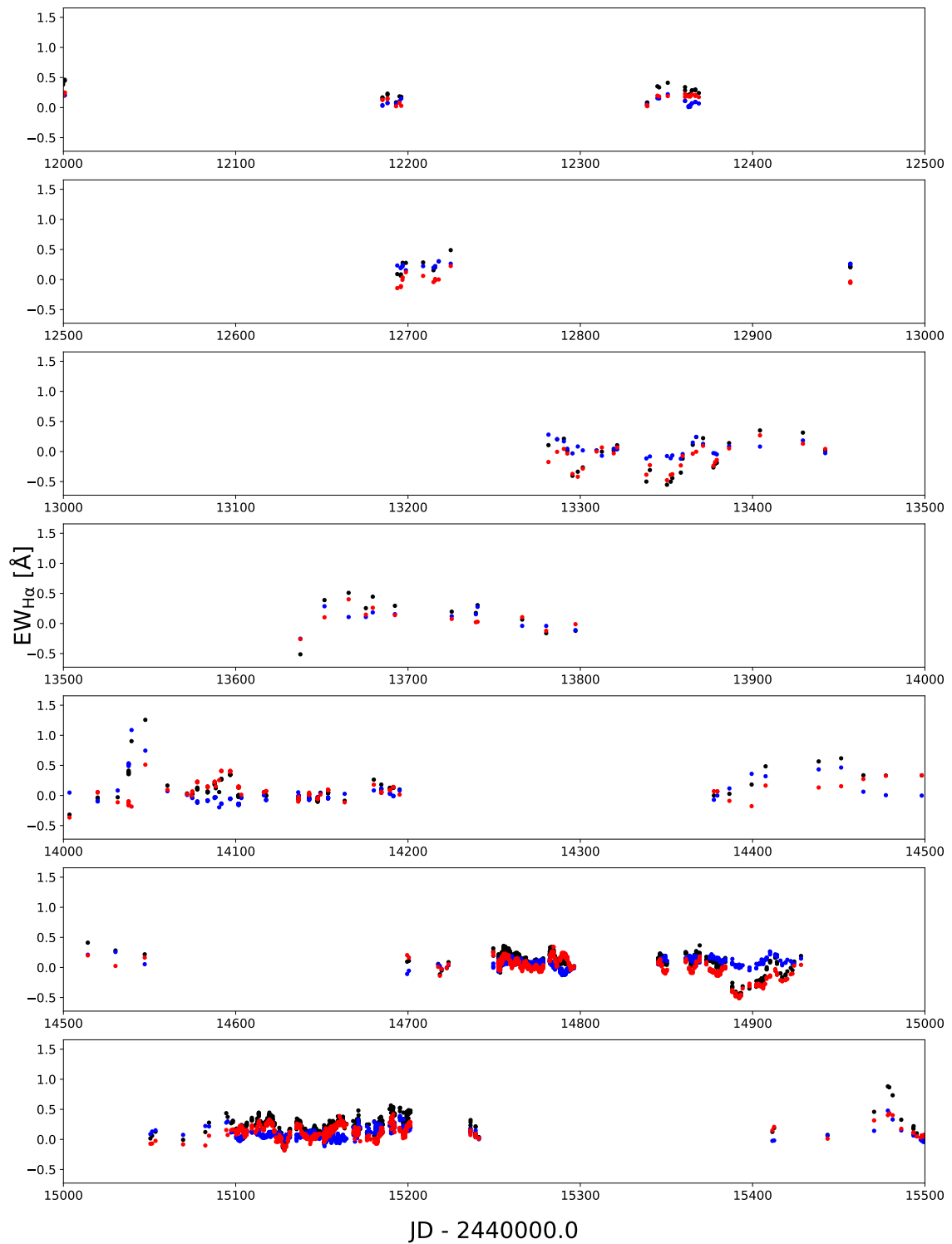


Figure 3.28: Zoomed part of Fig. 3.25.

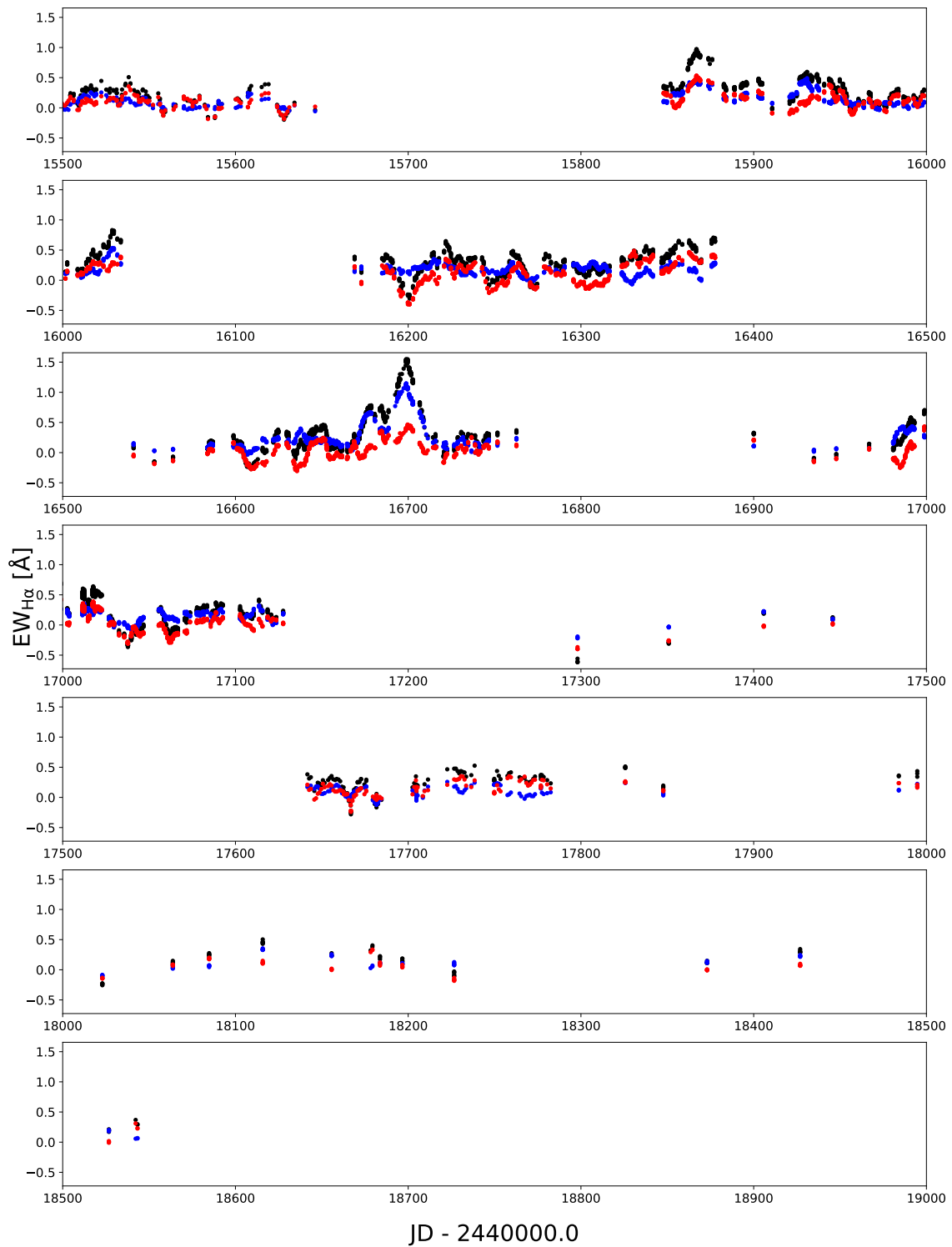


Figure 3.29: Zoomed part of Fig. 3.25.

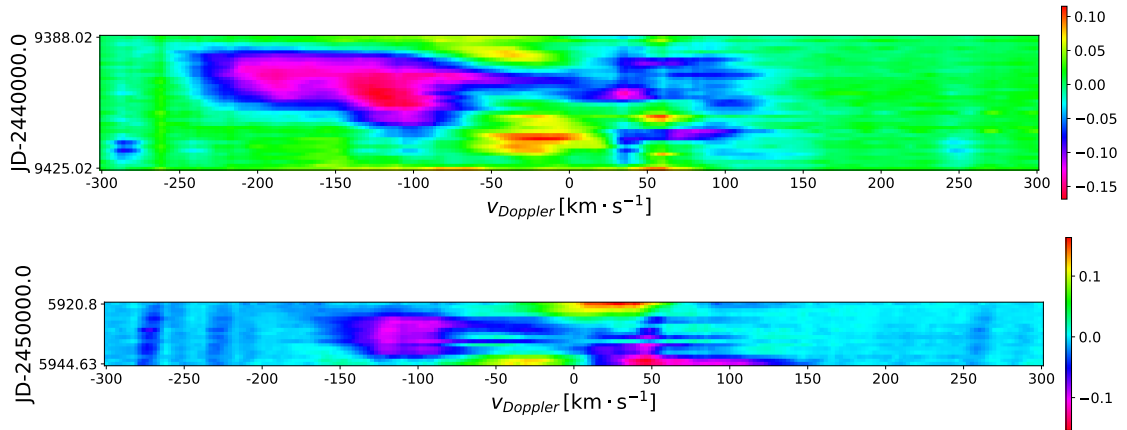


Figure 3.30: Dynamical spectra of H $\alpha$  line during HVA event in February/March 1994 (*top*) and December 2011/January 2012 (*bottom*).

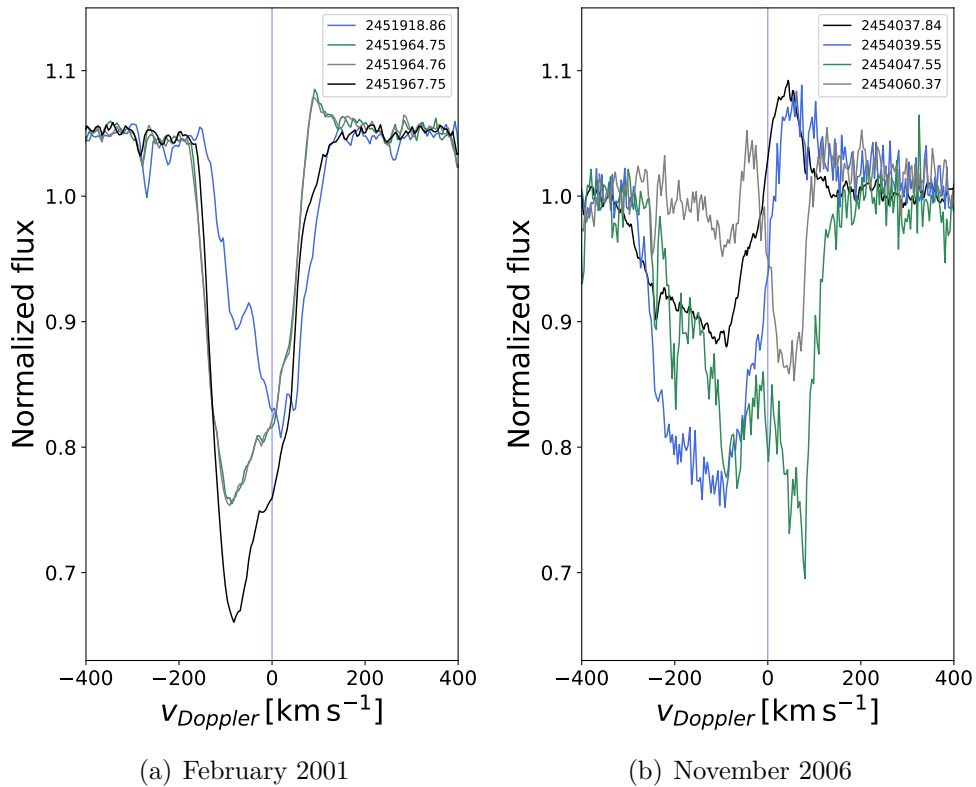


Figure 3.31: H $\alpha$  line profiles were taken during HVA events of 2001 (*left*) and 2006 years.

Based on the frequency of HVA event occurrence, it is reasonable to assume that the HVA event in 1994 (top panel of Fig. 3.30) is the same event previously identified by Kaufer et al. (1996a) and Israelian et al. (1997). While the 2006 event (right panel of Fig. 3.31), it may be considered a small fraction of the event previously analyzed

by Morrison et al. (2008) and Chesneau et al. (2014), with the measurements of both listed in Tab. 3.12.

As seen from bottom panel of Fig. 3.30 the HVA event in 2011-2012 was weak. At the onset of the event  $H\alpha$  was found in a P Cygni shape, while the event was enclosed by an inverse P Cygni profile with the absorption component stronger than the one observed during the preceding HVA event.

### 3.9 HD 197345 (Deneb)

Based on the previously published results by Richardson et al. (2011) regarding the events observed in Deneb's spectra, it appears that Deneb sets the lower limit for the temperature of objects that could potentially exhibit HVA events. This assertion is primarily derived from the rarity of events observed in Deneb compared to other supergiants. Despite Deneb being considered rare in terms of these events, the analysis revealed the presence of HVA events. One event was identified in two snapshots taken within a single observational night by FIES (see the top two lines in Tab. 3.13) in September 2010, and the second event with a duration of more than 105 days was detected in a six-year campaign from 2017 to 2023 using D700 with its measures listed in Tab. 3.13.

The majority of spectral data for Deneb were acquired using the D700 spectrograph, with only two observational nights available from the IACOB database. Conversely, the Temporal Variability Spectrum (TVS) composed of IACOB spectra can be seen in Fig. 3.32.

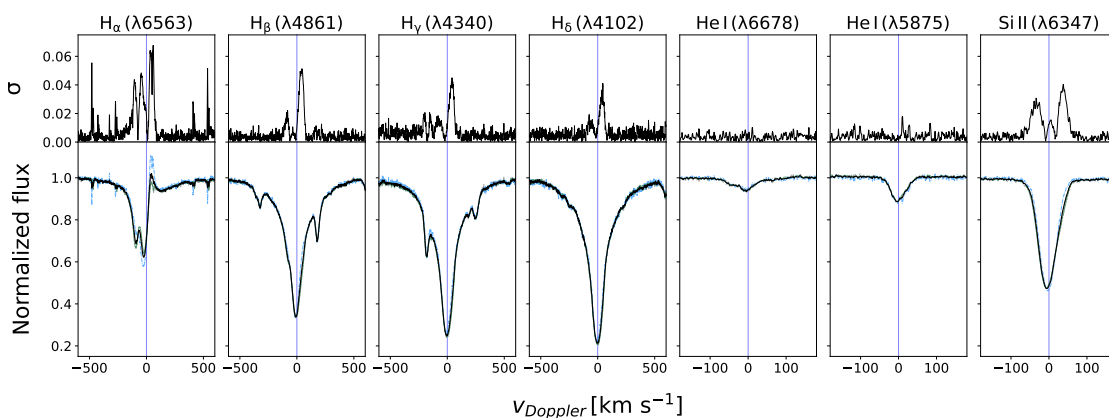


Figure 3.32: The Temporal Variance Spectrum (TVS) of HD 197345 focusing on seven selected spectral lines. *Bottom panels:* the black line represents the averaged spectrum, while the composite spectra are illustrated in different colors. *Top panels:* the deviation from the average spectra, providing insights into the general variability observed in each line.

Table 3.13: Estimated velocities and intensities of H $\alpha$  during HVA event recorded for HD 197345 in September 2010 and June-October 2020.

JD	max. depth [cont. lvl]	Velocity [km s <sup>-1</sup> ]	
		blue-edge	blue-shifted core
2455449.3	0.66	-559.9	-90.2
2455449.3	0.66	-523.0	-90.2
2459027.4	0.67	-276.9	-92.4
2459042.3	0.68	-279.0	-82.8
2459043.3	0.68	-298.0	-85.5
2459054.3	0.77	-296.3	-90.8
2459056.6	0.74	-308.0	-88.2
2459057.3	0.74	-307.2	-87.5
2459073.3	0.68	-287.9	-67.0
2459112.2	0.56	-303.2	-86.0
2459113.2	0.55	-312.1	-85.5
2459114.2	0.54	-313.2	-85.2
2459117.2	0.52	-306.3	-80.7
2459125.4	0.49	-303.4	-83.8
2459131.2	0.50	-317.0	-77.1
2459132.2	0.50	-335.0	-78.6
2459132.3	0.50	-322.1	-78.7
2459132.4	0.50	-301.5	-79.4

With the aim of tracing the event in photospheric lines, the equivalent widths (EWs) for H $\alpha$  and other lines (see Fig. 3.33) together with radial velocities were measured. In particular, the event can be observed in Fig. 3.33 at the right edge of the middle blue region where the EWs of H $\alpha$  exceed 1.5 Å, suggesting that the event was still evolving towards its maximum.

A slight imprint of the event is seen in the EWs of the Si II lines (middle panel of Fig. 3.33, both in green color), but no sign of an extreme event was identified in the radial velocities.

Regarding the EWs in Fig. 3.33, it is important to note that in about one-half of the spectra, the Fe II  $\lambda$ 6517 line is surrounded by two unidentified weaker lines at both wings. The presence of neighboring lines makes the estimation of radial velocities impossible. Consequently, the equivalent width is also affected by their presence.

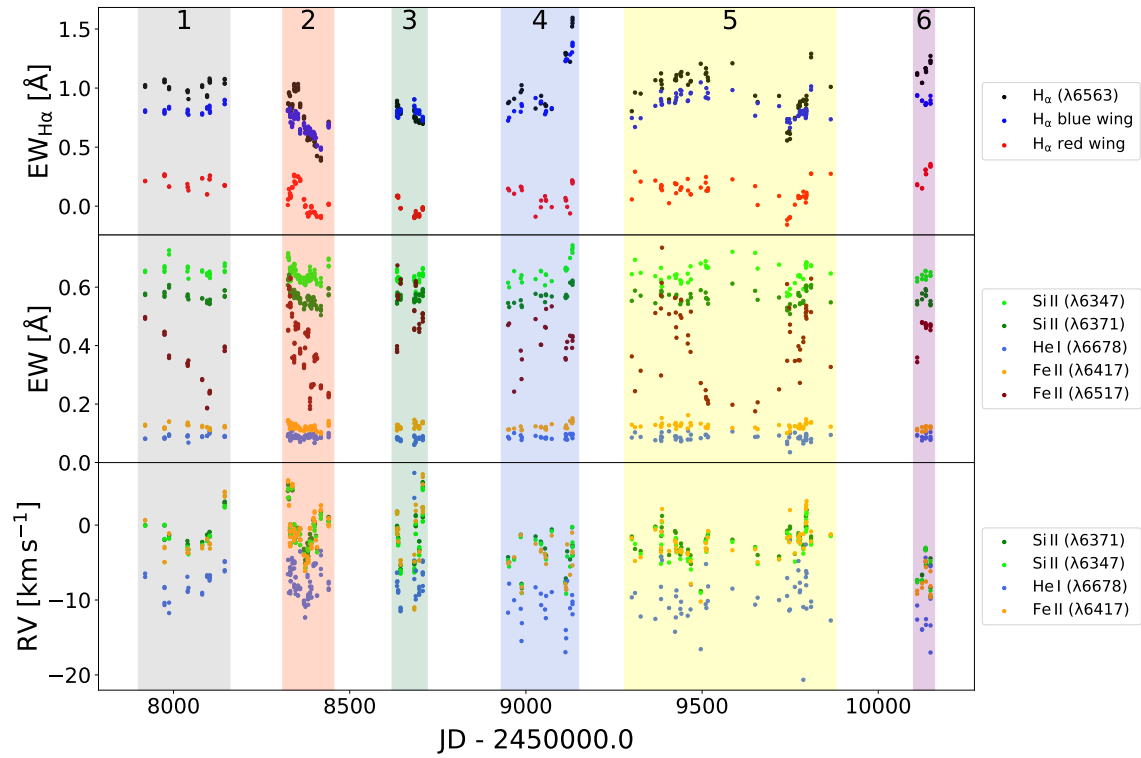


Figure 3.33: Equivalent widths of H $\alpha$  (top panel); Si II, Fe II and He I (middle panel) and radial velocities of Si II, Fe II and He I (bottom panel) measured across whole time-series from 2017 up to 2023. Each region with background color marked also by number in top panel is then shown zoomed in following Fig. 3.34 - 3.36.



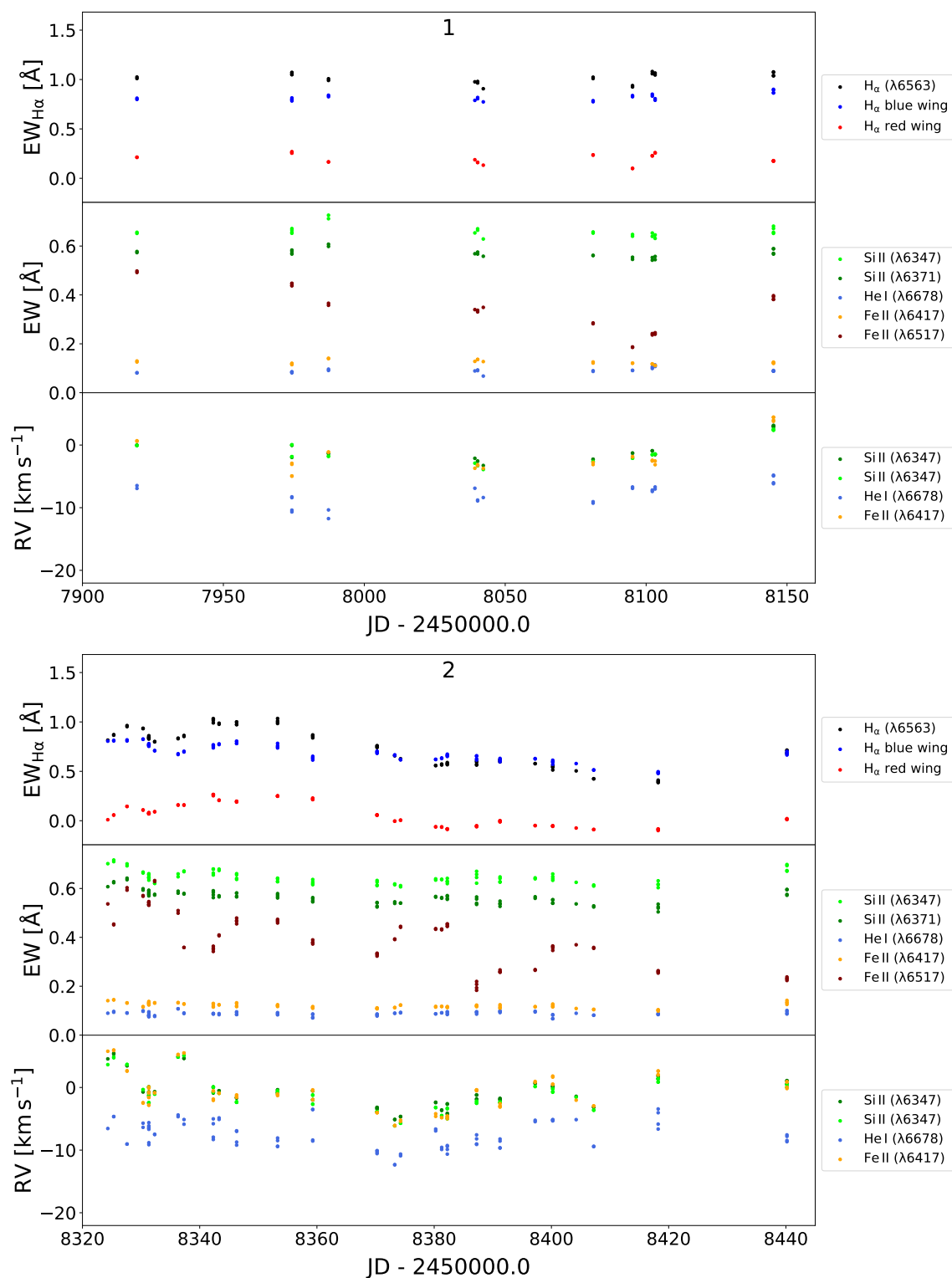


Figure 3.34: Zoomed parts 1 and 2, from top to bottom respectively, in Fig. 3.33.

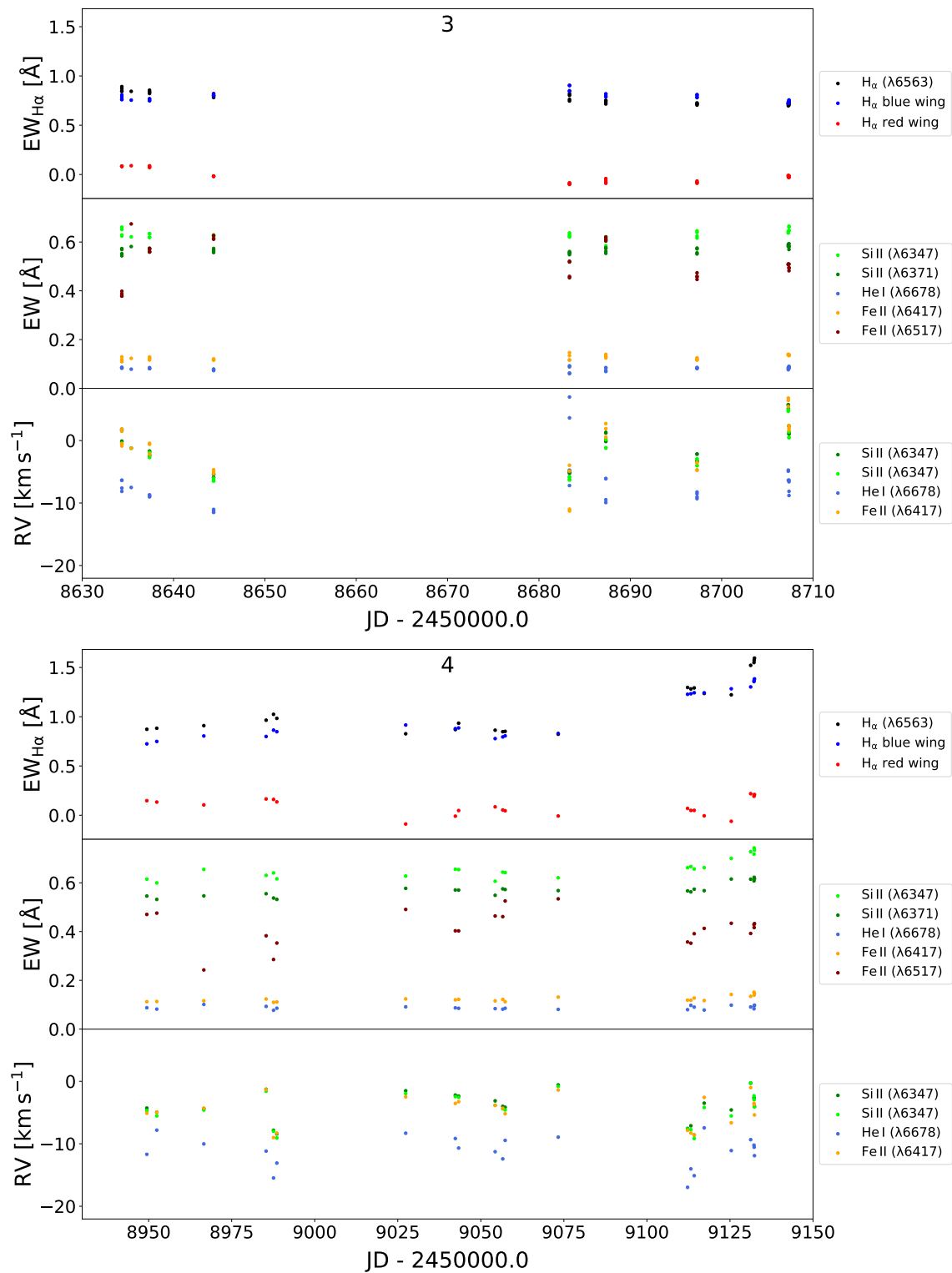


Figure 3.35: Zoomed parts 3 and 4, from top to bottom respectively, in Fig. 3.33.

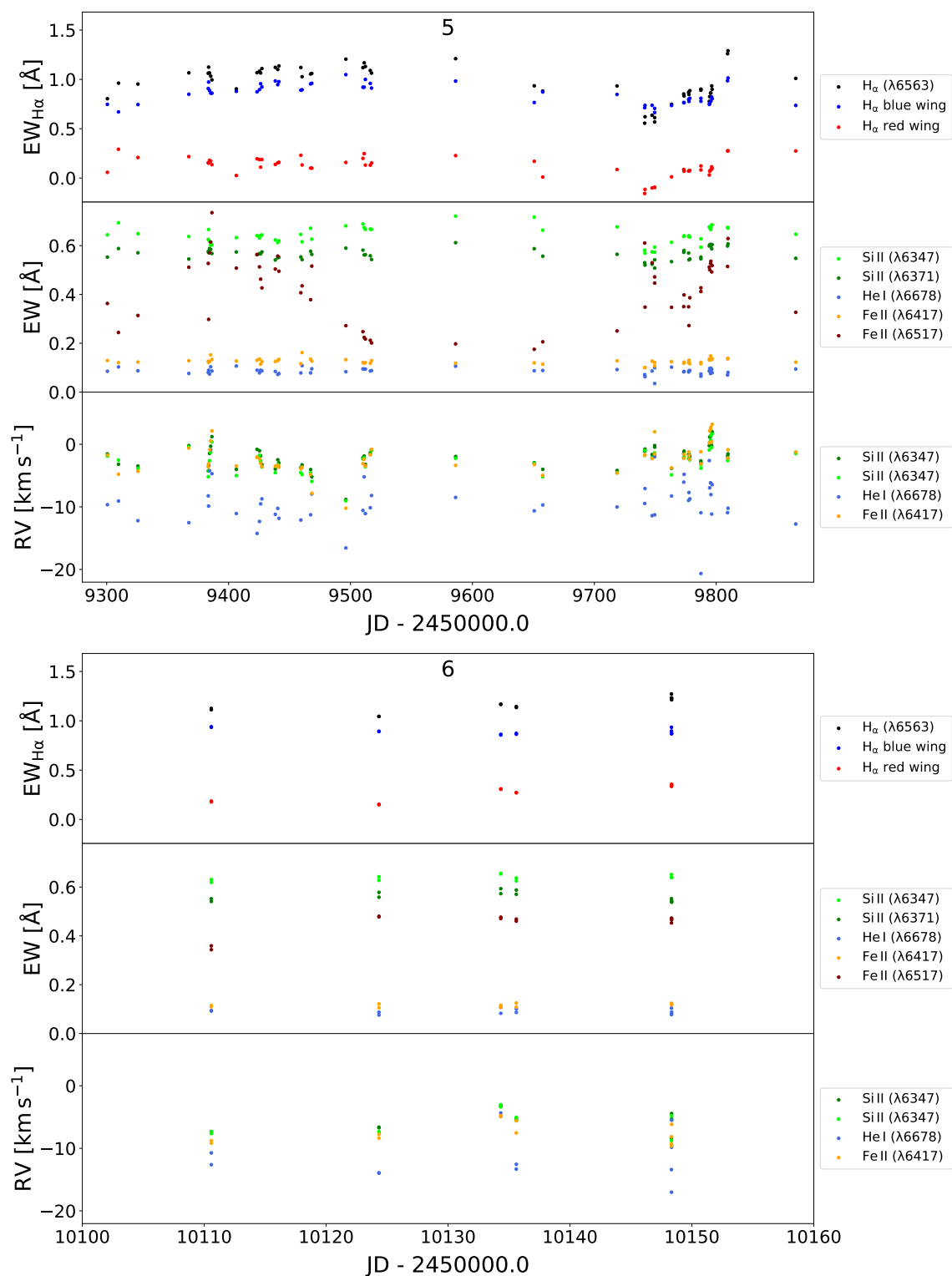


Figure 3.36: Zoomed parts 5 and 6, from top to bottom respectively, in Fig. 3.33.

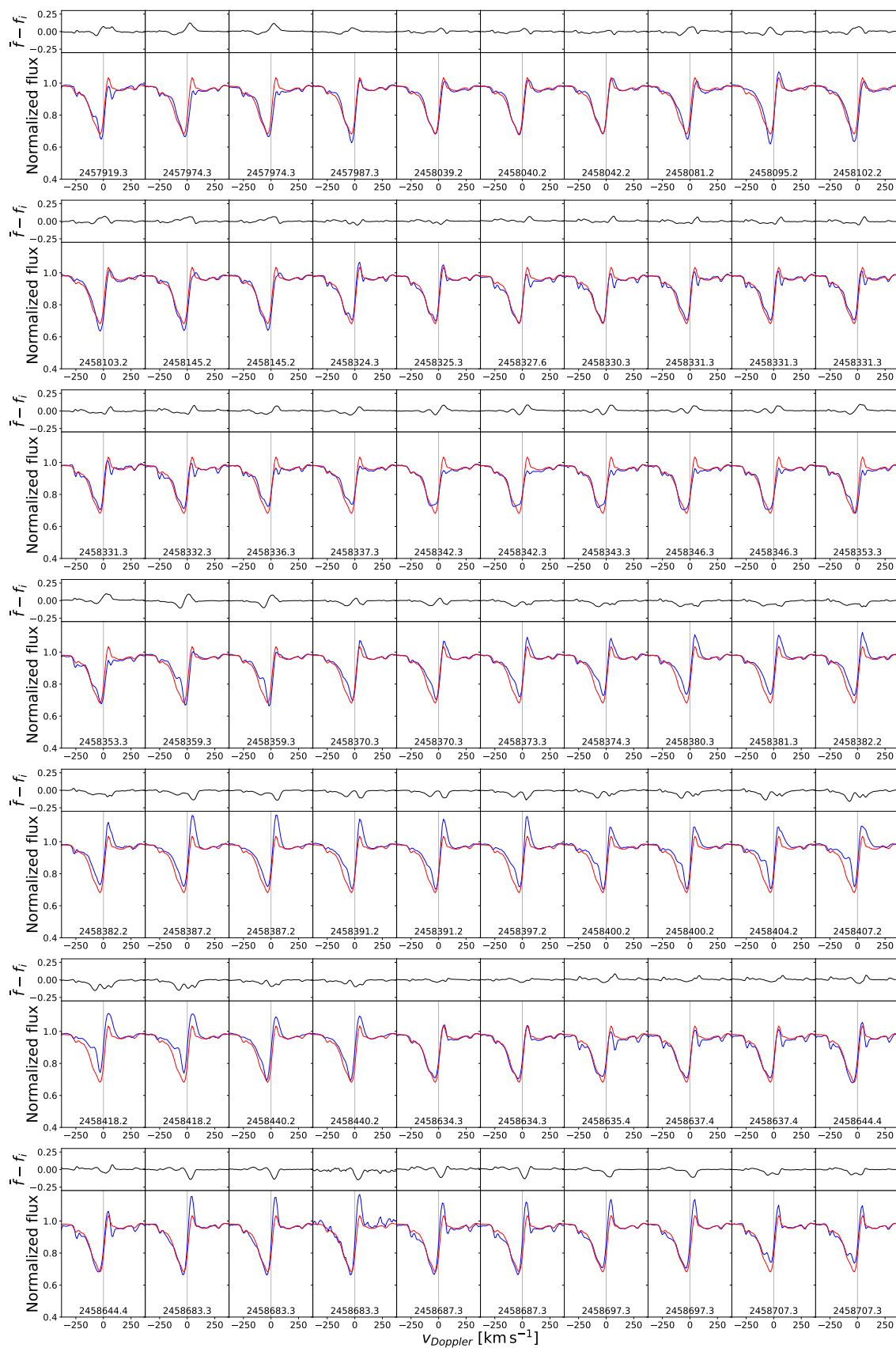


Figure 3.37: Detailed view on H $\alpha$  line profiles of Deneb. Each window contains the profile corresponding to the Julian date in blue line, the red profile is averaged one and is plotted for comparison. Top panels showing the difference between actual profile and the average simply by subtracting (average - actual profile).

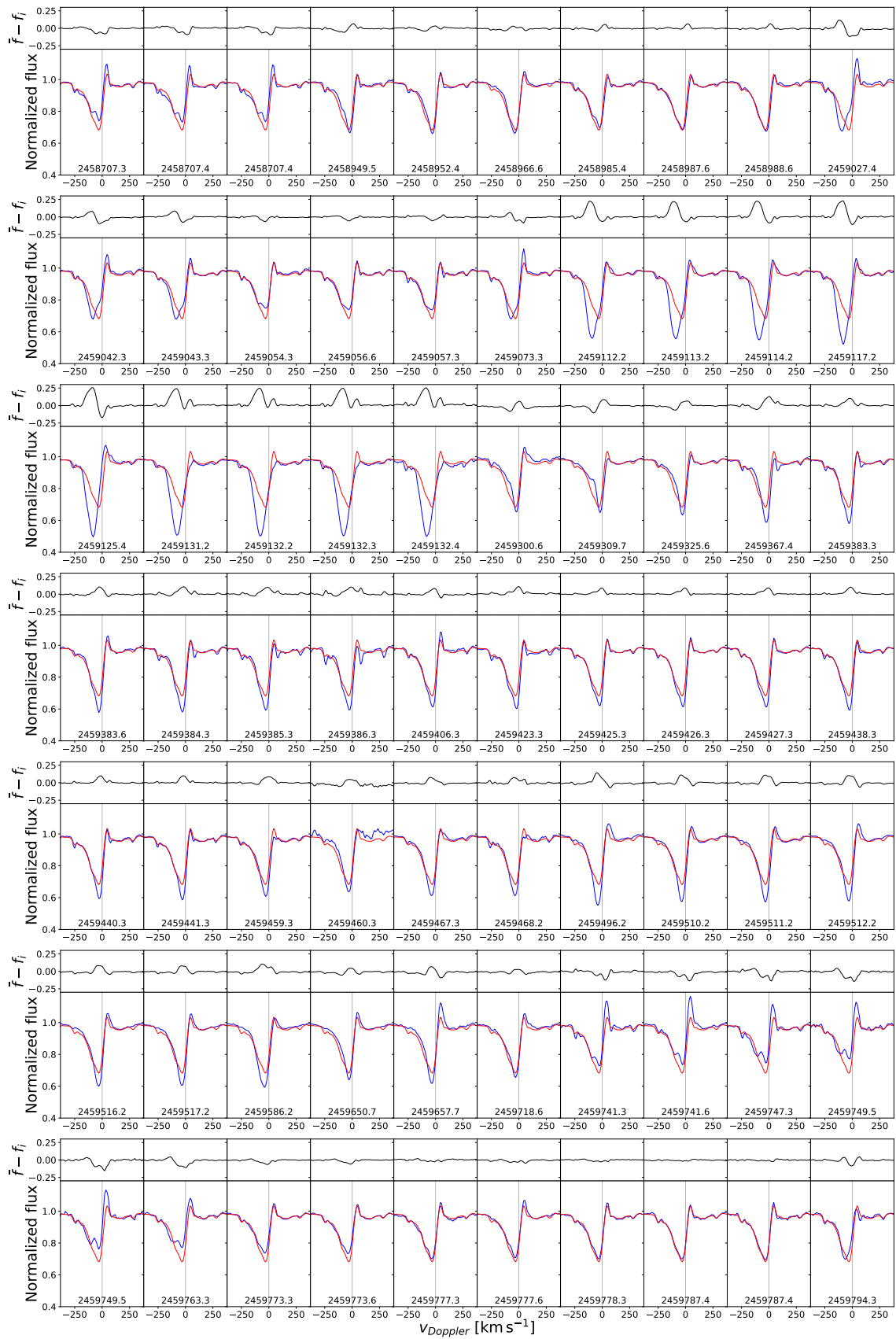


Figure 3.38: Continued from Fig. 3.38

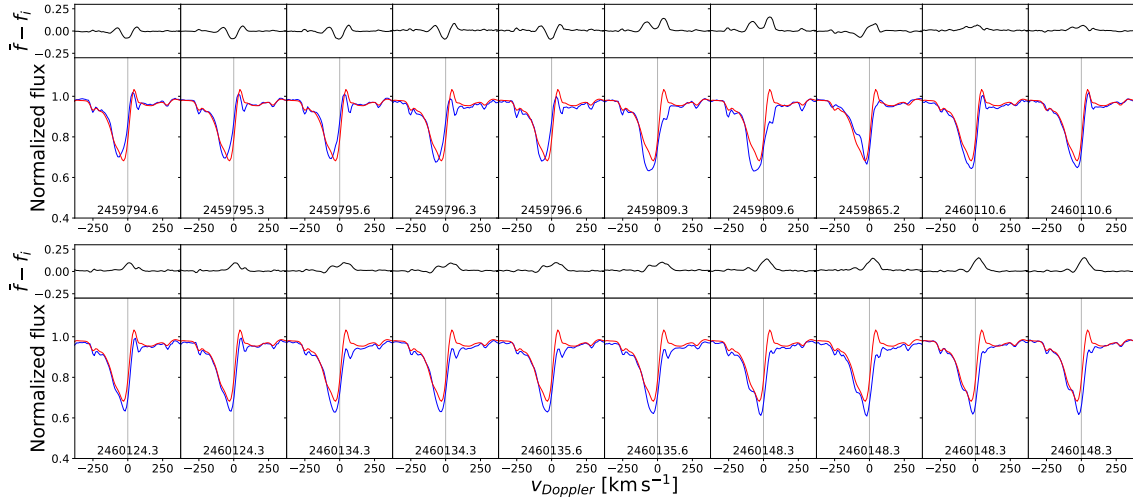


Figure 3.39: Continued from Fig. 3.39

### Morphology of H $\alpha$ line profiles

In the beginning of observational period we can see slow formation of P Cygni component (Fig. 3.37). The strength of red-shifted emission oscillates and finally disappears on 2458337.3. On 2458145.2 the core of absorption part consist of two components which then become one broad and two components are again seen approximately in 10 days. At this point (2458359.3) the P Cygni profile emission starts to grow and remains present up to 2459125.4 during the HVA event (Fig. 3.38). The first few panels from the very bottom line are remarkably different. Around 2459112.2 the profile becomes deeper and is significantly shifted towards the blue. The same behavior may be seen for the next 20 days up to 2459132.4, which is the last recorded similar profile. Because the events may last several dozens of days Markova et al. (2008) and the fact that the very beginning and the end of the event were not observed, this particular event could last longer than 50 days.

The absorption component mostly repeats the previous behavior. The core is slightly asymmetric, on 2459741.3 additional component appears and in one month turns back to one component absorption. Sign of P Cygni component is than present in the rest of spectra.

H $\alpha$  line profile is asymmetric for whole observational period which is the reason why the radial velocities are not plotted in Fig. 3.33.

The HVA event is clearly evident in the residual dynamic spectra, located in the middle part as a magenta region (see Fig. 3.40). Additionally, the dynamic spectra revealed a cyclical behavior that is not apparent from the series of H $\alpha$  line profiles (Fig. 3.37 - 3.39). This cyclic pattern becomes even more pronounced in the Fe II lines (Fig. 3.42 and Fig. 3.43), where the residual flux oscillates around zero velocity (between  $-40 \text{ km s}^{-1}$  and  $40 \text{ km s}^{-1}$ ) with an estimated period of approximately 112 days. After ruling out incorrect barycentric velocity correction as a source of the pattern, pulsations were suggested as a possible explanation.

In the study by Lucy (1976), the multi-periodic pulsational modes of Deneb were examined by analyzing radial velocities. The results indicated periods ranging from

6.9 to 100.8 days, which is slightly lower than what is observed in the dynamic spectra in this thesis. However, it's essential to note that the estimation of periods in this thesis is only a rough approximation, whereas the results by Lucy (1976) are based on a proper analysis.

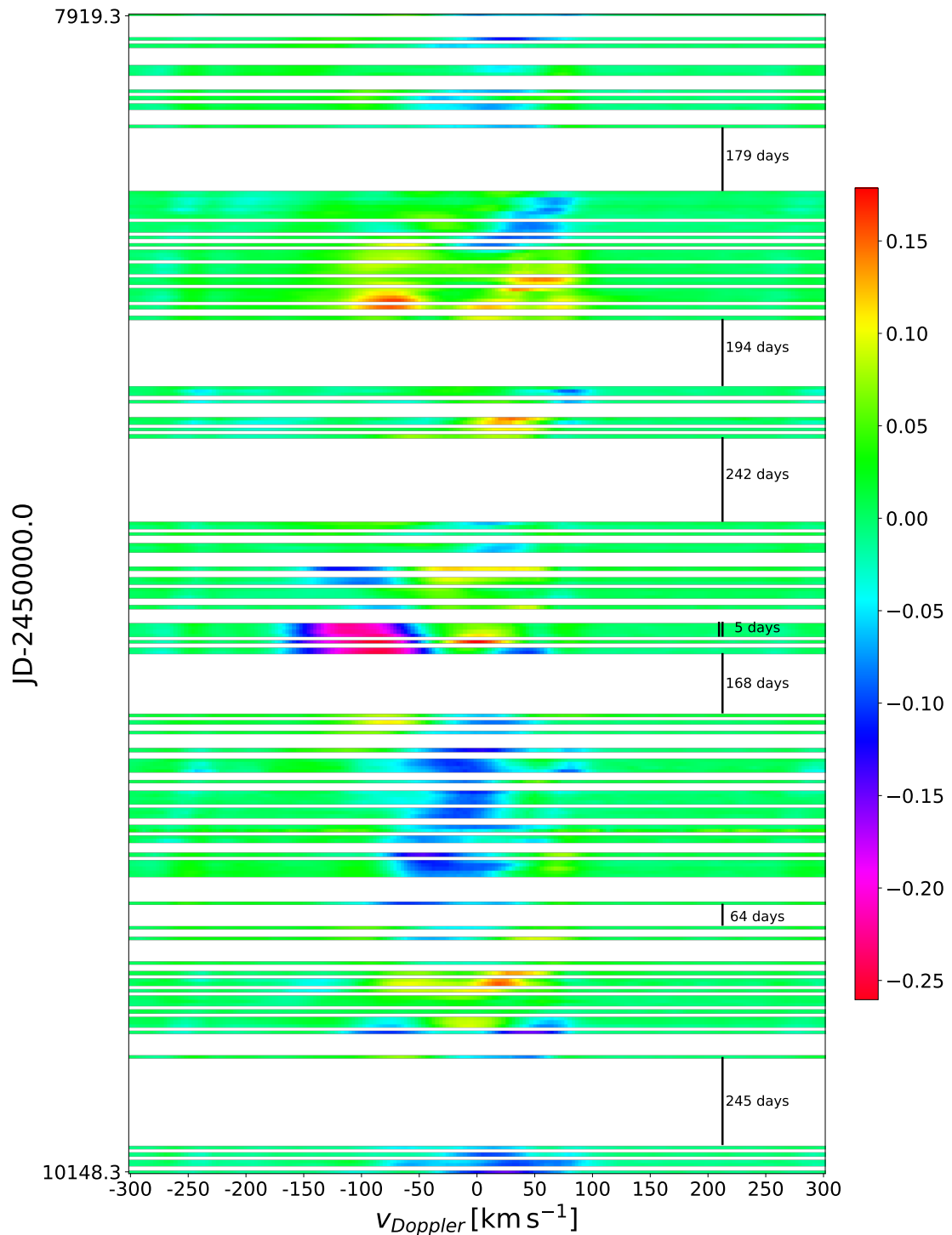


Figure 3.40: Residual dynamic spectra of Deneb's time-series seen in H $\alpha$  ( $\lambda 6563$ ) line and composed of D700 spectra.

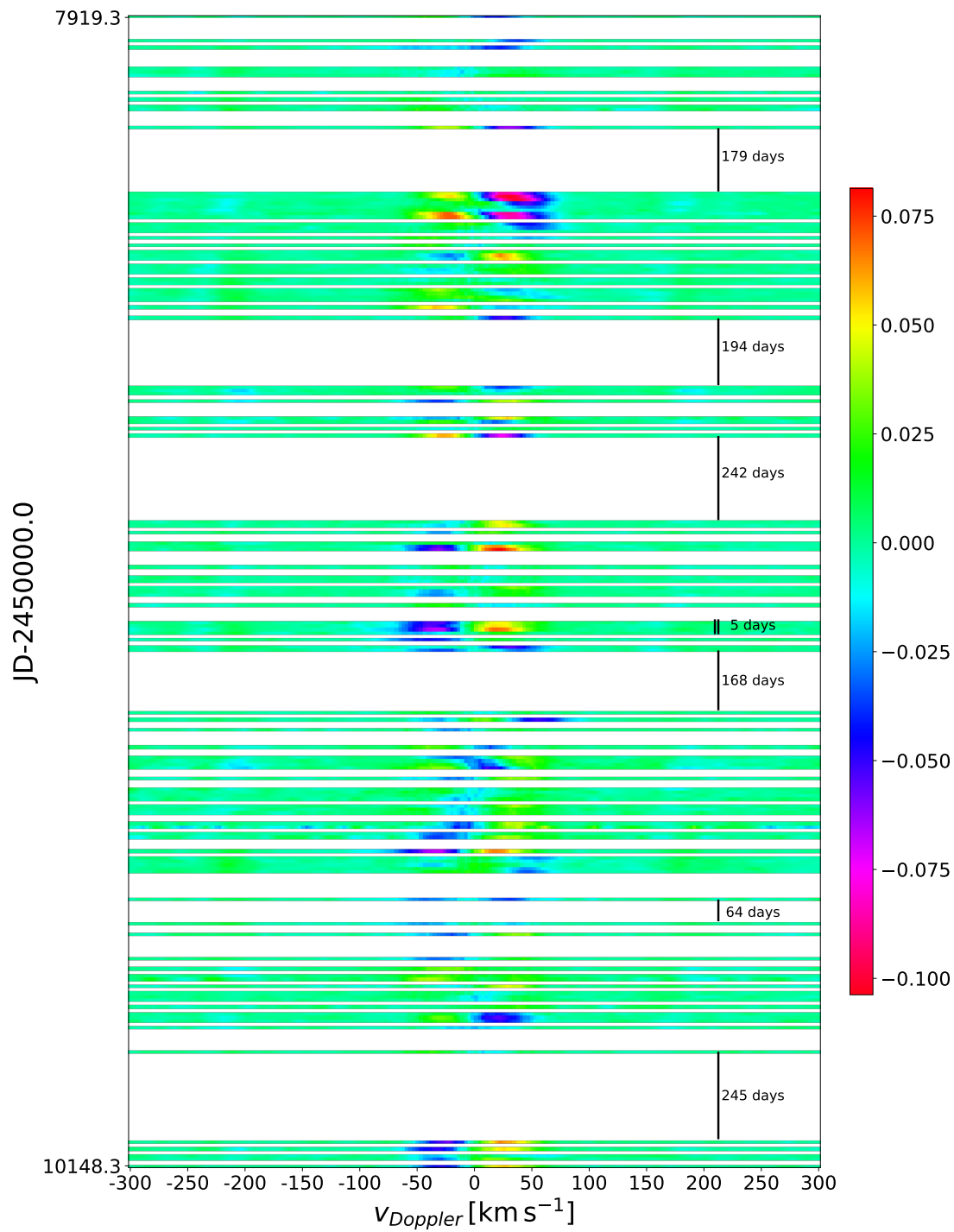


Figure 3.41: Residual dynamic spectra of Deneb's time-series seen in Si II ( $\lambda 6347$ ) line and composed of D700 spectra.



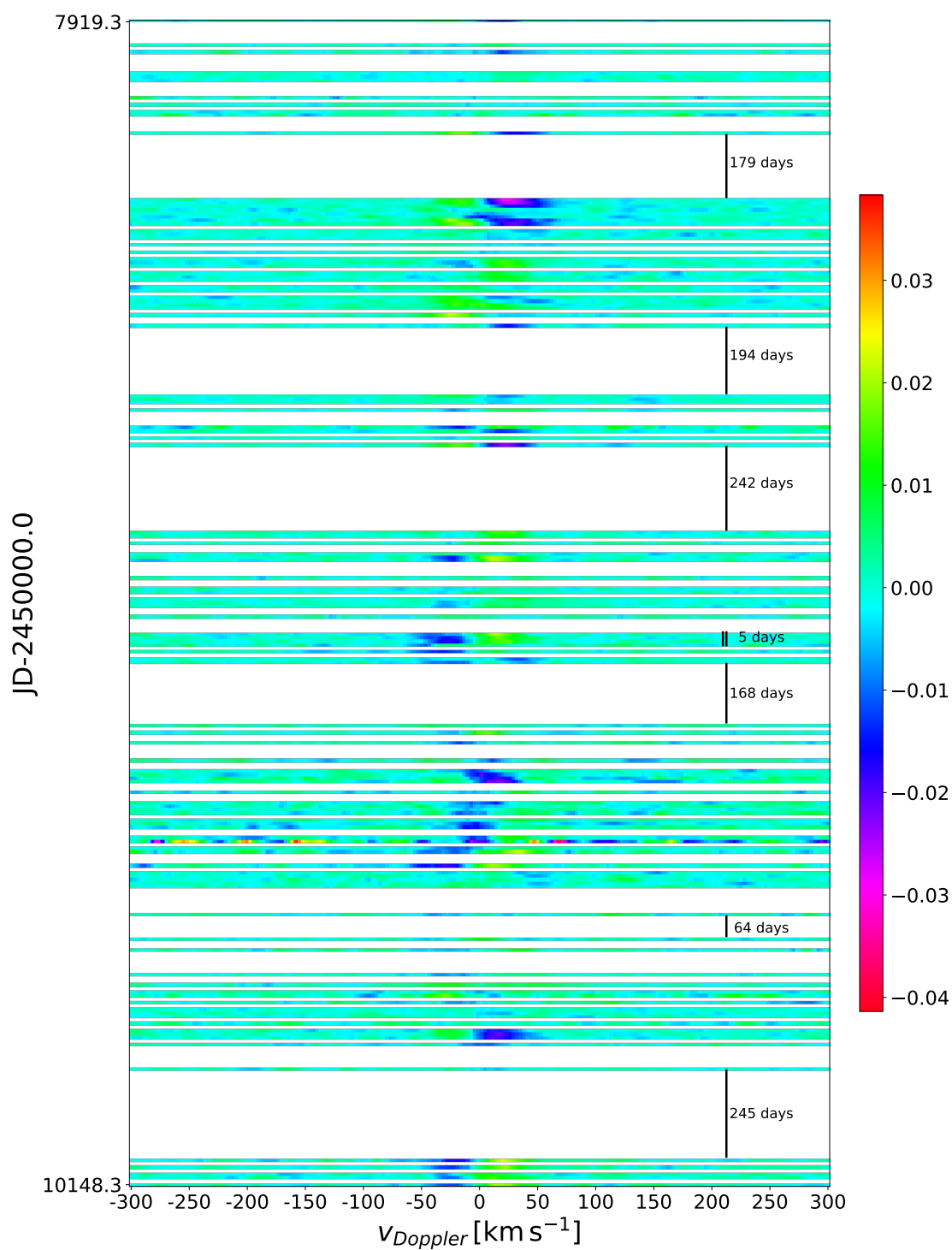


Figure 3.42: Residual dynamic spectra of Deneb's time-series seen in Fe II ( $\lambda 6417$ ) line and composed of D700 spectra.

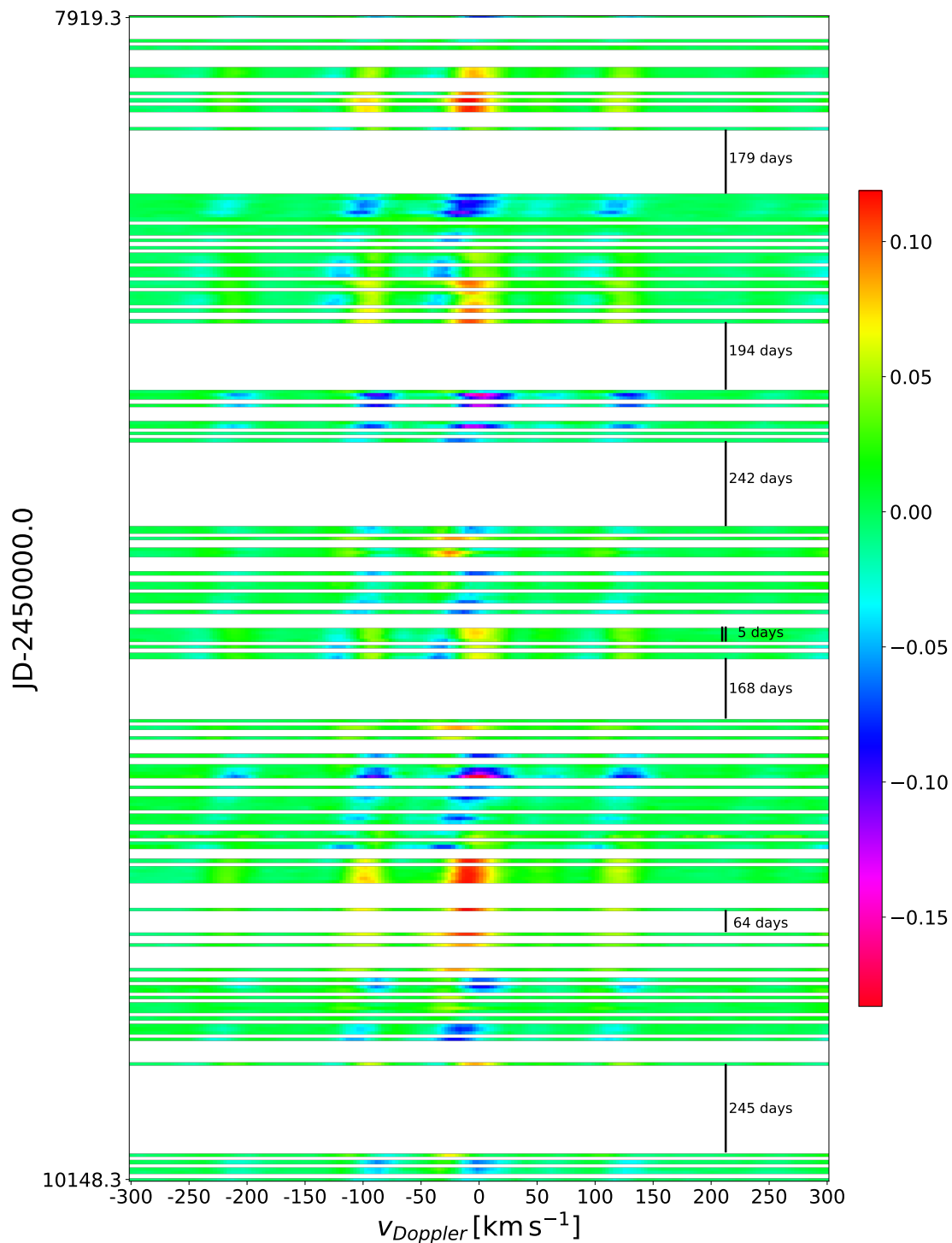


Figure 3.43: Residual dynamic spectra of Deneb's time-series seen in Fe II ( $\lambda 6517$ ) line and composed of D700 spectra.

However Deneb is one of the brightest stars of northern night sky and its spectroscopic observations goes long to the past, the first recorded HVA event occurred in 1991 as part of an extensive study of A- and B-type supergiants by Kaufer et al. (1996a). During this event, a second absorption component of a P Cygni profile

appeared in the  $H\alpha$  line and persisted for approximately 60 days. Subsequently, Morrison and Mulliss (1998) identified another HVA event for Deneb in 1997, which developed from a P Cygni type profile and lasted for about 40 days. The details of both events are listed in Tab. 3.14.

A comprehensive study by Richardson et al. (2011) provided further insight into HVA events in Deneb. Over five years of observations from 1997 to 2001, several weak events and one strong event in 2001 were detected. Although parameters for the weak events were not provided, the 2001 event was analyzed in detail. At the onset of the event, a very strong P Cygni component appeared, gradually fading as the event progressed. Additionally, a second, weaker event was identified, overlapping with the first event for a duration of approximately 40 days.

Last discovered HVA event for Deneb is found in the study by Shultz et al. (2014), however is recognized just in one snapshot and thus the evolution cannot be constrained. The parameters estimated from Shultz et al. (2014) Fig. 1 are listed in Tab. 3.14 together with the event from 2001 (Richardson et al., 2011).

Table 3.14: Characteristics of HVA events recorded for HD 197345.

	Kaufer et al. (1996a)	Morrison and Mulliss (1998)
JD	2448440 – 2448500	
Dates	Jul 2. - Aug 31. 1991	Aug 1997
$v_{blue\ core}$ [km s <sup>-1</sup> ]	-180	–
$v_{blue\ edge}$ [km s <sup>-1</sup> ]	≈ -200	–
Depth*	0.63	–
Duration of event [d]	60	≈ 40
	Richardson et al. (2011)	Shultz et al. (2014)
JD	2452180 – 2452240	2453544
Dates	Sept/Oct 2001	Jun 22. 2005
$v_{blue\ core}$ [km s <sup>-1</sup> ]	≈ -100	≈ -110
$v_{blue\ edge}$ [km s <sup>-1</sup> ]	≈ -200	≈ -200
Depth*	≈ 0.7	≈ 0.6
Duration of event [d]	≈ 60	–

\* Depth (in continuum lvl) of blue-shifted absorption component.

### 3.10 Broad emission wings around $H\alpha$

All the supergiants showing HVA events under study were also found to exhibit broad emission wings (Fig. 3.44). Exception is only HD 197345. The emission wings extend to about  $\pm 1500$  km s<sup>-1</sup> and they often exceeding 5 % of the continuum level. Moreover, the strength and extent of this feature depend on the central profile and display slightly correlated variability.

It's important to note that the feature is highly sensitive to reduction processes, such as normalization, where it may inadvertently be marked as part of the continuum and subsequently subtracted entirely. Recent findings have also revealed that

broad emission wings are susceptible to telluric correction procedure.

This particular feature has been already presented by Ebbets (1982) for several supergiants where it was initially attributed to stellar wind, particularly to its high expansion velocity. Nowadays understanding, however, attributes such effects to electron scattering. Non-LTE effects in the atmospheres of Luminous Blue Variables (LBVs), as presented by Hubeny and Leitherer (1989), result in extended wings with approximately three times weaker strength in terms of velocity. As discussed in Kaufer et al. (1996a), considering the potential influence of deep-seated  $H\alpha$  emission spread by photons scattered by electrons could yield a comparable extension in velocity.

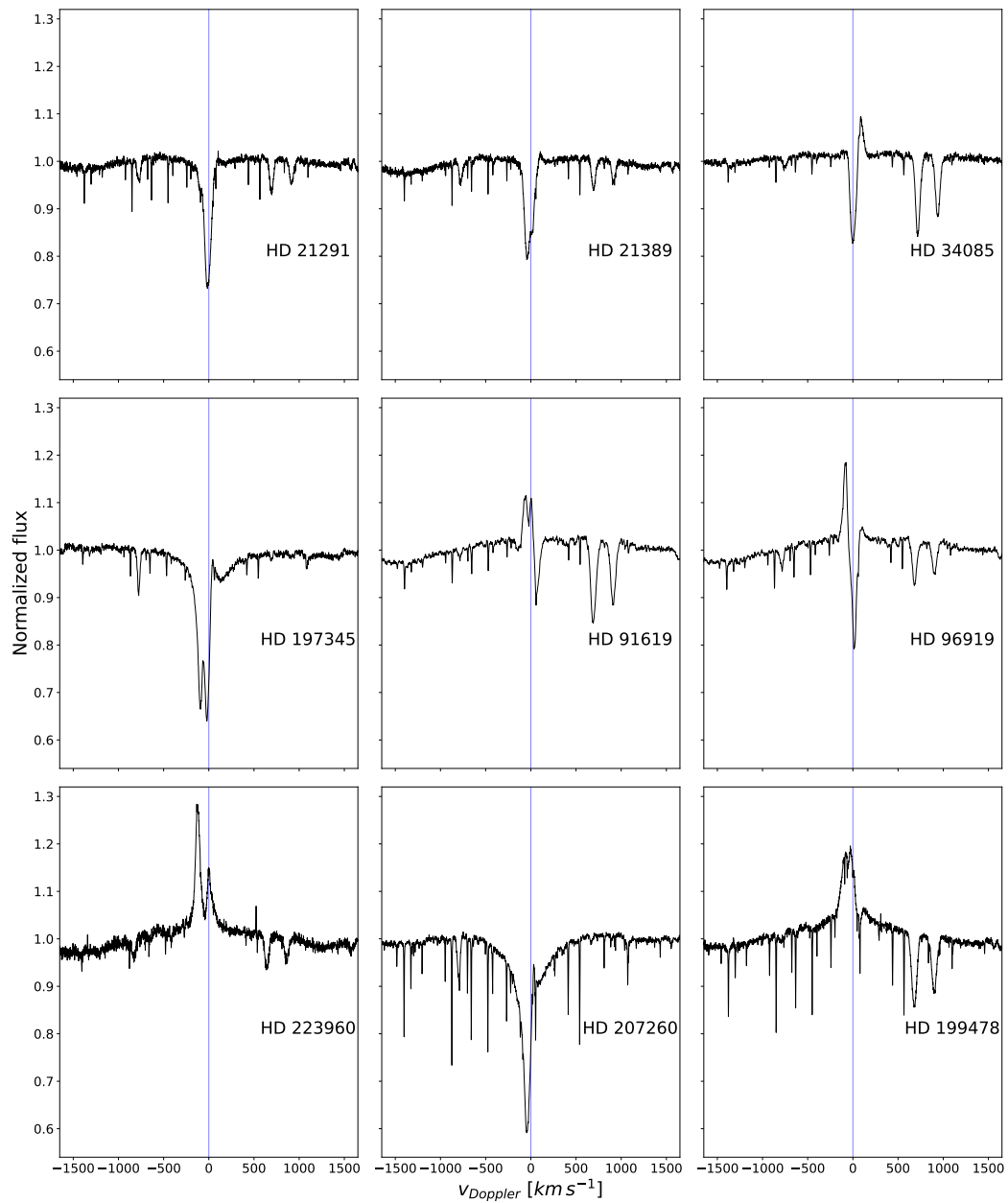


Figure 3.44: The H $\alpha$  profiles with broad emission wings in spectra of nine supergiants exhibiting HVAs.



# Chapter 4

## Explanation for HVA events

### 4.1 Evolutionary status

The modern theory of stellar evolution became reliable instrument for studying the stars. By discerning a star's placement within the Hertzsprung-Russell (HR) diagram, insights into its internal structure can be directly inferred. The study of various phases in the life of stars is important for different fields of modern astrophysics. It can also provide a key parameter for understanding the chemical evolution of interstellar matter and, consequently, the evolution of galaxies, where massive stars play a crucial role in material recycling processes.

In the Hertzsprung-Russell (HR) diagram, certain regions pose challenges to determining the evolutionary status of stars. One such area is the domain of Blue Supergiants (BSGs), through which stars with masses exceeding  $15, M_{\odot}$  traverse twice during their evolution. Initially, they cross this region as they transition from the Main Sequence (MS) to Red Supergiants (RSGs). Subsequently, after the RSG phase, they pass through this region once again as they evolve back. This dual passage through the BSGs region complicates the interpretation of the evolutionary pathways of massive stars.

One of the persisting challenges in the study of massive stars is establishing a reliable criterion for discerning whether BSGs are in a pre- or post-RSGs stage. Theoretically, distinguishing between these scenarios is feasible. Additional insights can be derived from mass-loss and chemical composition. During the RSGs phase, substantial mass loss occurs through stellar wind. By comparing the spectroscopic and evolutionary masses, it becomes possible to eliminate unsuitable scenarios and refine our understanding of the star's evolutionary path. Possible criterion for this distinction lies in the abundance of CNO elements. The CNO cycle generates helium through successive reactions involving hydrogen, nitrogen, carbon, and oxygen. Subsequently, the products are transported and mixed into the stellar atmosphere. This implies that stars in their first crossing, evolving towards RSGs have not yet experienced internal mixing, resulting in abundances comparable to solar values. Conversely, in the second case, as the star evolves leftwards, the atmospheric composition should exhibit the influence of the preceding RSG stage, manifested as chemical enhancements.

The point about evolutionary stage B-A-type supergiants (post MS or blue loop) seems to be crucial when considering that all the supergiants examined in this study are classified as  $\alpha$  Cyg variables. Saio et al. (2013) showed that during the RSG stage, peculiar mode pulsations are excited in stars with initial masses slightly higher than approximately  $14 M_{\odot}$ . As stars undergo the RSG stage, they lose a significant amount of mass, leading to an increase in the luminosity-to-mass ratio (L/M ratio). Consequently, it is the mass loss that causes the luminosity of the instability boundary in the second crossing to decrease by an order of magnitude. This shift in the instability boundary results in most  $\alpha$  Cyg variables falling within this instability domain. Now the question arises: what is then the reason for spectral and photometric variability of supergiants evolving redwards to RSGs? According to Saio et al. (2013), pulsations (radial and most non-radial), characteristic of these variables, are typically excited after the RSG stage when significant mass-loss occurs. However, it is noteworthy that the derived results from models, such as very high N/O and N/C ratios, do not align with the observed data. This discrepancy poses a challenge that warrants further investigation and refinement of theoretical frameworks and mainly spectroscopic observations.

The collected parameters of the stars exhibiting HVA events (Chapter 2) allow us to position them on the HR diagram. As it is illustrated in Fig. 4.1, the initial evolutionary mass of HVA stars falls within the  $15 - 25 M_{\odot}$  range. Some of them have lower masses, around  $15 M_{\odot}$  indicating that they are definitively in a pre-RSG phase. For a  $15 M_{\odot}$  star, the evolution terminates with a supernova explosion immediately following the RSG phase.

About more massive stars, as mentioned above (Chapter 2.6), Schiller and Przybilla (2008) performed a detailed abundance analysis for Deneb which they consequently used to ascertain its evolutionary status. Notably, the authors emphasized the N/C ratio, which exhibited a more pronounced deviation than predicted from models. Surprisingly, it surpassed even the values observed in other similar supergiants examined through the same method (Przybilla et al., 2006). However, the derived mass aligns more with the scenario where Deneb is still in its first crossing, evolving toward the RSG stage. The higher N/C ratios, as a sign of mixing, are then attributed to its rapidly rotating MS progenitor.

Georgy et al. (2014) compared period of Rigel pulsations, estimated by Moravveji et al. (2012) to be  $4 - 70$  days, with predictions of evolutionary model for star with an initial mass of  $25 M_{\odot}$ . The analysis led to the conclusion that Rigel is in the post-RSG stage.

For another star in the sample under investigation, HD 21389, the assessment of its evolutionary status was undertaken by Corliss et al., 2015. The examination of cluster/association membership did not yield a definitive statement regarding whether the star is older or younger than 10 million years. However, by comparing the N/C and N/O ratios with Rigel, a star confidently placed on the blue loop in its second crossing, the results for HD 21389 approached solar values. This suggests that HD 21389 is likely still in the process of evolving towards the RSG stage. The absence of pulsations exhibiting long-term periodic behavior, typical for stars in a blue loop (Georgy et al., 2014), further supports the hypothesis that HD 21389 is in



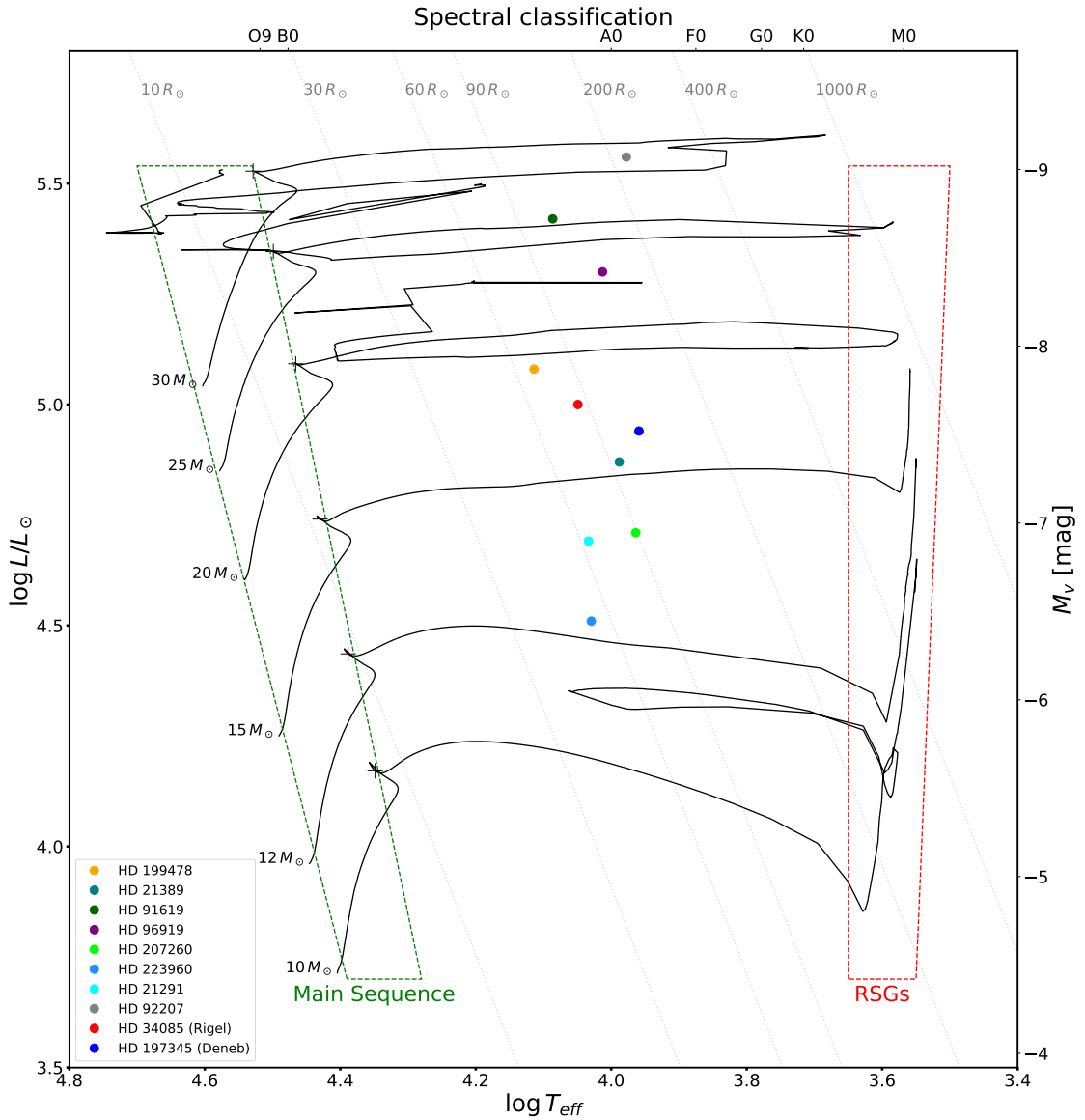


Figure 4.1: HR diagram encompasses evolutionary tracks for rotating stars with solar metallicity ( $Z_{\odot} = 0.014$ ) taken from Yusof et al. (2022). The evolution starts from the Zero-Age Main Sequence (ZAMS). Terminal Age Main Sequence (TAMS) is denoted by black crosses, marking the end of the Main Sequence phase. Additionally, the colored markers in the HR diagram correspond to all identified supergiants manifesting High-Velocity Absorption (HVA) components.

its first crossing of the HR diagram.

So, as evident from the paragraphs above, the evolutionary stages of HVA supergiants vary. Some, like HD 21389, are directly post-main sequence, while deeper analysis, as in the case of Rigel, reveals it to be even more evolved, found in the blue loop evolving bluewards from the RSG stage. This suggests that there is no direct link between HVA phenomenon and evolutionary status.

## 4.2 Hypothesis behind HVA events

The first-ever discussion about driving mechanism behind the observation of HVA events is attributed to Kaufer et al. (1996a). It is conceivable that such features were observed before without anyone paying significant attention to them<sup>1</sup>. This becomes particularly evident when considering that such types of stars exhibit a wide range of spectral variability (manifesting in the shape of line profiles, variations in line intensities, and alterations in radial velocities). The most pronounced changes consistently manifest in the H $\alpha$  line, recognized as the most sensitive optical indicator of stellar wind in late B and early A type supergiants, as it was suggested by eg. de Jager (1984) and Verdugo et al. (1999b). With this and the fact that there is still no systematic long-time high-resolution monitoring of these stars, the registration of HVA components is more like a miracle.

Concrete interpretations are discussed on the following pages. The first reference to peculiar events is traceable to the work by Kaufer et al. (1996a) and Kaufer et al. (1996b) who investigated spectral variability of ten  $\alpha$  Cyg variables. Among other results, they also captured several extraordinary events, the sudden appearance of highly shifted absorption to blue with unusual continuum depth for  $\beta$  Ori (in 1994), HD 91619 (1994), and HD 96919 (1993, 1994). Consequently, they provide a discussion about the possible nature of such behavior.

One possible way is a **mass-loss event at the base of stellar wind**. Such an event may then be responsible for the appearance of the HVA component propagating outwards in the stellar wind.

**Effects of critical ionization structure in the envelope** are considered as a second plausible scenario. This interpretation, previously mentioned in Kaufer et al. (1996a), is primarily based on the relatively short time scale characterizing HVA events. The rationale behind this scenario is rooted in the prompt manifestation of ionization structure, given the short recombination time scale for B-type supergiants at the base of H $\alpha$  formation, typically on the order of one day. According to Lamers et al. (1995), the crucial transition in ionization stages, and correspondingly the dominant driving lines, occurs in the effective temperature range of approximately 10 000 K, commonly referred to as the second bi-stability jump. Subsequent recombinations in this temperature regime lead to a less effective line acceleration, growth of the wind density, and a reduction in terminal velocity. This cascade induces further recombinations, ultimately giving rise to a sudden deepening of the absorption during HVA events. The recombinations then result in less effective line acceleration that increases the wind density and reduces the terminal velocity. It brings even more recombinations and finally gives a rise to sudden deepening of absorption during HVA events.

The final proposed explanation involves **the rotation of already existing azimuthally extended 'clump' within the envelope into the line of sight** and is based on the observation of the HVA component in HD 96919. Notably, the second

---

<sup>1</sup>An example of such study would be Luud et al. (1978). Where authors detected absorption profiles for H $\alpha$  and Fe II lines, however without velocity estimations we can not consider it as HVA event.

observed HVA event for this star exhibited a duration exceeding 90 days, indicating the likely persistence of the structure across the rotational cycle. However, this perspective does not provide the mechanism responsible for the formation of such an extended 'clump' in the stellar envelope.

The **extended close magnetic loops hypothesis** proposed by Israelian et al. (1997) stems from the observation of Rigel during an event in November 1993. This event was serendipitously captured by another group from Heidelberg (Kaufer et al. (1996a)). Both observations coincided in capturing the phase when the red-shifted absorption feature appeared (are there other observations with a red shift?). This feature was interpreted as simultaneous mass infall and outflow.

The suggested explanation posits the existence of an extended stellar spot on the surface as the source. Under certain conditions, a mass-loss event near the spot could lead to the formation of an extended magnetically supported loop. This loop, in turn, interacts with streams of matter and the fast wind, resulting in the creation of Corotating Interacting Regions, commonly referred to as CIRs. The authors based this model on observational properties and were inspired by real loops observed on solar corona.

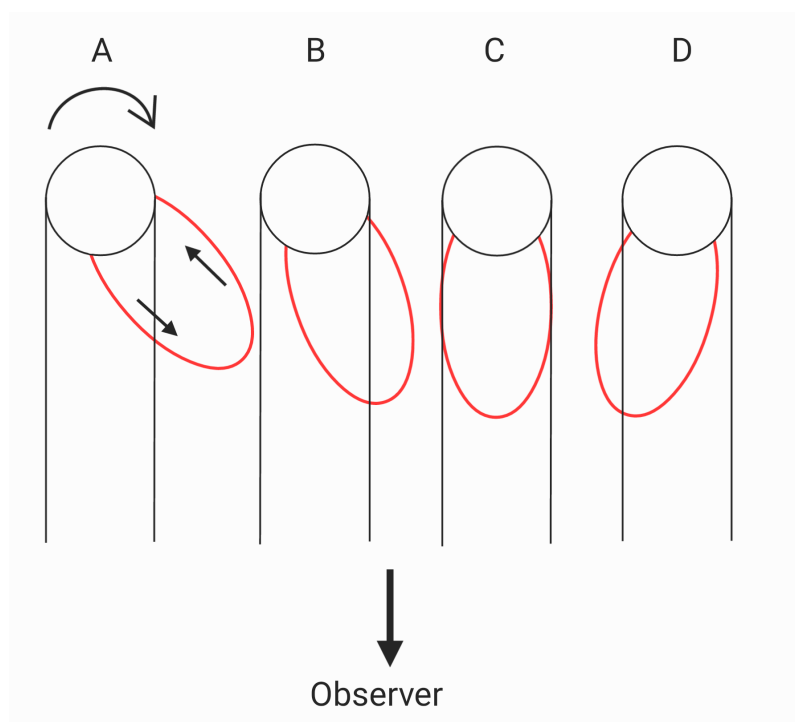


Figure 4.2: An illustration of rotating loop in equatorial plane. The arrows inside the loop indicate the direction of a mass flow. Inspired by the scheme of Israelian et al., 1997.

A schematic representation of the rotation loop is presented in Fig. 4.2. The observation is then interpreted according to the scheme.

The maximum velocity within the loop is attained between the lowest and highest point (Fig. 4.2 case A). The redshift, indicating the minimum velocity, manifests at

the foot of the descending leg. Case C (Fig. 4.2) then explain why the blue-shifted absorption diminishes as the red one starts increasing. The authors emphasize that observed solar corona loops exhibit non-homogeneous characteristics, suggesting a similar non-uniformity for loops in other stars.

The scheme illustrating the detailed time evolution of HVA events warrants some comments. Firstly, studies investigating the presence of magnetic fields in B-A type supergiants, such as Verdugo et al. (2003) and Verdugo et al. (2005) and Shultz et al. (2014), have not conclusively detected the Zeeman effect in the spectra of HVA supergiants. Even spectro-polarimetric observations have failed to reveal the presence of strong magnetic fields. Consequently, even if there are a strong enough magnetic field present, Owocki et al. (2022) demonstrated that the magnetically supported material would be elevated on both legs of a loop, rather than starting at one leg and passing around the loop over time to end in the second leg.

These arguments render the scenario proposed by Israelian et al. (1997) unsuitable as it relies on the presence of strong magnetic fields and magnetically supported loops, which have not been conclusively observed in B-A type supergiants exhibiting HVA events.

### 4.3 Hypothesis based on the results of this work

Based on up-to-date observational properties of the phenomenon known as High-Velocity Absorption (HVA) events, we can summarize several key points and use them to constrain a possible triggering mechanism:

- 1.: HVA events are observed within the effective temperature range  $\approx 9000 \div 13000$  K, corresponding to early A-type and late B-type supergiants, respectively, for stars with initial masses  $14 \div 25 M_{\odot}$ .
- 2.: The events manifest as abrupt changes in the Balmer line, particularly in  $H\alpha$  line, often exhibiting a significant blue-shifted component at high velocities (significant fraction of the terminal wind velocity  $v_{\infty}$ ), superimposed on the regular stellar absorption or with an additional blue-shifted absorption component.
  - The event's influence may also be discerned in certain photospheric lines, although this has been observed only in the case of HD 199478.
- 3.: The events occur sporadically, typically once every 1 to 10 years, depending on the individual supergiant, with durations ranging from several dozen days to several months ( $\approx 20$  to  $\approx 150$  days).
- 4.: Both the blue-shift and depth of the line (especially for  $H\alpha$ ) increase towards the event's maximum, when its parameters are most extreme. After reaching the maximum, the line gradually returns to normal over a similar timescale.
- 5.: Based on observational evidence, two types of events can be distinguished. Weak events are typically observed in  $H\alpha$  as a single absorption component with

a lower blue-shift ( $< -100 \text{ km s}^{-1}$ ) and usually disappear within several weeks. Strong events manifest as an additional blue-shifted absorption component, with velocities sometimes exceeding the wind terminal velocity, and persist over a period of several months.

- 6.: Pre- and post-HVA event observations in the  $\text{H}\alpha$  line have revealed that the event may be preceded and succeeded by P Cygni or inverse P Cygni profiles, suggesting a connection with the stellar wind.

Based on this, we propose that source of observed spectral variability is optically thick structure propagating through the upper part of the stellar atmosphere (Fig. 4.3). Size of this structure should be several  $R_{\odot}$ , because small size clump would not be visible.

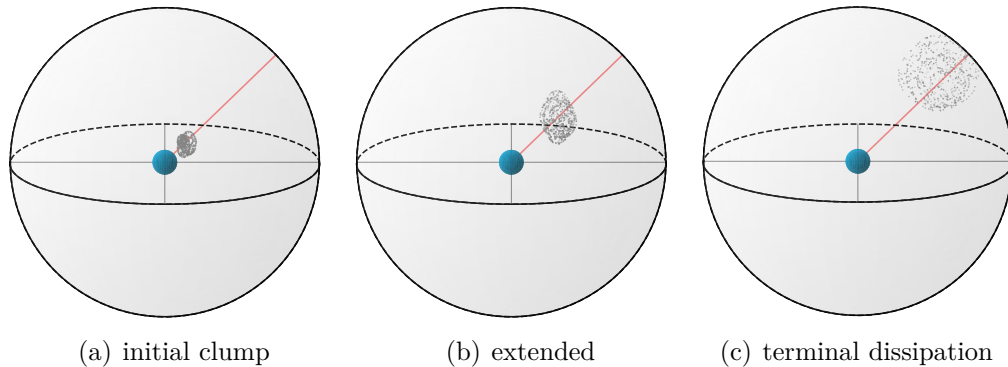


Figure 4.3: Schematic illustration of propagation of the optically thick asymmetric clump in the stellar wind effective region. Assumed size of wind zone is  $70 R_{*}$ , typical for B-type supergiants. The blue sphere in the centre represents blue supergiant and it needs to be noted is not in the scale.

The remaining question is whether such large structures within the stellar atmosphere move independently or are locked, rotating together with the star. As was shown by Kaufer et al. (1996b) Rigel’s event in 1994 and also our analysis revealed the same, these structures do not survive the rotational cycle as the rotational periods may be in some cases shorter than the duration of the HVA event.

Given the observational properties of HVA events described above, several mechanisms for their triggering can be proposed. One such scenario involves tidal effects within the binary or multiple star systems. The idea is that during periastron passage tidal forces release matter that forms an optically thick asymmetric structure, which then propagates away from the star. If this were indeed true, two main implications would follow: Firstly, the incidence of HVA would display strict periodicity. Secondly, the binary motion should be evident in the spectra, yet no such observation has been documented. Additionally, the orbital periods of these systems appear to be longer than the frequency of HVA event occurrences, thus excluding this scenario as a plausible explanation.

Another proposed scenario involves material released due to non-radial pulsations, as all HVA event-exhibiting supergiants are classified as  $\alpha$  Cygni type variables, known for such pulsations. However, if this were the case, it would likely be discernible from most of the spectral lines, which is not observed. Additionally, according to Saio et al. (2013), pulsations become observable after the red supergiant stage, which most of these stars have not yet reached. Hence, this scenario is also considered unlikely.

The last proposed mechanism involves the concept of the iron sub-surface convective zone (CZ) as a triggering mechanism for HVA events. This idea was inspired by the study of Cantiello et al. (2009), who discusses the observational consequences of sub-surface iron convective zones in massive stars. Massive stars generally possess convective cores and radiative envelopes, as outlined by Kippenhahn and Weigert (1990). However, according to prediction by Stothers and Chin (1993), massive stars also can have small convection zones in envelopes, related with “iron peak” in stellar opacities. Besides micro-clumping, such CZ could also be responsible for releasing macro-structures.

The sub-surface iron CZ of Sun-like stars, modified by stellar rotation, is thought to be capable of exhibiting magnetic fields via the  $\alpha\Omega$ -dynamo effect (Parker, 1975). If such dynamo effect alters the sub-surface iron CZ of supergiants at the moment of its instability, together they may give a rise to the creation of abnormally enlarged eddies. These structures may be forced out via localized magnetic fields and, as they interact with the stellar wind, potentially causing a large structure to be ejected from the stellar surface. This phenomenon could manifest as a considerably large, optically thick clump propagating through the atmosphere, producing the observed HVA events. Important to note that this is only a preliminary assumption, which requires detailed investigation through proper modeling.

We aimed to establish criteria for distinguish stars with and without HVA events. For that we decided to search for similarities in internal structure of stars exhibiting HVA events using Modules for Experiments in Stellar Astrophysics (MESA Paxton et al., 2011; Paxton et al., 2013; Paxton et al., 2015; Paxton et al., 2018; Paxton et al., 2019; Jermyn et al., 2023). We calculated evolutionary tracks for stars using the template *7M\_premsto\_AGB* with metallicity fixed to solar value of  $Z = 0.02$ , and varying only initial masses in the range  $14 \div 26 M_{\odot}$ . Model evolutionary tracks are shown in Fig. 4.4, while Fig. 4.5 - 4.8 present internal structure of stars during first crossing HR diagram from the Main sequence to RSG phase. It corresponds to the interval of effective temperatures from 15 000 K to 5 000 K. Results of calculations clearly show presence of two convective zones, interaction between which may be the reason for the appearances of HVA events. For more massive stars ( $M_* > 26 M_{\odot}$ ) CZ do not form in the certain temperature region. Hence sub-surface CZ form in stars with initial mass in range  $14 \div 26 M_{\odot}$ , i.e. exactly in the same range of mass where we observe HVA event. Thus MESA calculations support our hypothesis about the link between iron sub-surface CZ and HVA phenomenon. However the presence of sub-surface CZ is found in temperature interval  $\log T_{\text{eff}} 12500 \div 4000$ , while the events are observed in narrower interval  $T_{\text{eff}} 12500 \div 9500$ . Therefore, further research of the connection between sub-surface CZ and opacities in Fe III/FeII and He I is required.

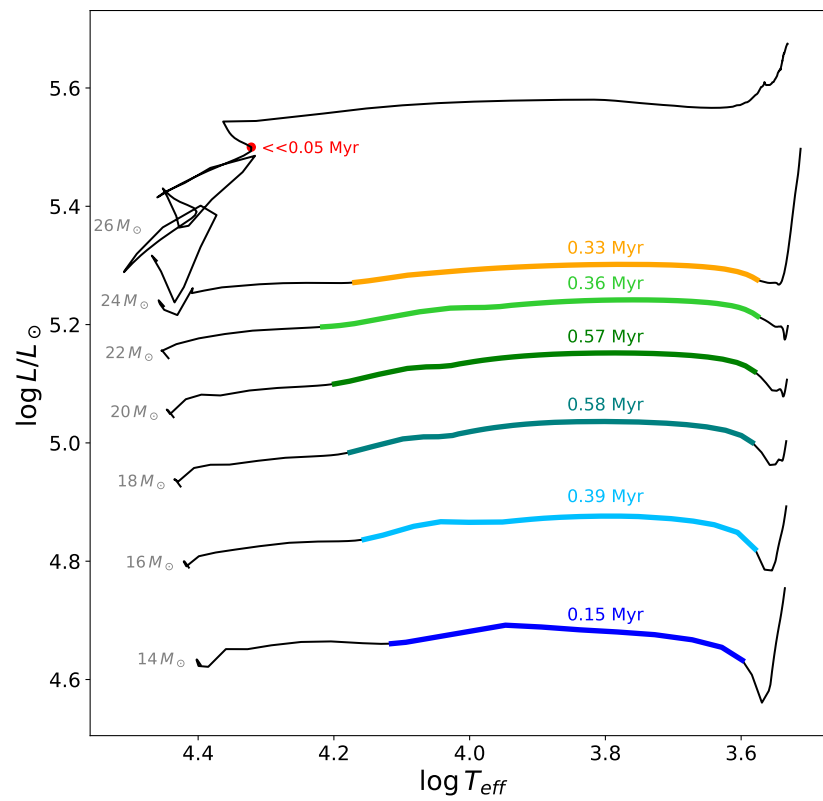


Figure 4.4: The Hertzsprung-Russell (HR) diagram composed of MESA evolutionary tracks. Different colors indicate the timing of two convective zones (CZ) occurrences: one situated just below the surface, and the second one with its bottom boundary approximately halfway through the stellar radius.

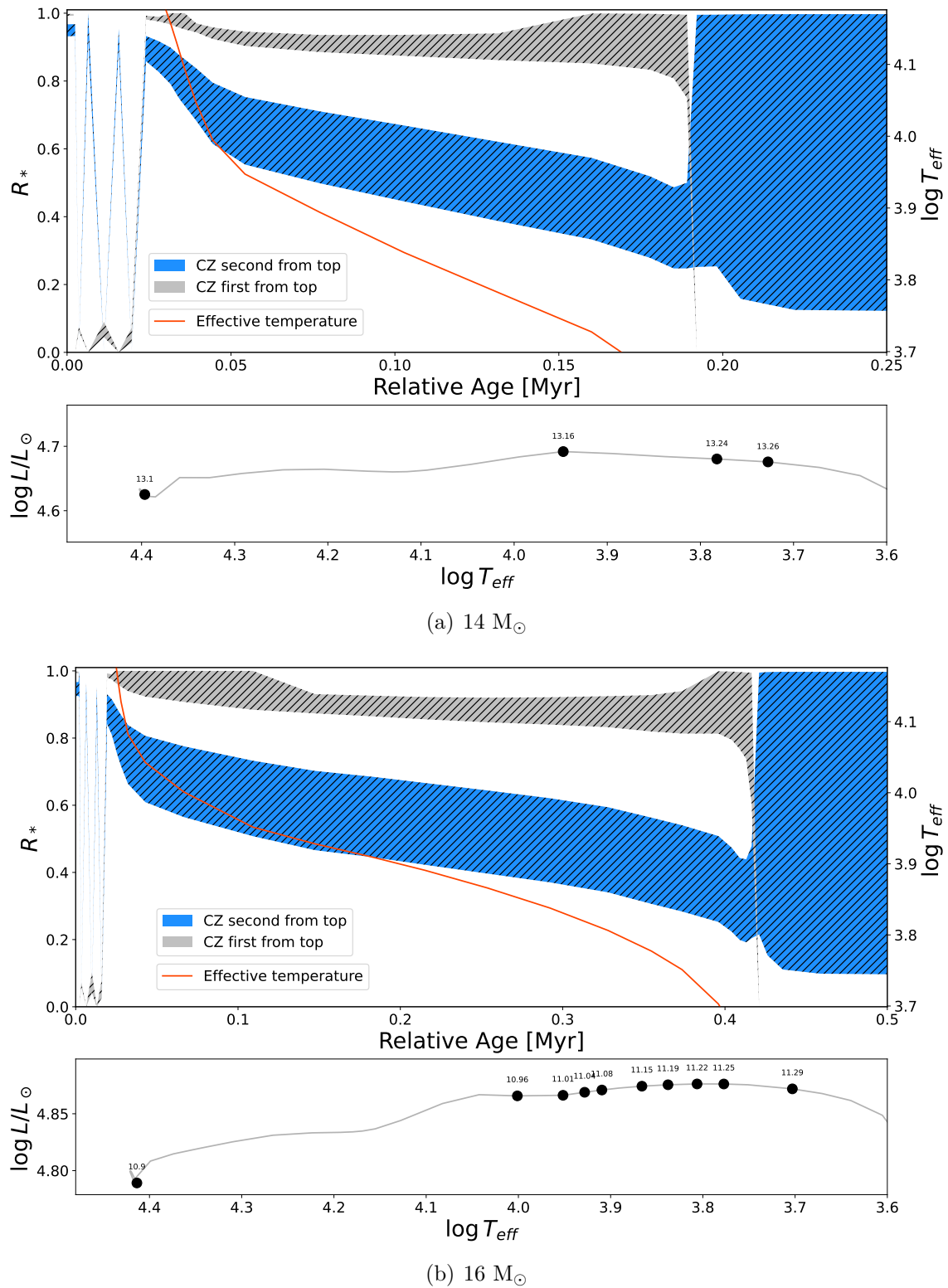


Figure 4.5: The time evolution (in relative age – starting by the end of MS with zero) of two upper most convective zones for stars with initial masses of  $14 \div 25 M_{\odot}$  and metallicity of  $Z = 0.02$ .



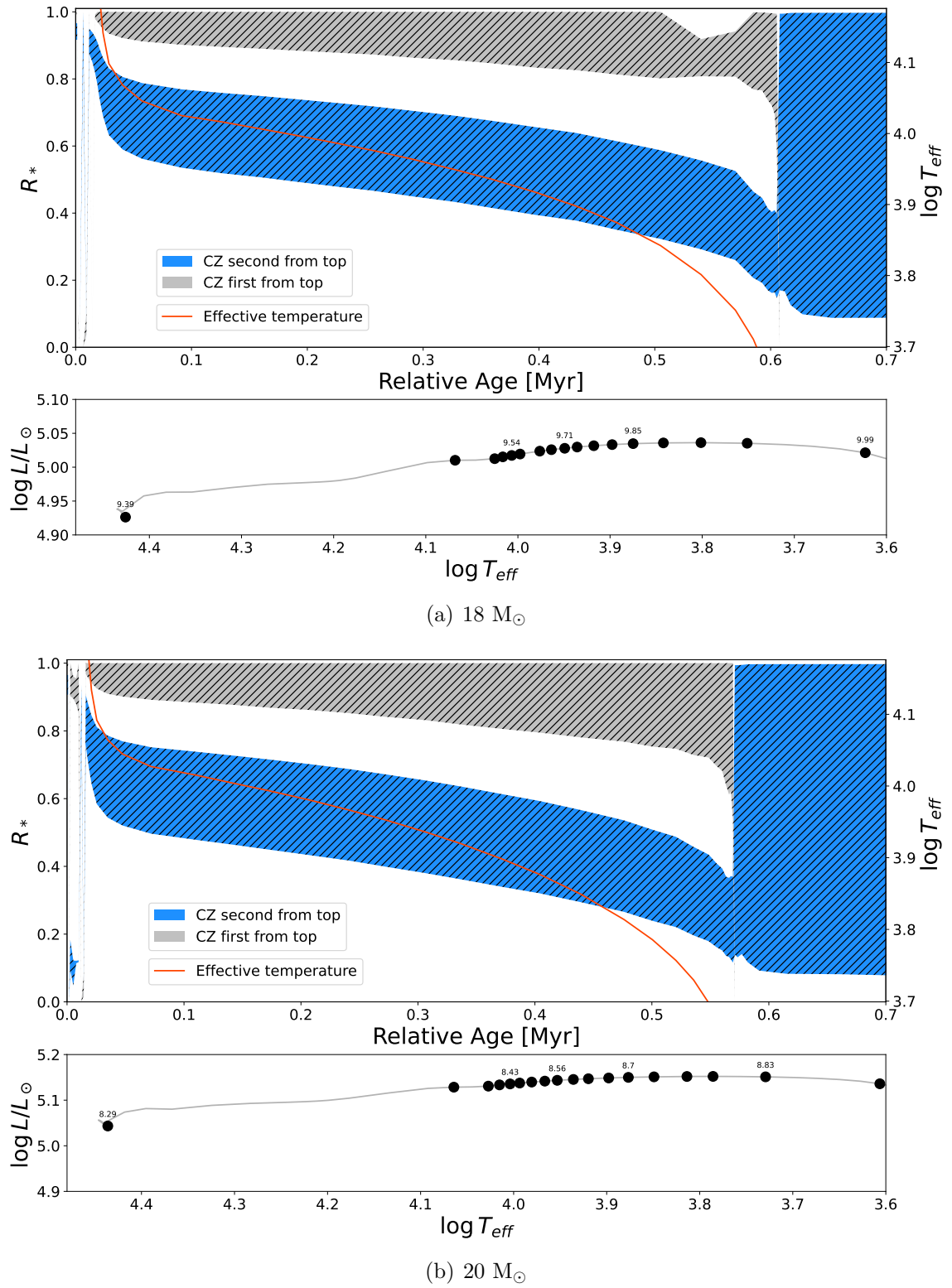


Figure 4.6: Continue of Fig. 4.5.

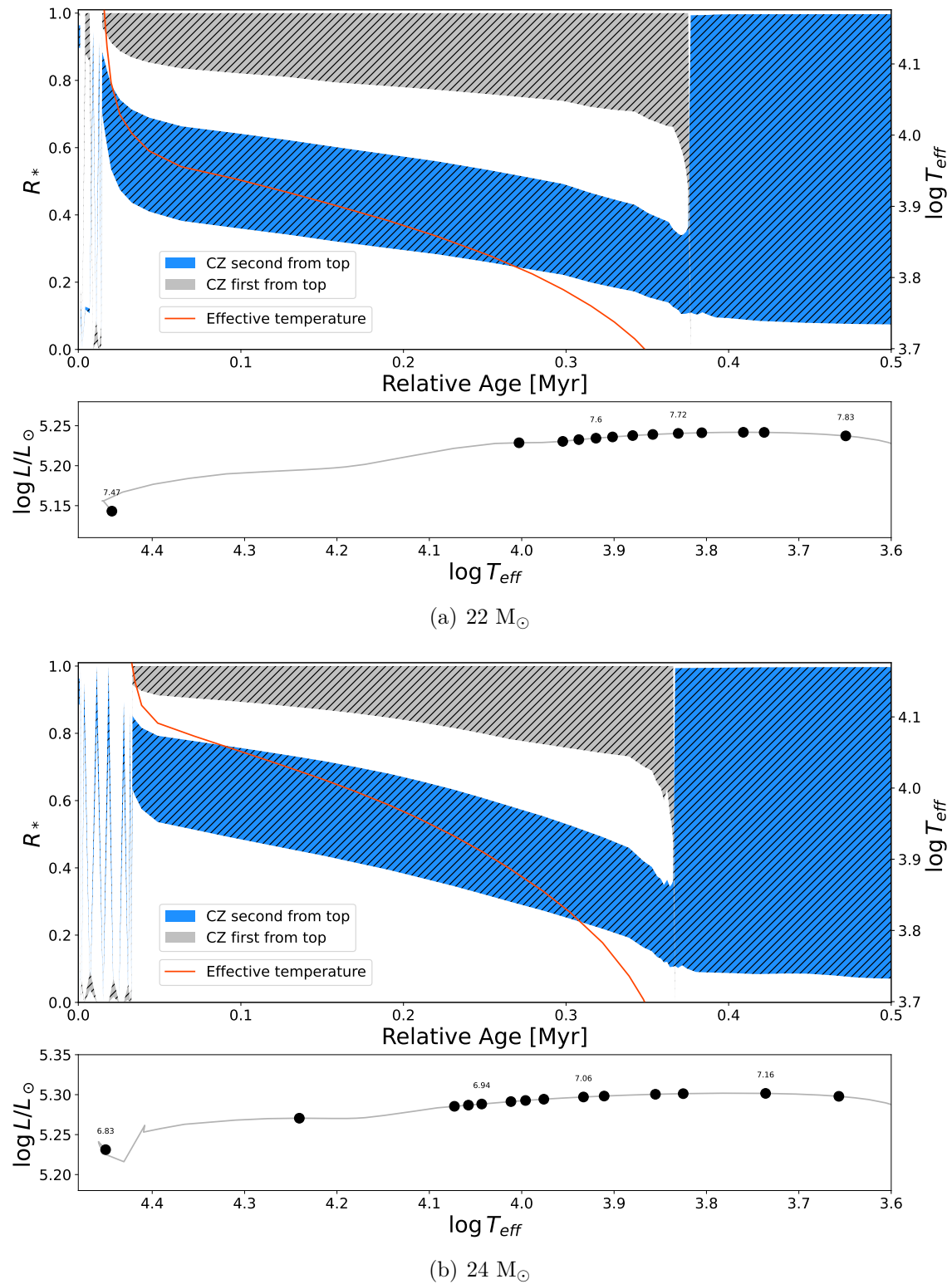


Figure 4.7: Continue of Fig. 4.5

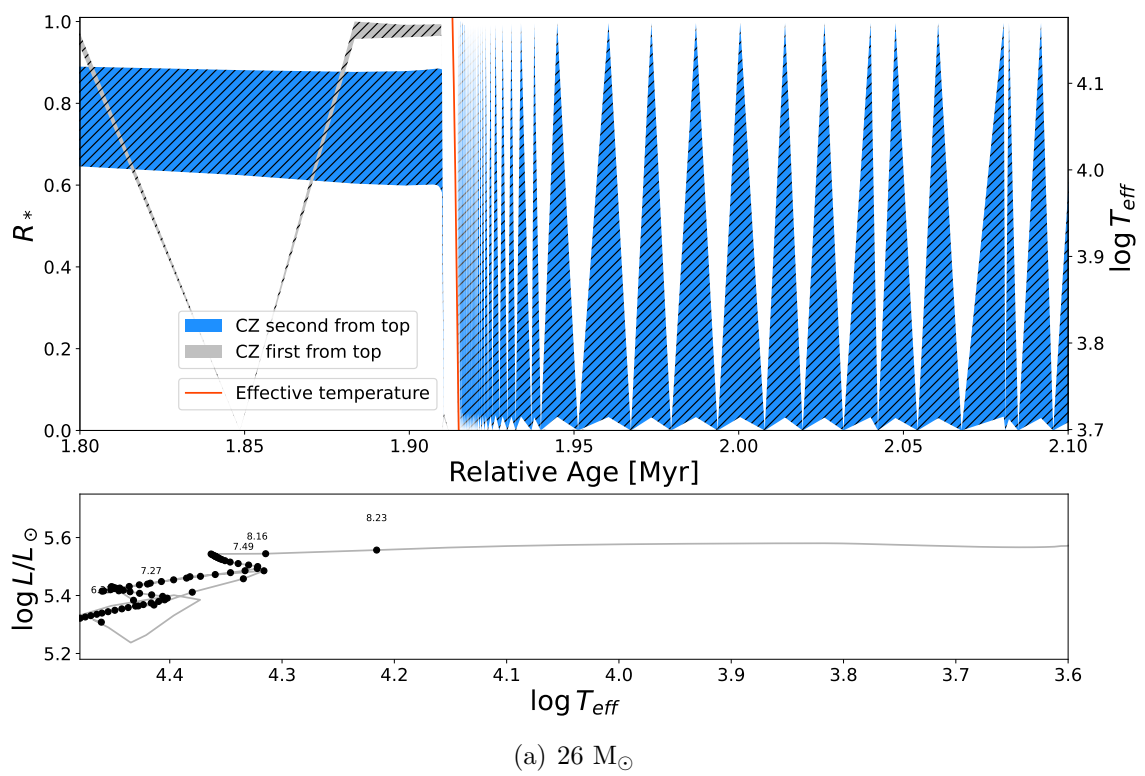


Figure 4.8: Continue of Fig. 4.5



# Conclusion and Future Insights

Late B- and early A-type supergiants are evolved stars found in the transitional region between the Main Sequence and Red Supergiants, that are known for exhibiting a wide range of spectral variations. In addition to exhibiting asymmetries in line wings, variability in line depth, and radial velocities, these stars occasionally display a phenomenon known as High-Velocity Absorption (HVA) events manifesting in the hydrogen Balmer series (most prominently in the  $H\alpha$  line) as a dramatic increase in intensity accompanied by a significant blue shift.

As of now, the presented work is a unique study, which systematizes all available information about B-, and A-type supergiants exhibiting HVAs. The work consists of a historical overview of observed events and the results of analysis of several thousand spectra including the evolution of hypotheses about the processes governing these phenomena.

We analyzed previously published observations of HVA events and extended them with the results of our investigations. Based on the analysis of a large amount of high- and medium-resolution spectra collected from the IACOB database and the database of 2m Perek telescope of Czech Academy of Science we were able to discover several new HVA events (two for HD 199478, one for HD 21291, three for HD 34085 and two for HD 197345), for which we measured main observational properties in  $H\alpha$  line such as blue-edge and core velocities or the time duration of the event. Additionally, in all cases of newly identified events, sudden alternations were found in higher Balmer lines in the form of asymmetries in the blue wing. And, except for HD 199478, no imprint of the event was discovered in photospheric lines, probably suggesting slightly different conditions in the photosphere of HD 199478 during the events.

The duration of the events (several dozens of days up to 4 – 5 months) depends on its strength. The strong ones in which larger deepening and higher blue shift of  $H\alpha$  line profile is observed, last longer than weak events during which the changes in  $H\alpha$  line are not that dramatic. The events generally occur once in 1 – 10 years depending on individual stars. In some cases, especially for Rigel, the strong event is accompanied by a weak one that is distant no more than several months.

Based on collected data we may conclude that supergiants exhibiting HVAs are stars with initial masses in range  $15 \div 25 M_{\odot}$ . At the same time, they show HVA events only in the narrow temperature range  $12\,500 \div 9\,500$  K, which corresponds to spectral classes B6-A2. Magnetic field, binarity, and proper rotation are not the key factors for the occurrence of HVA events. Furthermore, in our quest to identify common parameters among stars exhibiting HVA events, we investigated the internal

structure of stars using the MESA modeling code to reproduce example stars as are represented by HVA events exhibiting supergiants. Specifically, we focused on the processes occurring near the stellar surface which in this case is the existence of sub-surface iron convective zone. Consequently, the processes arising due to the dynamo effect inside this convective zone are proposed as the triggering mechanism behind these peculiar HVA events.

The results of the study provide a considerable basis for future theoretical investigations of the physical processes leading to the HVA phenomenon.

# Bibliography

- [1] Helmut A. Abt. “The Variability of Supergiants.” In: *ApJ* 126 (July 1957), p. 138. DOI: [10.1086/146379](https://doi.org/10.1086/146379).
- [2] Helmut A. Abt and Nidia I. Morrell. “The Relation between Rotational Velocities and Spectral Peculiarities among A-Type Stars”. In: *ApJS* 99 (July 1995), p. 135. DOI: [10.1086/192182](https://doi.org/10.1086/192182).
- [3] L. Achmad, H. J. G. L. M. Lamers, and L. Pasquini. “Radiation driven wind models for A, F and G supergiants.” In: *A&A* 320 (Apr. 1997), pp. 196–208.
- [4] C. Aydin. “Atmospheres of A-type supergiants.” In: *A&A* 19 (July 1972), p. 369.
- [5] S. Bagnulo et al. “The importance of non-photon noise in stellar spectropolarimetry. The spurious detection of a non-existing magnetic field in the A0 supergiant HD 92207”. In: *A&A* 559, A103 (Nov. 2013), A103. DOI: [10.1051/0004-6361/201322319](https://doi.org/10.1051/0004-6361/201322319). arXiv: [1309.2158](https://arxiv.org/abs/1309.2158) [[astro-ph.IM](#)].
- [6] C. A. L. Bailer-Jones et al. “Estimating Distance from Parallaxes. IV. Distances to 1.33 Billion Stars in Gaia Data Release 2”. In: *AJ* 156.2, 58 (Aug. 2018), p. 58. DOI: [10.3847/1538-3881/aacb21](https://doi.org/10.3847/1538-3881/aacb21). arXiv: [1804.10121](https://arxiv.org/abs/1804.10121) (astro-ph.SR).
- [7] C. A. L. Bailer-Jones et al. “Estimating Distances from Parallaxes. V. Geometric and Photogeometric Distances to 1.47 Billion Stars in Gaia Early Data Release 3”. In: *AJ* 161.3, 147 (Mar. 2021), p. 147. DOI: [10.3847/1538-3881/abd806](https://doi.org/10.3847/1538-3881/abd806). arXiv: [2012.05220](https://arxiv.org/abs/2012.05220) [[astro-ph.SR](#)].
- [8] M. J. Barlow and M. Cohen. “Infrared photometry and mass loss rates for OBA supergiants and Of stars.” In: *ApJ* 213 (May 1977), pp. 737–755. DOI: [10.1086/155204](https://doi.org/10.1086/155204).
- [9] R. A. Bartaya et al. “Hypergiant 6 Cas and association Cas OB5.” In: *Bulletin of the Special Astrophysics Observatory* 38 (Jan. 1994), pp. 103–118.
- [10] B. Bates, D. R. Halliwell, and W. Brown-Kerr. “Ultraviolet Spectroscopy of Mass Loss from Late B-Type Supergiants”. In: *Irish Astronomical Journal* 17 (Mar. 1986), p. 256.
- [11] B. Bates et al. “Discrete absorption components and stellar wind features in spectra of beta Ori.” In: *ESA Special Publication*. Ed. by N. Longdon and E. J. Rolfe. Vol. 2. ESA Special Publication. June 1988, pp. 151–154.

- [12] H. Bouy and J. Alves. “Cosmography of OB stars in the solar neighbourhood”. In: *A&A* 584, A26 (Dec. 2015), A26. DOI: [10.1051/0004-6361/201527058](https://doi.org/10.1051/0004-6361/201527058).
- [13] W. Buscombe. “Variations in the spectra of A-type supergiants”. In: *The Observatory* 94 (June 1974), pp. 120–122.
- [14] William Buscombe. “Four Southern A-Type Supergiants”. In: *Astrophysics and Space Science* 23.2 (Aug. 1973), pp. 431–441. DOI: [10.1007/BF00645170](https://doi.org/10.1007/BF00645170).
- [15] William Wallace Campbell et al. “Sixty-eight stars whose radial velocities vary”. In: *Lick Observatory Bulletin* 199 (Jan. 1911), pp. 140–154. DOI: [10.5479/ADS/bib/1911LicOB.6.140C](https://doi.org/10.5479/ADS/bib/1911LicOB.6.140C).
- [16] M. Cantiello et al. “Sub-surface convection zones in hot massive stars and their observable consequences”. In: *A&A* 499.1 (May 2009), pp. 279–290. DOI: [10.1051/0004-6361/200911643](https://doi.org/10.1051/0004-6361/200911643). arXiv: [0903.2049](https://arxiv.org/abs/0903.2049) [[astro-ph.SR](#)].
- [17] M. Catelan and H. A. Smith. *Pulsating Stars*. 2015.
- [18] O. Chesneau et al. “The variable stellar wind of Rigel probed at high spatial and spectral resolution”. In: *A&A* 566, A125 (June 2014), A125. DOI: [10.1051/0004-6361/201322894](https://doi.org/10.1051/0004-6361/201322894). arXiv: [1405.0907](https://arxiv.org/abs/1405.0907) [[astro-ph.SR](#)].
- [19] R. Chini et al. “A spectroscopic survey on the multiplicity of high-mass stars”. In: *MNRAS* 424.3 (Aug. 2012), pp. 1925–1929. DOI: [10.1111/j.1365-2966.2012.21317.x](https://doi.org/10.1111/j.1365-2966.2012.21317.x). arXiv: [1205.5238](https://arxiv.org/abs/1205.5238) [[astro-ph.SR](#)].
- [20] J. S. Clark et al. “On the nature of the galactic early-B hypergiants”. In: *A&A* 541, A145 (May 2012), A145. DOI: [10.1051/0004-6361/201117472](https://doi.org/10.1051/0004-6361/201117472). arXiv: [1202.3991](https://arxiv.org/abs/1202.3991) [[astro-ph.SR](#)].
- [21] David J. Corliss, Nancy D. Morrison, and Saul J. Adelman. “Spectroscopic and Photometric Variability in the A0 Supergiant HR 1040”. In: *AJ* 150.6, 190 (Dec. 2015), p. 190. DOI: [10.1088/0004-6256/150/6/190](https://doi.org/10.1088/0004-6256/150/6/190).
- [22] E. S. G. de Almeida et al. “Combined spectroscopy and intensity interferometry to determine the distances of the blue supergiants P Cygni and Rigel”. In: *MNRAS* 515.1 (Sept. 2022), pp. 1–12. DOI: [10.1093/mnras/stac1617](https://doi.org/10.1093/mnras/stac1617). arXiv: [2204.00372](https://arxiv.org/abs/2204.00372) [[astro-ph.SR](#)].
- [23] A. de Burgos et al. “High-resolution spectroscopic study of massive blue and red supergiants in Perseus OB1. I. Definition of the sample, membership, and kinematics”. In: *A&A* 643, A116 (Nov. 2020), A116. DOI: [10.1051/0004-6361/202039019](https://doi.org/10.1051/0004-6361/202039019). arXiv: [2008.13299](https://arxiv.org/abs/2008.13299) [[astro-ph.SR](#)].
- [24] C. de Jager. *The brightest stars*. 1984.
- [25] C. de Jager, H. Nieuwenhuijzen, and K. A. van der Hucht. “Mass loss rates in the Hertzsprung-Russell diagram.” In: *A&AS* 72 (Feb. 1988), pp. 259–289.
- [26] L. Denizman and M. Hack. “Spectra and radial velocities of white supergiants.” In: *A&AS* 75 (Oct. 1988), pp. 79–92.



- [27] Trevor Z. Dorn-Wallenstein et al. “Short-term Variability of Evolved Massive Stars with TESS. II. A New Class of Cool, Pulsating Supergiants”. In: *ApJ* 902.1, 24 (Oct. 2020), p. 24. DOI: [10.3847/1538-4357/abb318](https://doi.org/10.3847/1538-4357/abb318). arXiv: [2008.11723](https://arxiv.org/abs/2008.11723) [astro-ph.SR].
- [28] J. R. Ducati. “VizieR Online Data Catalog: Catalogue of Stellar Photometry in Johnson’s 11-color system.” In: *VizieR Online Data Catalog* (Jan. 2002).
- [29] J. A. Eaton and M. H. Williamson. “Managing the operations of the TSU 2-m Automatic Spectroscopic Telescope”. In: *Astronomische Nachrichten* 325.6 (Oct. 2004), pp. 522–526. DOI: [10.1002/asna.200410272](https://doi.org/10.1002/asna.200410272).
- [30] D. Ebbets. “The structure and variability of H  $\alpha$  emission in early-type supergiants.” In: *ApJS* 48 (Apr. 1982), pp. 399–414. DOI: [10.1086/190783](https://doi.org/10.1086/190783).
- [31] Edward Arthur Fath. “Pulsation in stellar atmospheres ; Atmospheric extinction at Mt. Hamilton”. In: *Lick Observatory Bulletin* 474 (Jan. 1935), pp. 115–121. DOI: [10.5479/ADS/bib/1935LicOB.17.115F](https://doi.org/10.5479/ADS/bib/1935LicOB.17.115F).
- [32] M. Firnstein and N. Przybilla. “Quantitative spectroscopy of Galactic BA-type supergiants. I. Atmospheric parameters”. In: *A&A* 543, A80 (July 2012), A80. DOI: [10.1051/0004-6361/201219034](https://doi.org/10.1051/0004-6361/201219034). arXiv: [1207.0308](https://arxiv.org/abs/1207.0308) (astro-ph.SR).
- [33] William J. Fischer and Nancy D. Morrison. “Spectrum Variability of the A-Type Supergiant Star HD 223960”. In: *Publications of the ASP* 113.785 (July 2001), pp. 821–828. DOI: [10.1086/322141](https://doi.org/10.1086/322141).
- [34] A. W. Fullerton, D. R. Gies, and C. T. Bolton. “Absorption Line Profile Variations among the O Stars. I. The Incidence of Variability”. In: *ApJS* 103 (Apr. 1996), p. 475. DOI: [10.1086/192285](https://doi.org/10.1086/192285).
- [35] Gaia Collaboration. *VizieR Online Data Catalog: Gaia DR3 Part 1. Main source (Gaia Collaboration, 2022)*. VizieR On-line Data Catalog: I/355. Originally published in: *Astron. Astrophys.*, in prep. (2022). May 2022. DOI: [10.26093/cds/vizier.1355](https://doi.org/10.26093/cds/vizier.1355).
- [36] Gaia Collaboration. “VizieR Online Data Catalog: Gaia EDR3 (Gaia Collaboration, 2020)”. In: *VizieR Online Data Catalog*, I/350 (Nov. 2020), pp. I/350.
- [37] Gaia Collaboration et al. “Gaia Data Release 2. Summary of the contents and survey properties”. In: *A&A* 616, A1 (Aug. 2018), A1. DOI: [10.1051/0004-6361/201833051](https://doi.org/10.1051/0004-6361/201833051). arXiv: [1804.09365](https://arxiv.org/abs/1804.09365) [astro-ph.GA].
- [38] R. F. Garrison and R. O. Gray. “The Late B-Type Stars: Refined MK Classification, Confrontation With Stromgren Photometry, And The Effects of Rotation”. In: *AJ* 107 (Apr. 1994), p. 1556. DOI: [10.1086/116967](https://doi.org/10.1086/116967).
- [39] A. Gautschy. “Deneb’s variability: a hint of a deep-lying convection zone?” In: *A&A* 498.1 (Apr. 2009), pp. 273–279. DOI: [10.1051/0004-6361/200911666](https://doi.org/10.1051/0004-6361/200911666).
- [40] A. Gautschy. “Exciting alpha Cygni.” In: *MNRAS* 259 (Nov. 1992), pp. 82–88. DOI: [10.1093/mnras/259.1.82](https://doi.org/10.1093/mnras/259.1.82).

- [41] C. Georgy, H. Saio, and G. Meynet. “The puzzle of the CNO abundances of  $\alpha$  Cygni variables resolved by the Ledoux criterion.” In: *MNRAS* 439 (Mar. 2014), pp. L6–L10. DOI: [10.1093/mnrasl/slt165](https://doi.org/10.1093/mnrasl/slt165). arXiv: [1311.4744](https://arxiv.org/abs/1311.4744) [[astro-ph.SR](#)].
- [42] E. Gerth et al. “Magnetic field measurements of the supergiant  $\nu$  Cep.” In: *Astronomische Nachrichten* 312 (Feb. 1991), p. 107. DOI: [10.1002/asna.2113120209](https://doi.org/10.1002/asna.2113120209).
- [43] Wolfgang Glatzel and Stefanie Mehren. “Non-radial pulsations and stability of massive stars”. In: *MNRAS* 282.4 (Oct. 1996), pp. 1470–1482. DOI: [10.1093/mnras/282.4.1470](https://doi.org/10.1093/mnras/282.4.1470).
- [44] G. A. Gontcharov. “Pulkovo Compilation of Radial Velocities for 35 495 Hipparcos stars in a common system”. In: *Astronomy Letters* 32.11 (Nov. 2006), pp. 759–771. DOI: [10.1134/S1063773706110065](https://doi.org/10.1134/S1063773706110065). arXiv: [1606.08053](https://arxiv.org/abs/1606.08053) [[astro-ph.SR](#)].
- [45] R. O. Gray and R. F. Garrison. “The Early A-Type Stars: Refined MK Classification, Confrontation with Stroemgren Photometry, and the Effects of Rotation”. In: *ApJS* 65 (Dec. 1987), p. 581. DOI: [10.1086/191237](https://doi.org/10.1086/191237).
- [46] F. Grundahl et al. “SONG - getting ready for the prototype”. In: *GONG-SoHO 24: A New Era of Seismology of the Sun and Solar-Like Stars*. Vol. 271. Journal of Physics Conference Series. IOP, Jan. 2011, 012083, p. 012083. DOI: [10.1088/1742-6596/271/1/012083](https://doi.org/10.1088/1742-6596/271/1/012083).
- [47] G. L. H. Harris. “Evolved stars in open clusters.” In: *ApJS* 30 (Apr. 1976), pp. 451–490. DOI: [10.1086/190368](https://doi.org/10.1086/190368).
- [48] M. Haucke et al. “Wind properties of variable B supergiants. Evidence of pulsations connected with mass-loss episodes”. In: *A&A* 614, A91 (June 2018), A91. DOI: [10.1051/0004-6361/201731678](https://doi.org/10.1051/0004-6361/201731678). arXiv: [1902.01341](https://arxiv.org/abs/1902.01341) ([astro-ph.SR](#)).
- [49] G. M. Hill, G. A. H. Walker, and S. Yang. “The MV - W (H-gamma) calibration for O6 to A3 supergiants.” In: *Publications of the ASP* 98 (Nov. 1986), pp. 1186–1192. DOI: [10.1086/131919](https://doi.org/10.1086/131919).
- [50] N. Houk and A. P. Cowley. *University of Michigan Catalogue of two-dimensional spectral types for the HD stars. Volume I. Declinations -90 to -53 $^{\circ}$ 00'*. 1975.
- [51] Ian D. Howarth. “Discrete absorption components in O-type stars”. In: *The Atmospheres of Early-Type Stars*. Ed. by Ulrich Heber and C. Simon Jeffery. Vol. 401. 1992, p. 131. DOI: [10.1007/3-540-55256-1\\_293](https://doi.org/10.1007/3-540-55256-1_293).
- [52] Ivan Hubeny and Claus Leitherer. “On the Interpretation of Emission Wings of Balmer Lines in Luminous Blue Variables”. In: *Publications of the ASP* 101 (Jan. 1989), p. 114. DOI: [10.1086/132408](https://doi.org/10.1086/132408).
- [53] S. Hubrig et al. “Magnetic field detection in the bright A0-type supergiant HD 92207”. In: *A&A* 546, L6 (Oct. 2012), p. L6. DOI: [10.1051/0004-6361/201220265](https://doi.org/10.1051/0004-6361/201220265).

- [54] R. M. Humphreys. “Studies of luminous stars in nearby galaxies. I. Supergiants and O stars in the Milky Way.” In: *ApJS* 38 (Dec. 1978), pp. 309–350. DOI: [10.1086/190559](https://doi.org/10.1086/190559).
- [55] M. O. Inoue. “Variation in radial velocities and line profiles of Alpha Cygni (A2 Ia).” In: *Publications of the ASJ* 31 (Jan. 1979), pp. 11–21.
- [56] N. Ismailov and Sh Ismayilova. “High-velocity absorption and emission in the spectrum of supergiant HD 199478”. In: *Monthly Notices of the Royal Astronomical Society* 485 (May 2019), pp. 3558–3568. DOI: [10.1093/mnras/stz646](https://doi.org/10.1093/mnras/stz646).
- [57] N. Z. Ismailov and Sh. K. Ismailova. “Photospheric Variability of the Late B-Supergiant HD199478”. In: *Azerbaijani Astronomical Journal* 16.1 (Nov. 2021), pp. 56–82.
- [58] N. Z. Ismailov and Sh K. Ismayilova. “High-velocity absorption and emission in the spectrum of supergiant HD 199478”. In: *MNRAS* 485.3 (May 2019), pp. 3558–3568. DOI: [10.1093/mnras/stz646](https://doi.org/10.1093/mnras/stz646).
- [59] N. Z. Ismailov and Sh K. Ismayilova. “Photospheric variability of the late B supergiant HD 199478”. In: *MNRAS* 502.1 (Mar. 2021), pp. 157–175. DOI: [10.1093/mnras/staa3542](https://doi.org/10.1093/mnras/staa3542).
- [60] Sh. K. Ismayilova and N. Z. Ismailov. “On the Variation of Absorption Lines in the Spectrum of the Late SG Star HD 199478”. In: *Azerbaijani Astronomical Journal* 15.2 (Dec. 2020), pp. 147–153.
- [61] G. Israelian, E. Chentsov, and F. Musaev. “The inhomogeneous circumstellar envelope of Rigel (beta Orionis A)”. In: *MNRAS* 290.3 (Sept. 1997), pp. 521–532. DOI: [10.1093/mnras/290.3.521](https://doi.org/10.1093/mnras/290.3.521).
- [62] Adam S. Jermyn et al. “Modules for Experiments in Stellar Astrophysics (MESA): Time-dependent Convection, Energy Conservation, Automatic Differentiation, and Infrastructure”. In: *ApJS* 265.1, 15 (Mar. 2023), p. 15. DOI: [10.3847/1538-4365/acae8d](https://doi.org/10.3847/1538-4365/acae8d). arXiv: [2208.03651](https://arxiv.org/abs/2208.03651) [[astro-ph.SR](#)].
- [63] A. Kaufer, O. Stahl, and B. Wolf. “Spectroscopic monitoring of BA-type supergiants.” In: *Astronomische Gesellschaft Abstract Series*. Vol. 10. Astronomische Gesellschaft Abstract Series. Jan. 1994, pp. 41–41.
- [64] A. Kaufer et al. “FEROS, the fiber-fed extended range optical spectrograph for the ESO 1.52-m telescope.” In: *The Messenger* 89 (Sept. 1997), pp. 1–4.
- [65] A. Kaufer et al. “Long-term spectroscopic monitoring of BA-type supergiants. I.  $H_{\alpha}$ -line-profile variability.” In: *A&A* 305 (Jan. 1996), p. 887.
- [66] A. Kaufer et al. “Long-term spectroscopic monitoring of BA-type supergiants. II. High-velocity absorptions in  $\beta$ Ori and HD96919.” In: *A&A* 314 (Oct. 1996), pp. 599–608.
- [67] A. Kaufer et al. “Long-term spectroscopic monitoring of BA-type supergiants. III. Variability of photospheric lines.” In: *A&A* 320 (Apr. 1997), pp. 273–286.

- [68] A. Kaufer et al. “The Circumstellar Environment of Rigel Probed at High Spatial and Spectral Resolution”. In: *Circumstellar Dynamics at High Resolution*. Ed. by A. C. Carciofi and Th. Rivinius. Vol. 464. Astronomical Society of the Pacific Conference Series. Dec. 2012, p. 35.
- [69] Andreas Kaufer. “Variable Circumstellar Structure of Luminous Hot Stars: the Impact of Spectroscopic Long-term Campaigns”. In: *Reviews in Modern Astronomy* 11 (Jan. 1998), p. 177.
- [70] P. Kervella et al. “The angular sizes of dwarf stars and subgiants. Surface brightness relations calibrated by interferometry”. In: *A&A* 426 (Oct. 2004), pp. 297–307. DOI: [10.1051/0004-6361:20035930](https://doi.org/10.1051/0004-6361:20035930). arXiv: [astro-ph/0404180](https://arxiv.org/abs/astro-ph/0404180) [[astro-ph](#)].
- [71] Pierre Kervella et al. “Stellar and substellar companions of nearby stars from Gaia DR2. Binarity from proper motion anomaly”. In: *A&A* 623, A72 (Mar. 2019), A72. DOI: [10.1051/0004-6361/201834371](https://doi.org/10.1051/0004-6361/201834371). arXiv: [1811.08902](https://arxiv.org/abs/1811.08902) [[astro-ph.SR](#)].
- [72] N. V. Kharchenko and S. Roeser. *VizieR Online Data Catalog: All-Sky Compiled Catalogue of 2.5 million stars (Kharchenko+ 2009)*. VizieR On-line Data Catalog: I/280B. Originally published in: 2001KFNT...17e.409K. Sept. 2009.
- [73] N. V. Kharchenko et al. “Astrophysical supplements to the ASCC-2.5: Ia. Radial velocities of  $\sim 55000$  stars and mean radial velocities of 516 Galactic open clusters and associations”. In: *Astronomische Nachrichten* 328.9 (Nov. 2007), p. 889. DOI: [10.1002/asna.200710776](https://doi.org/10.1002/asna.200710776). arXiv: [0705.0878](https://arxiv.org/abs/0705.0878) [[astro-ph](#)].
- [74] S. Kikuchi. “Time Variation of the  $H\alpha$  Profile of Beta Orionis”. In: *Publications of the ASJ* 20 (Jan. 1968), p. 190.
- [75] Rudolf Kippenhahn and Alfred Weigert. *Stellar Structure and Evolution*. 1990.
- [76] P. Koubský et al. “Ondřejov Echelle Spectrograph - OES”. In: *Publications of the Astronomical Institute of the Czechoslovak Academy of Sciences* 92 (Jan. 2004), pp. 37–43.
- [77] R. P. Kudritzki et al. “The wind momentum-luminosity relationship of galactic A- and B-supergiants”. In: *A&A* 350 (Oct. 1999), pp. 970–984. arXiv: [astro-ph/9910449](https://arxiv.org/abs/astro-ph/9910449) [[astro-ph](#)].
- [78] H. J. G. L. M. Lamers. “Mass loss from O and B stars.” In: *ApJ* 245 (Apr. 1981), pp. 593–608. DOI: [10.1086/158835](https://doi.org/10.1086/158835).
- [79] Henny J. G. L. M. Lamers, Theodore P. Snow, and Douglas M. Lindholm. “Terminal Velocities and the Bistability of Stellar Winds”. In: *ApJ* 455 (Dec. 1995), p. 269. DOI: [10.1086/176575](https://doi.org/10.1086/176575).
- [80] O. J. Lee. “The radial velocity of alpha Cygni.” In: *ApJ* 34 (Nov. 1911), pp. 303–307. DOI: [10.1086/141890](https://doi.org/10.1086/141890).

- [81] K. Lefever, J. Puls, and C. Aerts. “Statistical properties of a sample of periodically variable B-type supergiants. Evidence for opacity-driven gravity-mode oscillations”. In: *A&A* 463.3 (Mar. 2007), pp. 1093–1109. DOI: [10.1051/0004-6361:20066038](https://doi.org/10.1051/0004-6361:20066038). arXiv: [astro-ph/0611484](https://arxiv.org/abs/astro-ph/0611484) [astro-ph].
- [82] O. H. Levato. “Rotational Velocities and Spectral Types of Some A-Type Stars”. In: *Publications of the ASP* 84.500 (Aug. 1972), p. 584. DOI: [10.1086/129336](https://doi.org/10.1086/129336).
- [83] L. B. Lucy. “An analysis of the variable radial velocity of Alpha Cygni.” In: *ApJ* 206 (June 1976), pp. 499–508. DOI: [10.1086/154405](https://doi.org/10.1086/154405).
- [84] L. S. Luud, E. A. Ruusalepp, and A. A. Kaasik. “Anomalous line profiles for the Fe II (42) multiplet in the spectrum of Deneb.” In: *Soviet Astronomy Letters* 4 (Apr. 1978), pp. 151–152.
- [85] David A. Lyder. “The Stars in Camelopardalis OB1: Their Distance and Evolutionary History”. In: *AJ* 122.5 (Nov. 2001), pp. 2634–2643. DOI: [10.1086/323705](https://doi.org/10.1086/323705).
- [86] Y. M. Maharramov and A. Sh. Baloglanov. “Spectroscopic Variability of the Supergiants HD21389 and HD187982”. In: *Odessa Astronomical Publications* 28 (Jan. 2015), p. 39.
- [87] J. Maíz Apellániz et al. “Lucky spectroscopy, an equivalent technique to lucky imaging. II. Spatially resolved intermediate-resolution blue-violet spectroscopy of 19 close massive binaries using the William Herschel Telescope”. In: *A&A* 646, A11 (Feb. 2021), A11. DOI: [10.1051/0004-6361/202039479](https://doi.org/10.1051/0004-6361/202039479). arXiv: [2011.12250](https://arxiv.org/abs/2011.12250) [astro-ph.SR].
- [88] H. Mandel. “High Resolution Spectroscopy with a Fibre-Linked Echelle - Spectrograph”. In: *The Impact of Very High S/N Spectroscopy on Stellar Physics*. Ed. by G. Cayrel de Strobel and Monique Spite. Vol. 132. Jan. 1988, p. 9.
- [89] N. Markova and J. Puls. “Bright OB stars in the Galaxy. IV. Stellar and wind parameters of early to late B supergiants”. In: *A&A* 478.3 (Feb. 2008), pp. 823–842. DOI: [10.1051/0004-6361:20077919](https://doi.org/10.1051/0004-6361:20077919). arXiv: [0711.1110](https://arxiv.org/abs/0711.1110) (astro-ph).
- [90] N. Markova and T. Valchev. “Spectral variability of luminous early type stars. I. Peculiar supergiant HD199478”. In: *A&A* 363 (Nov. 2000), pp. 995–1004.
- [91] N. Markova et al. “Wind structure of late B supergiants. I. Multi-line analyses of near-surface and wind structure in HD 199 478 (B8 Iae)”. In: *A&A* 487.1 (Aug. 2008), pp. 211–221. DOI: [10.1051/0004-6361:200809376](https://doi.org/10.1051/0004-6361:200809376). arXiv: [0806.0929](https://arxiv.org/abs/0806.0929) [astro-ph].
- [92] Paul W. Merrill and Cora G. Burwell. “Catalogue and Bibliography of Stars of Classes B and A whose Spectra have Bright Hydrogen Lines”. In: *ApJ* 78 (Sept. 1933), p. 87. DOI: [10.1086/143490](https://doi.org/10.1086/143490).

- [93] Paul W. Merrill and Cora G. Burwell. “Supplement to the Mount Wilson Catalogue and Bibliography of Stars of Classes B and a whose Spectra have Bright Hydrogen Lines.” In: *ApJ* 98 (Sept. 1943), p. 153. DOI: [10.1086/144557](https://doi.org/10.1086/144557).
- [94] Ehsan Moravveji, Andres Moya, and Edward F. Guinan. “Asteroseismology of the nearby SN II Progenitor Rigel. II. epsilon-mechanism Triggering Gravity-mode Pulsations?” In: *ApJ* 749.1, 74 (Apr. 2012), p. 74. DOI: [10.1088/0004-637X/749/1/74](https://doi.org/10.1088/0004-637X/749/1/74). arXiv: [1202.1836](https://arxiv.org/abs/1202.1836) [[astro-ph.SR](#)].
- [95] W. W. Morgan and Nancy G. Roman. “Revised Standards for Supergiants on the System of the Yerkes Spectral Atlas.” In: *ApJ* 112 (Nov. 1950), pp. 362–364. DOI: [10.1086/145351](https://doi.org/10.1086/145351).
- [96] N. D. Morrison and C. L. Mulliss. “Recent Results from High-Resolution H $\alpha$  Spectroscopic Monitoring of alpha Cygni”. In: *Bulletin of the American Astronomical Society*. Vol. 191. Jan. 1998, 125.04, p. 125.04.
- [97] N. D. Morrison, R. Rother, and N. Kurschat. “H $\alpha$  line profile variability in the B8Ia-type supergiant Rigel ( $\beta$  Ori)”. In: *Clumping in Hot-Star Winds*. Ed. by Wolf-Rainer Hamann, Achim Feldmeier, and Lidia M. Oskinova. Apr. 2008, p. 155.
- [98] D. J. Mullan. “Corotating interaction regions in stellar winds”. In: *ApJ* 283 (Aug. 1984), pp. 303–312. DOI: [10.1086/162307](https://doi.org/10.1086/162307).
- [99] S. P. Owocki et al. “Centrifugal breakout reconnection as the electron acceleration mechanism powering the radio magnetospheres of early-type stars”. In: *MNRAS* 513.1 (June 2022), pp. 1449–1458. DOI: [10.1093/mnras/stac341](https://doi.org/10.1093/mnras/stac341). arXiv: [2202.05449](https://arxiv.org/abs/2202.05449) [[astro-ph.SR](#)].
- [100] E. N. Parker. “The generation of magnetic fields in astrophysical bodies. X. Magnetic buoyancy and the solar dynamo.” In: *ApJ* 198 (May 1975), pp. 205–209. DOI: [10.1086/153593](https://doi.org/10.1086/153593).
- [101] Bill Paxton et al. “Modules for Experiments in Stellar Astrophysics (MESA)”. In: *ApJS* 192.1, 3 (Jan. 2011), p. 3. DOI: [10.1088/0067-0049/192/1/3](https://doi.org/10.1088/0067-0049/192/1/3). arXiv: [1009.1622](https://arxiv.org/abs/1009.1622) [[astro-ph.SR](#)].
- [102] Bill Paxton et al. “Modules for Experiments in Stellar Astrophysics (MESA): Binaries, Pulsations, and Explosions”. In: *ApJS* 220.1, 15 (Sept. 2015), p. 15. DOI: [10.1088/0067-0049/220/1/15](https://doi.org/10.1088/0067-0049/220/1/15). arXiv: [1506.03146](https://arxiv.org/abs/1506.03146) [[astro-ph.SR](#)].
- [103] Bill Paxton et al. “Modules for Experiments in Stellar Astrophysics (MESA): Convective Boundaries, Element Diffusion, and Massive Star Explosions”. In: *ApJS* 234.2, 34 (Feb. 2018), p. 34. DOI: [10.3847/1538-4365/aaa5a8](https://doi.org/10.3847/1538-4365/aaa5a8). arXiv: [1710.08424](https://arxiv.org/abs/1710.08424) [[astro-ph.SR](#)].
- [104] Bill Paxton et al. “Modules for Experiments in Stellar Astrophysics (MESA): Planets, Oscillations, Rotation, and Massive Stars”. In: *ApJS* 208.1, 4 (Sept. 2013), p. 4. DOI: [10.1088/0067-0049/208/1/4](https://doi.org/10.1088/0067-0049/208/1/4). arXiv: [1301.0319](https://arxiv.org/abs/1301.0319) [[astro-ph.SR](#)]. ■



- [105] Bill Paxton et al. “Modules for Experiments in Stellar Astrophysics (MESA): Pulsating Variable Stars, Rotation, Convective Boundaries, and Energy Conservation”. In: *ApJS* 243.1, 10 (July 2019), p. 10. DOI: [10.3847/1538-4365/ab2241](https://doi.org/10.3847/1538-4365/ab2241). arXiv: [1903.01426](https://arxiv.org/abs/1903.01426) [astro-ph.SR].
- [106] J. R. Percy and D. L. Welch. “Photometric variability of B- and A-type supergiants.” In: *Publications of the ASP* 95 (Aug. 1983), pp. 491–505. DOI: [10.1086/131198](https://doi.org/10.1086/131198).
- [107] K. Pivonková et al. “Spectral Variability of Supergiant HD21389”. In: *Azerbaijani Astronomical Journal* 17.2 (Dec. 2022), pp. 88–99.
- [108] Kateřina Pivoňková. *Spectral variability of evolved supergiants: study of HD 21389*. Bakalářská práce. Brno, 2022. URL: <https://is.muni.cz/th/eo077/>.
- [109] J. S. Plaskett. “The spectroscopic binary beta Orionis.” In: *ApJ* 30 (July 1909), pp. 26–32. DOI: [10.1086/141674](https://doi.org/10.1086/141674).
- [110] R. K. Prinja and I. D. Howarth. “The effects of episodic mass-loss enhancements on theoretical P Cygni profiles.” In: *A&A* 149 (Aug. 1985), pp. 73–82.
- [111] N. Przybilla et al. “Quantitative spectroscopy of BA-type supergiants”. In: *A&A* 445.3 (Jan. 2006), pp. 1099–1126. DOI: [10.1051/0004-6361:20053832](https://doi.org/10.1051/0004-6361:20053832). arXiv: [astro-ph/0509669](https://arxiv.org/abs/astro-ph/0509669) [astro-ph].
- [112] G. Raskin et al. “HERMES: a high-resolution fibre-fed spectrograph for the Mercator telescope”. In: *A&A* 526, A69 (Feb. 2011), A69. DOI: [10.1051/0004-6361/201015435](https://doi.org/10.1051/0004-6361/201015435). arXiv: [1011.0258](https://arxiv.org/abs/1011.0258) [astro-ph.IM].
- [113] N. D. Richardson et al. “A Five-year Spectroscopic and Photometric Campaign on the Prototypical  $\alpha$  Cygni Variable and A-type Supergiant Star Deneb”. In: *AJ* 141.1, 17 (Jan. 2011), p. 17. DOI: [10.1088/0004-6256/141/1/17](https://doi.org/10.1088/0004-6256/141/1/17). arXiv: [1009.5994](https://arxiv.org/abs/1009.5994) [astro-ph.SR].
- [114] J. D. Rosendhal. “A survey of H-alpha emission in early-type high-luminosity stars.” In: *ApJ* 186 (Dec. 1973), p. 909. DOI: [10.1086/152555](https://doi.org/10.1086/152555).
- [115] J. D. Rosendhal. “Observations of some early-type supergiants with variable Halpha profiles.” In: *ApJ* 182 (June 1973), p. 523. DOI: [10.1086/152160](https://doi.org/10.1086/152160).
- [116] Sara Rother. “A Time Series Study of Rigel, a B8Ia Supergiant”. MA thesis. University of Toledo, Ohio, Nov. 2009.
- [117] A. Kh. Rzaev, S. K. Zeinalov, and E. L. Chentsov. “Investigation of the non-stationarity of the HD 21291 atmosphere.” In: *Kinematika i Fizika Nebesnykh Tel* 5 (Jan. 1989), pp. 75–79.
- [118] Abid Kh Rzaev. “Peculiarities of radial velocity variability of lines in the spectrum of  $\alpha$  Cyg supergiant”. In: *MNRAS* 524.2 (Sept. 2023), pp. 1735–1745. DOI: [10.1093/mnras/stad1995](https://doi.org/10.1093/mnras/stad1995).
- [119] Saio et al. “MOST Detects g- and p-Modes in the B Supergiant HD 163899 (B2 Ib/II)”. In: *ApJ* 650.2 (Oct. 2006), pp. 1111–1118. DOI: [10.1086/507409](https://doi.org/10.1086/507409). arXiv: [astro-ph/0606712](https://arxiv.org/abs/astro-ph/0606712) [astro-ph].

- [120] Hideyuki Saio, Cyril Georgy, and Georges Meynet. “Evolution of blue supergiants and  $\alpha$  Cygni variables: puzzling CNO surface abundances”. In: *MNRAS* 433.2 (Aug. 2013), pp. 1246–1257. DOI: [10.1093/mnras/stt796](https://doi.org/10.1093/mnras/stt796). arXiv: [1305.2474](https://arxiv.org/abs/1305.2474) [astro-ph.SR].
- [121] Z. A. Samedov et al. “HD207260 (A2 Iae) Star Atmosphere: Fundamental Parameters, Abundance of Elements”. In: *Azerbaijani Astronomical Journal* 16.2 (Dec. 2021), pp. 80–85.
- [122] N. N. Samus’ et al. “General catalogue of variable stars: Version GCVS 5.1”. In: *Astronomy Reports* 61.1 (Jan. 2017), pp. 80–88. DOI: [10.1134/S1063772917010085](https://doi.org/10.1134/S1063772917010085).
- [123] Roscoe F. Sanford. “Spectroscopic Observations of Rigel with High Dispersion.” In: *ApJ* 105 (Mar. 1947), p. 222. DOI: [10.1086/144897](https://doi.org/10.1086/144897).
- [124] G. Schaller et al. “New Grids of Stellar Models from 0.8-SOLAR-MASS to 120-SOLAR-MASSSES at Z=0.020 and Z=0.001”. In: *A&AS* 96 (Dec. 1992), p. 269.
- [125] F. Schiller and N. Przybilla. “Quantitative spectroscopy of Deneb”. In: *A&A* 479.3 (Mar. 2008), pp. 849–858. DOI: [10.1051/0004-6361:20078590](https://doi.org/10.1051/0004-6361:20078590). arXiv: [0712.0040](https://arxiv.org/abs/0712.0040) [astro-ph].
- [126] G. Scholz and E. Gerth. “Magnetic field evidence for the supergiant  $\nu$  Cep.” In: *MNRAS* 195 (June 1981), pp. 853–855. DOI: [10.1093/mnras/195.4.853](https://doi.org/10.1093/mnras/195.4.853).
- [127] M. Shultz et al. “An observational evaluation of magnetic confinement in the winds of BA supergiants”. In: *MNRAS* 438.2 (Feb. 2014), pp. 1114–1126. DOI: [10.1093/mnras/stt2260](https://doi.org/10.1093/mnras/stt2260). arXiv: [1311.5116](https://arxiv.org/abs/1311.5116) [astro-ph.SR].
- [128] S. Simón-Díaz et al. “The IACOB project: A grid-based automatic tool for the quantitative spectroscopic analysis of O-stars”. In: *Journal of Physics Conference Series*. Vol. 328. Journal of Physics Conference Series. Dec. 2011, 012021, p. 012021. DOI: [10.1088/1742-6596/328/1/012021](https://doi.org/10.1088/1742-6596/328/1/012021). arXiv: [1111.1341](https://arxiv.org/abs/1111.1341) [astro-ph.SR].
- [129] Miroslav Slechta and Petr Skoda. “2-meter telescope devices: coudé slit spectrograph and HEROS”. In: *Publications of the Astronomical Institute of the Czechoslovak Academy of Sciences* 90 (Jan. 2002), pp. 1–4.
- [130] Jr. Snow T. P. “Long-term changes in ultraviolet P Cygni profiles observed with Copernicus.” In: *ApJ* 217 (Nov. 1977), pp. 760–770. DOI: [10.1086/155622](https://doi.org/10.1086/155622).
- [131] Jr. Snow T. P. and D. C. Morton. “Copernicus ultraviolet observations of mass-loss effects in O and B stars.” In: *ApJS* 32 (Nov. 1976), pp. 429–465. DOI: [10.1086/190404](https://doi.org/10.1086/190404).
- [132] *Stellar Classification Table*. <http://www.isthe.com/chongo/tech/astro/HR-temp-mass-table-byhrclass.html>. Accessed: 2024-04-03.
- [133] Richard B. Stothers and Chao-Wen Chin. “Dynamical Instability as the Cause of the Massive Outbursts in  $\eta$  Carinae and Other Luminous Blue Variables”. In: *ApJL* 408 (May 1993), p. L85. DOI: [10.1086/186837](https://doi.org/10.1086/186837).



- [134] V. Straižys and V. Laugalys. “Young Stars and Clouds in Camelopardalis”. In: *Handbook of Star Forming Regions, Volume I*. Ed. by B. Reipurth. Vol. 4. 2008, p. 294. DOI: [10.48550/arXiv.0811.2992](https://doi.org/10.48550/arXiv.0811.2992).
- [135] Yoichi Takeda and Masahide Takada-Hidai. “Helium and Carbon Abundances in Late-B and Early-A Supergiants”. In: *Publications of the ASJ* 52 (Feb. 2000), p. 113. DOI: [10.1093/pasj/52.1.113](https://doi.org/10.1093/pasj/52.1.113).
- [136] Yoichi Takeda and Masahide Takada-Hidai. “On the Abundances of Nitrogen and Sulfur in Late-B through F Supergiants Atmospheres”. In: *Publications of the ASJ* 47 (Apr. 1995), pp. 169–188.
- [137] A. Talavera and A. I. Gomez de Castro. “The UV high resolution spectrum of A-type supergiants.” In: *A&A* 181 (July 1987), pp. 300–314.
- [138] J. H. Telting et al. “FIES: The high-resolution Fiber-fed Echelle Spectrograph at the Nordic Optical Telescope”. In: *Astronomische Nachrichten* 335.1 (Jan. 2014), p. 41. DOI: [10.1002/asna.201312007](https://doi.org/10.1002/asna.201312007).
- [139] A. A. Tokovinin. “MSC - a catalogue of physical multiple stars”. In: *A&AS* 124 (July 1997), pp. 75–84. DOI: [10.1051/aas:1997181](https://doi.org/10.1051/aas:1997181).
- [140] F. van Leeuwen. “Validation of the new Hipparcos reduction”. In: *A&A* 474.2 (Nov. 2007), pp. 653–664. DOI: [10.1051/0004-6361:20078357](https://doi.org/10.1051/0004-6361:20078357). arXiv: [0708.1752](https://arxiv.org/abs/0708.1752) [[astro-ph](#)].
- [141] Kim A. Venn. “Atmospheric Parameters and LTE Abundances for 22 Galactic, A-Type Supergiants”. In: *ApJS* 99 (Aug. 1995), p. 659. DOI: [10.1086/192201](https://doi.org/10.1086/192201).
- [142] E. Verdugo, A. Talavera, and A. I. Gómez de Castro. “Understanding A-type supergiants. I. Ultraviolet and visible spectral atlas”. In: *A&AS* 137 (June 1999), pp. 351–362. DOI: [10.1051/aas:1999487](https://doi.org/10.1051/aas:1999487).
- [143] E. Verdugo, A. Talavera, and A. I. Gómez de Castro. “Understanding A-type supergiants. II. Atmospheric parameters and rotational velocities of Galactic A-type supergiants”. In: *A&A* 346 (June 1999), pp. 819–830.
- [144] E. Verdugo et al. “Do A-type Supergiants have Magnetic Fields?” In: *The Nature and Evolution of Disks Around Hot Stars*. Ed. by R. Ignace and K. G. Gayley. Vol. 337. Astronomical Society of the Pacific Conference Series. Nov. 2005, p. 324.
- [145] Eva Verdugo et al. “Search for magnetic fields in A-type supergiants”. In: *A Massive Star Odyssey: From Main Sequence to Supernova*. Ed. by Karel van der Hucht, Artemio Herrero, and César Esteban. Vol. 212. Jan. 2003, p. 255.
- [146] J. S. Vink, A. de Koter, and H. J. G. L. M. Lamers. “New theoretical mass-loss rates of O and B stars”. In: *A&A* 362 (Oct. 2000), pp. 295–309. DOI: [10.48550/arXiv.astro-ph/0008183](https://doi.org/10.48550/arXiv.astro-ph/0008183). arXiv: [astro-ph/0008183](https://arxiv.org/abs/astro-ph/0008183) [[astro-ph](#)].
- [147] J. S. Vink, A. de Koter, and H. J. G. L. M. Lamers. “On the nature of the bi-stability jump in the winds of early-type supergiants”. In: *A&A* 350 (Oct. 1999), pp. 181–196. DOI: [10.48550/arXiv.astro-ph/9908196](https://doi.org/10.48550/arXiv.astro-ph/9908196). arXiv: [astro-ph/9908196](https://arxiv.org/abs/astro-ph/9908196) [[astro-ph](#)].

- [148] Jorick S. Vink, A. de Koter, and H. J. G. L. M. Lamers. “Mass-loss predictions for O and B stars as a function of metallicity”. In: *A&A* 369 (Apr. 2001), pp. 574–588. DOI: [10.1051/0004-6361:20010127](https://doi.org/10.1051/0004-6361:20010127). arXiv: [astro-ph/0101509](https://arxiv.org/abs/astro-ph/0101509) [[astro-ph](#)].
- [149] D. Weßmayer, N. Przybilla, and K. Butler. “Quantitative spectroscopy of B-type supergiants”. In: *A&A* 668, A92 (Dec. 2022), A92. DOI: [10.1051/0004-6361/202243973](https://doi.org/10.1051/0004-6361/202243973). arXiv: [2208.02692](https://arxiv.org/abs/2208.02692) [[astro-ph.SR](#)].
- [150] Ralph Elmer Wilson. “General catalogue of stellar radial velocities.” In: *Carnegie Institute Washington D.C. Publication* (Jan. 1953), p. 0.
- [151] B. Wolf and C. Sterken. “HD 91619 (B5 Ia) and HD 96919 (B9 Ia), two peculiar H $\alpha$  variables.” In: *A&A* 53 (Dec. 1976), pp. 355–361.
- [152] Kutluay Yüce. “Spectral Analyses of 4 Lacertae and  $\nu$  Cephei”. In: *Publications of the ASP* 115.809 (July 2003), pp. 888–888. DOI: [10.1086/376397](https://doi.org/10.1086/376397).
- [153] Norhasliza Yusof et al. “Grids of stellar models with rotation VII: models from 0.8 to 300  $M_{\odot}$  at supersolar metallicity ( $Z = 0.020$ )”. In: *MNRAS* 511.2 (Apr. 2022), pp. 2814–2828. DOI: [10.1093/mnras/stac230](https://doi.org/10.1093/mnras/stac230). arXiv: [2201.08645](https://arxiv.org/abs/2201.08645) [[astro-ph.SR](#)].
- [154] S. K. Zeinalov and A. Kh. Rzaev. “Nonstationary Atmospheres of Supergiants - Part One - Systematic Movement of Matter in the Atmospheres of Stars HD21291 and HD21389”. In: *Astrophysics and Space Science* 172.2 (Oct. 1990), pp. 211–216. DOI: [10.1007/BF00643311](https://doi.org/10.1007/BF00643311).
- [155] S. K. Zeinalov and A. Kh. Rzaev. “Nonstationary Atmospheres of Supergiants - Part Two - the H $\alpha$  Profile Variations in the Spectra of HD21291 and HD21389”. In: *Astrophysics and Space Science* 172.2 (Oct. 1990), pp. 217–224. DOI: [10.1007/BF00643312](https://doi.org/10.1007/BF00643312).
- [156] E. B. Zvereva, S. K. Zeilanov, and E. L. Chentsov. “On the systematic movements of matter in the atmospheres of white supergiant HD 21291 and HD 21389.” In: *Astrofizicheskie Issledovaniia Izvestiya Spetsial'noj Astrofizicheskoy Observatorii* 18 (Jan. 1984), pp. 29–36.

# Appendix

# SPECTRAL VARIABILITY OF SUPERGIANT HD 21389

*K. Pivoňková<sup>a\*</sup>, O. V. Maryeva<sup>b</sup>, A. Aret<sup>c</sup>, V. Checha<sup>c</sup>*

<sup>a</sup> *Department of Theoretical Physics and Astrophysics, Faculty of Science, Masaryk University, Kotlářská 2, 61137 Brno, Czech Republic*

<sup>b</sup> *Astronomical Institute of the Czech Academy of Sciences, Fričova 298, 25165 Ondřejov, Czech Republic*

<sup>c</sup> *Tartu Observatory, University of Tartu, Observatooriumi 1, 61602, Tõravere, Tartumaa, Estonia*

Late B- and early A-type supergiants are interesting evolved stars exhibiting photometric variability accompanied by spectral changes. Particularly interesting is a group of pulsating stars named after Deneb as  $\alpha$  Cyg variables. Deneb-type variables are known for decades to show variability in both brightness and radial velocities. Despite this group of stars undergoing continuous observations, the mechanism responsible for such changes is not yet well understood. In order to better understand and possibly describe this mechanism, the continuous spectral monitoring of early-type supergiants is still a topical task. The main goal of our work is to characterize the spectral variability of one of the Deneb-type variables – HD 21389. We carried out the spectral variability analysis of its spectra taken within 6 years from 2017 up to now.

Radial velocities and lines' profiles of HD 21389 show variability across the whole observational period with the most prominent variability in the  $H\alpha$  line. Among other things, we captured the final phase of the High-Velocity Absorption event (HVA) which HD 21389 underwent in 2018, and observed broad emission features around Balmer lines.

**Keywords:** stars: early-type – stars: massive – stars: individual: HD 21389 – stars: atmospheres – techniques: spectroscopic – techniques: radial velocities

## 1. INTRODUCTION

Late B- and early A-type supergiants represent a progressive evolutionary phase of massive stars that are evolving redward after they leave the Main Se-

---

\* E-mail: pivonkova@mail.muni.cz

quence (MS) or already underwent the Red Supergiant (RSGs) stage and moving blueward in their second crossing of Hertzsprung–Russell (H–R) diagram.

Among these stars is a group of variables, called Deneb (or  $\alpha$  Cyg) type variables named after its prototype, and exhibiting low amplitude photometric variability ( $\Delta V \leq 0.1$  mag) and variability in radial velocity with period 1.2 – 100 days, as well as the variability of spectral lines’ profiles [1]. With their quite short lifetime (ranging from several to tens of millions of years), which leads to an unbalanced final stage in form of a core-collapsed supernova (SN), these objects are rare. Because of their significant variability, we need to know more about them.

HD 21389 is an A0 type supergiant located in Cam OB1 association (e.g., [2]) and included in a list of Galactic  $\alpha$  Cyg variables (e.g., [3]). The main parameters of HD 21389 are listed in Table 1.

The story of the HD 21389 started more than one century ago, in 1910 when Mr. Young performed spectroscopic observations and analysis of its spectra ([4]). Based on these results, the star was suggested as a spectroscopic binary [5]; however, its binarity has never been reliably confirmed. The vast majority of previous studies (e.g., [6–8]) discuss variability in radial velocities and profiles of Balmer lines (mainly  $H\alpha$  and  $H\beta$ ) that is strongly tied to the active phase. Some studies (e.g., [6, 9–11]) also revealed variability in metallic lines.

The most extended spectral study of this star was performed by Corliss et al. [12]. Authors analyzed 152 spectra taken with the 1-m telescope of Ritter Observatory between 1993 and 2007 and detected High-Velocity Absorption (HVA) events in spectra from the years 1993-1994. Their study also presents results based on simultaneous photometric observations, that show a strong correlation between photometric and spectroscopic variability with active and quiescent phases of the star. In this paper, we study the spectroscopic variability of HD 21389 using a set of new spectral observations covering 6 years. Our analysis revealed variability in radial velocities, and lines’ profiles, and also brought new results such as the presence of extended emission wings around the  $H\alpha$  line, as well as the detection of another episode of HVA.

## 2. OBSERVATIONS AND SPECTRAL DATA REDUCTION

Optical spectroscopic observations of HD 21389 mainly in  $H\alpha$  region were performed during 6 years from 2017 up to 2022 at the Perek 2-m telescope of Czech Academy of Science and AZT-12 1.5-m telescope of Tartu Observatory, University of Tartu, Estonia. Spectroscopic observations performed at the Perek 2-m telescope were done using two spectrographs: Single order spectrograph (CCD700) [13] and Ondřejov Echelle Spectrograph (OES) [14, 15].

Parameters	Values	References
Names	HR 1040, CE Cam, BD+58 607	
RA (J2000)	$3^h 29^m 54.74^s$	[26]
Dec (J2000)	$58^\circ 52' 43.5''$	[26]
$M_V$ [mag]	-7.56	
$V$ [mag]	4.54	[27]
$B$ [mag]	5.10	[27]
Spectral Type	A0 Ia	[2]
Parallax [mas]	$0.930 \pm 0.119$	[26]
$T_{eff}$ [K]	9730	[28]
$M$ [ $M_\odot$ ]	19.3	[28]
$R$ [ $R_\odot$ ]	97	[28]
$\log L/L_\odot$	4.87	[29]
$\log g$ [cgs]	1.7	[30]
$v_{esc}$ [ $\text{km} \cdot \text{s}^{-1}$ ]	233	[31]
$v \cdot \sin i$ [ $\text{km} \cdot \text{s}^{-1}$ ]	53	[28]
$\dot{M}$ [ $M_\odot \cdot \text{yr}^{-1}$ ]	$-4.2 \cdot 10^{-7}$	[32]
Distance [pc]	$1084^{+124}_{-112}$	[33]

Table 1: Stellar parameters for HD 21389.

Both spectrographs are connected to the primary focus by optical fiber and placed in separate rooms. Observations at the Tartu observatory were carried out using a Single slit spectrograph (ASP-32) that is directly attached to the Cassegrain focus [16]. The information about spectra used in the work is given in Table 2.

Data from ASP-32 and OES spectrographs were processed using standard IRAF tasks, while spectra taken by the CCD700 instrument were reduced using a dedicated IDL-based package including all standard steps. Additionally, the telluric correction was done using MOLECFIT 1.5.1. software [17, 18]. All spectra are normalized and corrected for barycentric velocity.

Telescope	Instrument	R	Sp. range [Å]	Obs. period	N
Perek 2m	CCD700	13 000	6260 – 6730	Aug 2017 - Aug 2022	86
	OES	50 000	3965 – 8740	Jul 2021 - Oct 2021	10
AZT-12	ASP-32	10 000	6300 – 6580	Aug 2018 - Nov 2021	30

Table 2: Summary of spectral data used in present work. R is spectral resolution, N is number of spectra.

### 3. RESULTS

In total, we performed a spectral analysis of 126 spectra of HD 21389. The sample spectrum taken on Sep 26, 2018, may be seen in Fig. 1. We mainly focused on the study of the variability of H $\alpha$  line profile, but we also measured radial velocities of selected absorption lines listed in Tab. 3 to test possible binary behavior and to trace the motion of matter in the atmosphere of the star.

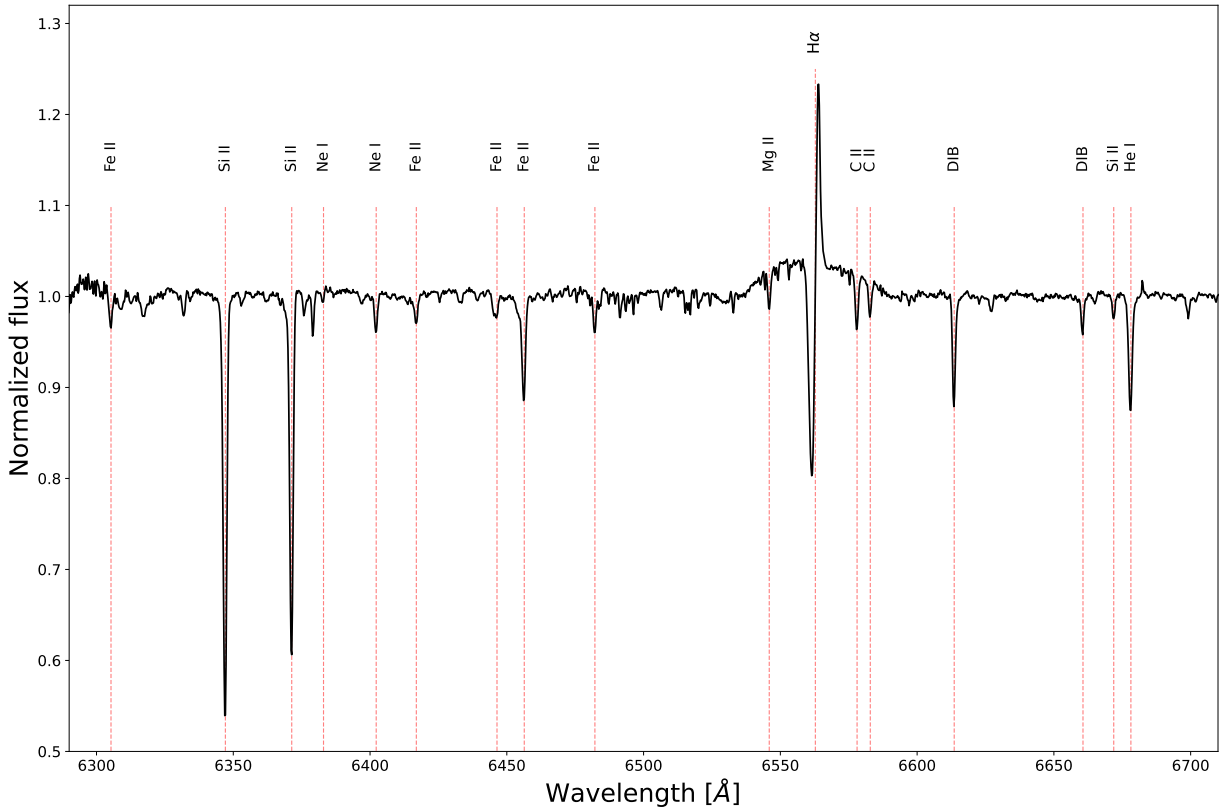


Fig. 1: Spectrum of HD 21389 taken on Sep 26, 2018 in H $\alpha$  region with Perek 2m, CCD700. Telluric lines are removed from the spectrum using MOLECFIT.

Spectral line	$\lambda$ [Å]	D700	ASP-32	OES	Spectral line	$\lambda$ [Å]	D700	ASP-32	OES
Si II	6347.11	✓	✓	✓	DIB	6613.56	✓		
Si II	6371.37	✓	✓	✓	DIB	6660.64	✓		
Fe II	6456.38	✓	✓	✓	H $\beta$	4861.32			✓
Mg II	6545.94	✓	✓	✓	H $\gamma$	4340.46			✓
H $\alpha$	6562.80	✓	✓	✓	H $\delta$	4101.73			✓
C II	6578.05	✓		✓	Na I	5889.95			✓
C II	6582.88	✓		✓	Na I	5895.92			✓
He I	6678.15	✓		✓					

Table 3: List of spectral lines of which the radial velocities were measured ( $\lambda$  is air wavelength).

### 3.1. Variability in H $\alpha$ line

As it is known, the best indicator of stellar wind in B- and A- type supergiants is H $\alpha$  line [19]. H $\alpha$  line in HD 21389 spectrum has a complex structure and displays significant variability across all our observations. Pure absorption, normal and inverse P Cyg, and double-peaked profiles were observed. Sometimes highly asymmetric profiles appear, but in our case, that was associated with fading of the HVA event (the left panel of Fig. 2). Selected lines' profiles are shown in the right panel of Fig. 2.

#### 3.1.1. High-velocity absorption event

As was already mentioned in the introduction, HD 21389 is one of the rare stars showing high-velocity absorption events (HVAs) [12]. HVA event is the occasional appearance of deep and highly blue-shifted absorption component detected only in the H $\alpha$  line. The kinematic properties of the HVAs are completely different from those of Discrete Absorption Components (DACs) observed in the ultraviolet spectra of O-type and early B-type stars. HVAs do not propagate outwards, but instead, extend to zero velocity and even indicate mass infall [20].

$\alpha$  Cyg variables with HVA events are rare. This behavior was already observed in a few late B- and early A- type supergiants HD 91619 (B7 Iae), HD 96919 (B9 Iae), HD 34085 (B8 Iae), HD 197345 (A2 Ia), HD 207260 (A2 Iab), and HD 199478 (B8 Iae) [20], [21], [22], [23], [24]. Such events are reported to last from dozens of days to several months [20]. There is currently no proper expla-



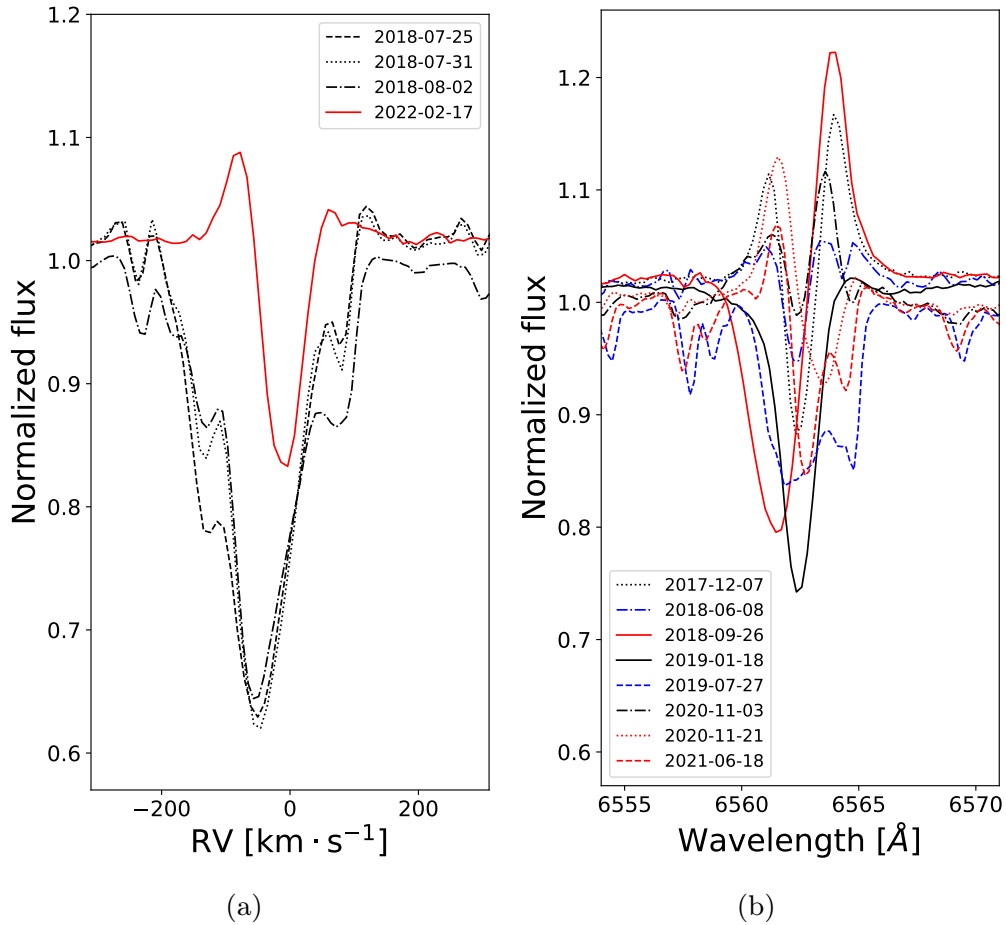


Fig. 2: (a) Lines' profile appearance during final phase of HVA event is demonstrated by black lines. Red solid line is to compare the intensity with profile taken out of HVA event. (b) Selected lines' profiles of H $\alpha$  line.

nation for the formation of HVAs. Israelian, Chentsov, & Musaev [25] attributed them to the effects of magnetic fields, but these stars do not have a such strong magnetic field to fit the observational properties of HVA.

Our data taken during July and August 2018 revealed the presence of unusually deep and blue-shifted absorption component of H $\alpha$  line profile when the intensity reached 0.6 of continuum level (Figure 3). We detected only one HVA event in our spectra of HD 21389 acquired over 6 years. This indicates that conditions in the atmosphere of HD 21389 necessary for the appearance of HVA events require at least several years to form. However, there is evidence of two consecutive HVA for Rigel (HD 34085) just several months apart [25].

Since these events are associated with significant variability in the H $\alpha$  line without any correlation in other lines, it may be said that the star switches between active phases represented by HVAs and quiescent ones containing no such events.

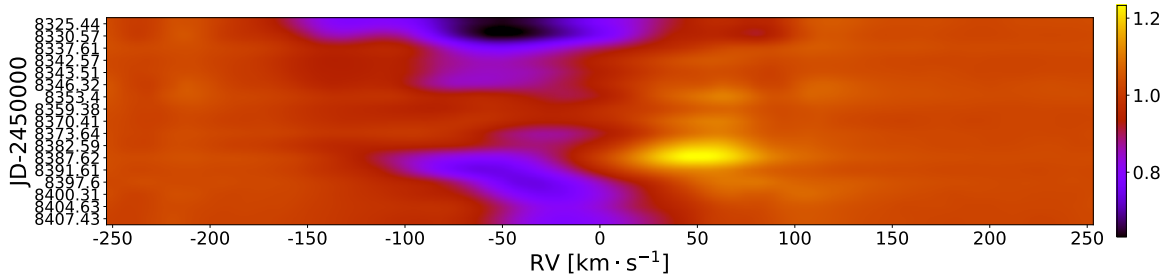


Fig. 3: Dynamic spectrum intercepting final phase of HVA that HD 21389 underwent during July and August 2018. Color bar at the right side represents the flux, thus the darkest part (top black region) shows HVA.

### 3.1.2. Broad emission wings around $H\alpha$ line

All data contains a prominent feature of extended emission wings around the  $H\alpha$  line. Although HD 21389 has been spectroscopically studied many times before, especially the  $H\alpha$  region, no one has mentioned this feature. The emission wings extend to about  $\pm 1400 \text{ km} \cdot \text{s}^{-1}$  as shown in Fig. 4. We performed the analysis of this feature. Broad emission wings in a few spectra were fitted with Gaussian profile and it turned out that this feature varies on a timescale of a few weeks and from time to time appears asymmetric without any pattern.

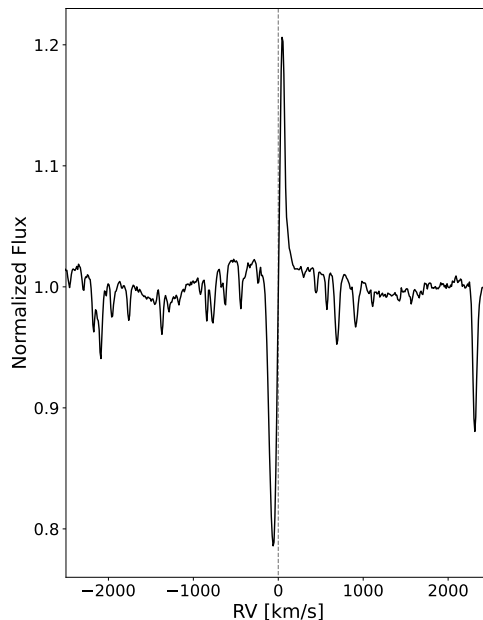


Fig. 4: Extended emission wings around  $H\alpha$  line.

### 3.2. Variability in other lines

All studied lines listed in Tab. 3 display variability in radial velocities (except the interstellar Na II doublet) across the whole observational period and also show asymmetries in lines' profiles while the most striking changes are recorded in Balmer lines, especially in the H $\alpha$  line (Fig. 5).

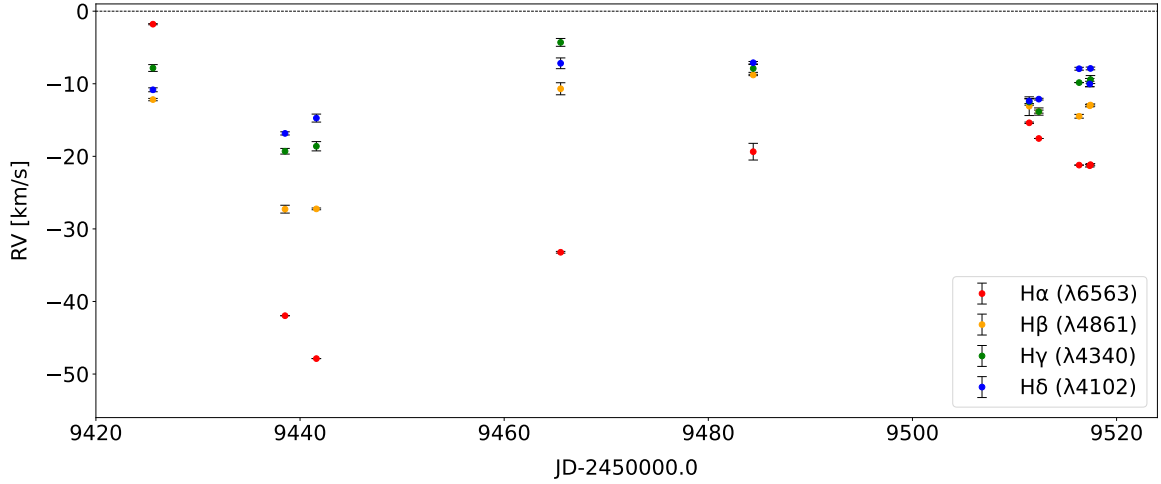


Fig. 5: Radial velocities of Balmer lines measured from OES spectra taken from July to October 2021.

In a study by Abt [11], the radial velocities of selected lines were measured. Among others, the surprising results were obtained for Si II  $\lambda$ 4028, 4030 and Fe II  $\lambda$ 4508, 4515, 4520, 4522 lines. Both velocity curves were almost the same in shape but slightly shifted in radial velocity. The same result may be seen in Fig. 6.

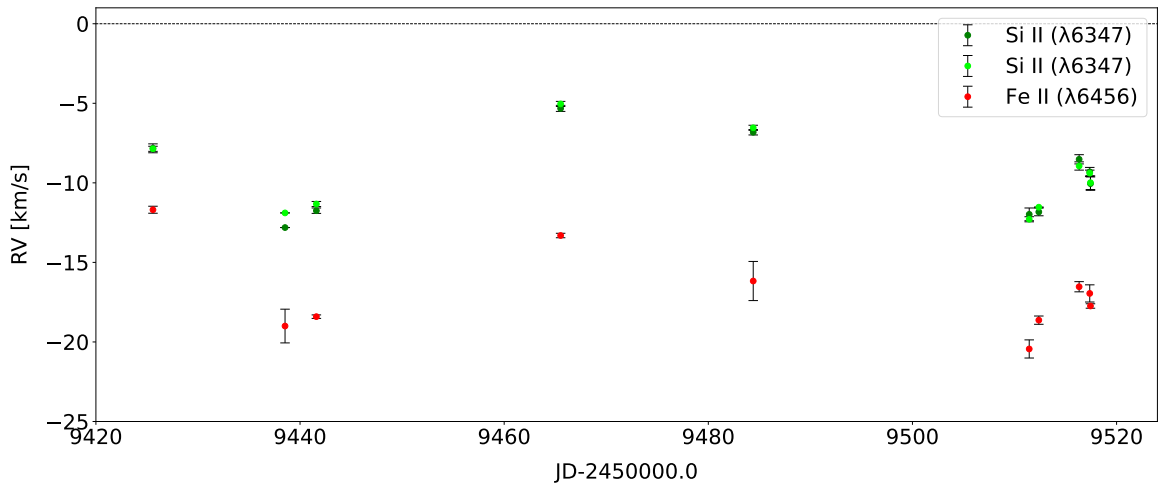


Fig. 6: Comparison of radial velocities of Fe II  $\lambda$ 6456 and Si II  $\lambda$ 6347; 6371 lines measured from the OES spectra.

Interesting results were obtained from the analysis of radial velocities of Mg II  $\lambda 6546$  line, see Fig. 7. The observations taken with AZT-12 telescope point to some signs of binarity with the period around 400 days, but we need more observational data to be sure.

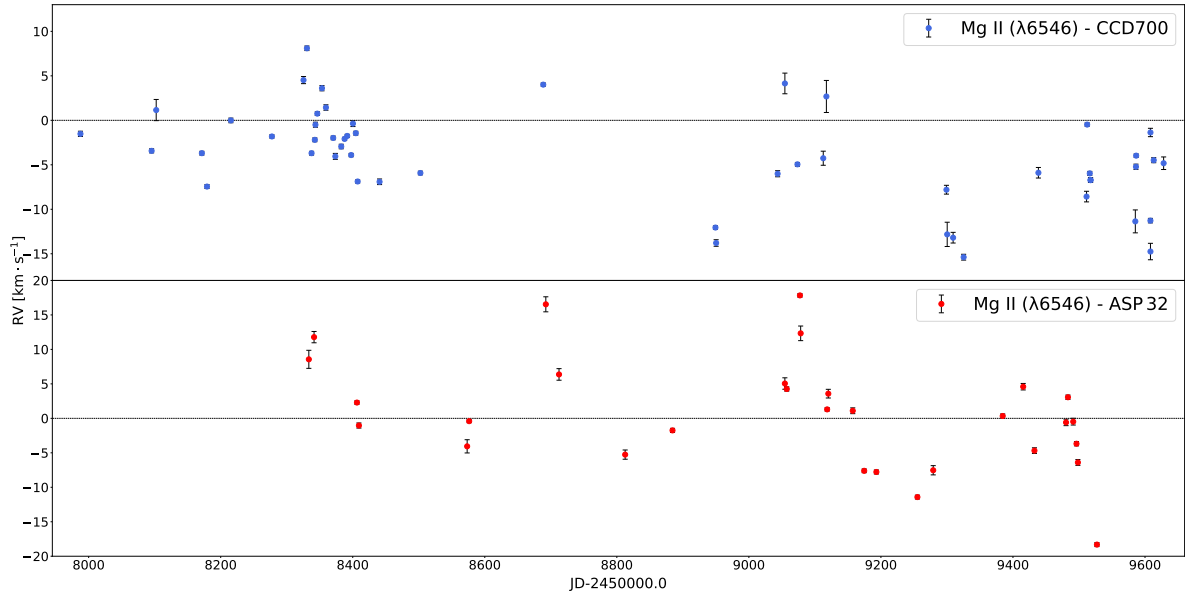


Fig. 7: Measured radial velocities of magnesium line Mg II  $\lambda 6546$ . Blue dots represent data from CCD700 and red ones are data from ASP-32.

Spectra taken with OES have the largest wavelength coverage in our data set, which allows us to analyze other Balmer lines ( $H\beta$ ,  $H\gamma$ ,  $H\delta$ ,  $H\epsilon$ ). A sample of lines' profiles variability in OES spectra is shown in Fig. 8. As mentioned above, noticeable asymmetries are clearly seen in the  $H\alpha$  line profile (Fig. 8 (c)).

#### 4. CONCLUSION

We analyzed spectral variability of A-type supergiant HD 21389 based on medium- and high-resolution spectra collected during 6 years. HD 21389 shows long-term variability (longer than a month) and variability on a short time scale (tens of minutes or several days) in both radial velocities and lines' profiles. The most striking changes were recorded for the  $H\alpha$  line. We observed variability with no obvious pattern in the width of extended emission wings and detected HVA (July and August 2018) during which the depth of the  $H\alpha$  line reached its maximum. All other measured lines show variability too. Asymmetry in lines' profiles reflects the actual condition of the  $H\alpha$  line which is associated with active or quiescent phases of the atmosphere.

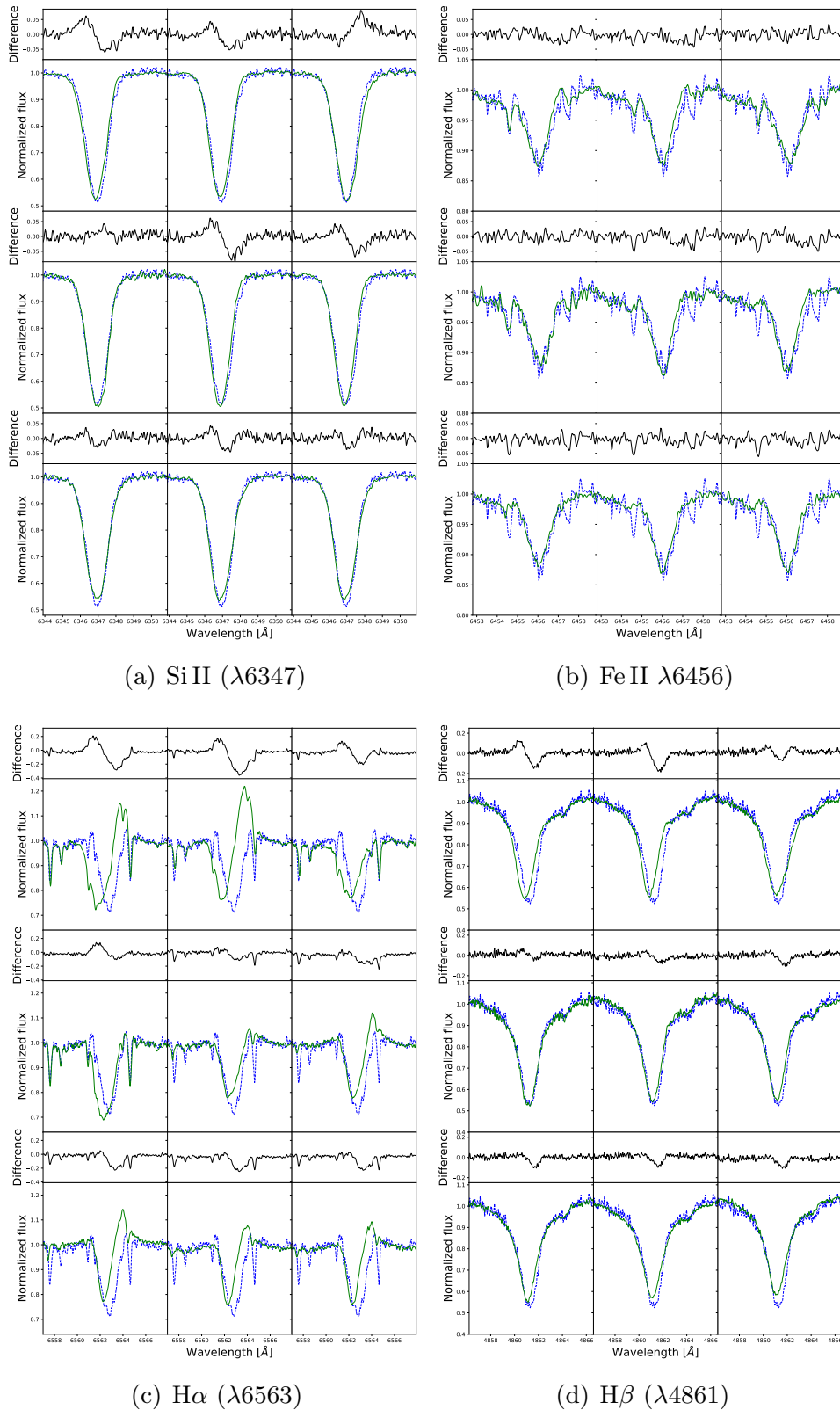


Fig. 8: Line profile variability of Si II, Fe II, H $\alpha$  and H $\beta$  lines. The blue dashed profile is a reference and the rest of the spectra compared to it are green. Their asymmetry is seen above (black line).

## 5. ACKNOWLEDGEMENT

We thank all observers at the Ondřejov Observatory and Tartu Observatory who participated in the observations of HD 21389 and subsequent discussion of results. The work is funded by the European Union's Framework Programme for Research and Innovation Horizon 2020 (2014-2020) under the Marie Skłodowska-Curie Grant Agreement No. 823734. This work is based on data taken with the Perek telescope at the Astronomical Institute of the Czech Academy of Sciences in Ondřejov, which is supported by the project RVO:67985815 of the Academy of Sciences of the Czech Republic.

## REFERENCES

1. Catelan, M. & Smith, H. A. 2015, *Pulsating Stars* (Wiley-VCH), 2015
2. Lyder, D. A. 2001, *AJ*, 122, 2634. doi:10.1086/323705
3. Straižys, V. & Laugalys, V. 2007, *Baltic Astronomy*, 16, 167
4. Kapteyn J. C., Frost E. B., 1910, *ApJ*, 32, 83. doi:10.1086/141786
5. Campbell, W. W., Moore, J. H., Wright, W. H., et al. 1911, *Lick Observatory Bulletin*, 199, 140. doi:10.5479/ADS/bib/1911LicOB.6.140C
6. Zeinalov, S. K. & Rzaev, A. K. 1990, *Astrophysics and Space Science*, 172, 211. doi:10.1007/BF00643311
7. Rosendhal, J. D. 1973, *ApJ*, 186, 909. doi:10.1086/152555
8. Aydin, C. 1972, *A&A*, 19, 369
9. Denizman, L. & Hack, M. 1988, *A&AS*, 75, 79
10. Maharramov, Y. M. & Baloglanov, A. S. 2015, *Odessa Astronomical Publications*, 28, 39
11. Abt, H. A. 1957, *ApJ*, 126, 138. doi:10.1086/146379
12. Corliss, D. J., Morrison, N. D., & Adelman, S. J. 2015, *AJ*, 150, 190. doi:10.1088/0004-6256/150/6/190
13. Slechta M., Skoda P. 2002, *PAICz*, 90, 1
14. Koubský P., Mayer P., Čáp J., Žďárský F., Zeman J., Pína L., Melich Z. 2004, *PAICz*, 92, 37
15. Kabáth P., Skarka M., Sabotta S., Guenther E., Jones D., Klocová T., Šubjak J., et al. 2020, *PASP*, 132, 035002. doi:10.1088/1538-3873/ab6752

16. Folsom, C. P., Kama, M., Eenme, T., et al. 2022, *A&A*, A105. doi:10.1051/0004-6361/202142124
17. Smette A., Sana H., Noll S., Horst H., Kausch W., Kimeswenger S., Barden M., et al., 2015, *A&A*, 576, A77. doi:10.1051/0004-6361/201423932
18. Kausch W., Noll S., Smette A., Kimeswenger S., Barden M., Szyszka C., Jones A. M., et al., 2015, *A&A*, 576, A78. doi:10.1051/0004-6361/201423909
19. Lamers H. J. G. L. M., Cassinelli J. P., 1999, *isw..book*, 452
20. Markova, N., Prinja, R. K., Markov, H., et al. 2008, *A&A*, 487, 211. doi:10.1051/0004-6361:200809376
21. Kaufer, A., Stahl, O., Wolf, B., et al. 1996, *A&A*, 314, 599
22. Kaufer, A., Stahl, O., Wolf, B., et al. 1996, *A&A*, 305, 887
23. Morrison, N. D., Rother, R., & Kurschat, N. 2008, *Clumping in Hot-Star Winds*, 155
24. Shultz, M., Wade, G. A., Petit, V., et al. 2014, *MNRAS*, 438, 1114. doi:10.1093/mnras/stt2260
25. Israelian, G., Chentsov, E., & Musaev, F. 1997, *MNRAS*, 290, 521. doi:10.1093/mnras/290.3.521
26. Gaia Collaboration 2020, *VizieR Online Data Catalog*, I/350
27. Ducati, J. R. 2002, *VizieR Online Data Catalog*
28. Verdugo, E., Talavera, A., & Gomez de Castro, A. I. 1999, *A&A*, 346, 819
29. de Jager, C., Nieuwenhuijzen, H., & van der Hucht, K. A. 1988, *A&AS*, 72, 259
30. Takeda Y., Takada-Hidai M., 2000, *PASJ*, 52, 113. doi:10.1093/pasj/52.1.113
31. Talavera, A. & Gomez de Castro, A. I. 1987, *A&A*, 181, 300
32. Barlow, M. J. & Cohen, M. 1977, *ApJ*, 213, 737. doi:10.1086/155204
33. Bailer-Jones, C. A. L., Rybizki, J., Foesneau, M., et al. 2021, *AJ*, 161, 147. doi:10.3847/1538-3881/abd806